

**ROLE OF ADROPIN IN ARTERIAL STIFFENING ASSOCIATED  
WITH OBESITY AND TYPE 2 DIABETES**

---

A Dissertation Presented to the  
Faculty of the Graduate School  
University of Missouri, Columbia

---

In Partial Fulfillment of the  
Requirements of the Degree:  
Doctorate of Philosophy

---

By Thomas J Jurrissen, III

Jaume Padilla, PhD, Dissertation Supervisor

December 2022

The undersigned, appointed by the dean of the Graduate School, have examined the dissertation entitled:

ROLE OF ADROPIN IN ARTERIAL STIFFENING ASSOCIATED WITH OBESITY AND TYPE 2 DIABETES

Presented by Thomas J Jurrissen, III, a candidate for the degree of Doctor of Philosophy, and hereby certify that, in their opinion, it is worthy of acceptance.

---

Associate Professor Jaume Padilla, PhD

---

Professor Luis A Martinez-Lemus, DVM, PhD

---

Professor Jill A. Kanaley, PhD

---

Associate Professor Victoria J. Vieira-Potter, PhD

---

Professor Shivendra D. Shukla, PhD

## DEDICATION

I would like to dedicate this dissertation to my family, Thomas W. Jurrissen, Stephen M. Jurrissen, Alexander C. Jurrissen, and Miranda M. Wallace for your kindness, compassion, love and support throughout this process. Without you, this would not have been possible.

## ACKNOWLEDGEMENTS

This work would not have been possible without the help and contributions of many great people here at the University of Missouri. First, and foremost, I would like to thank my mentor, Jaume Padilla, and my unofficial co-advisor Luis Martinez-Lemus, who have been incredibly patient mentors. Together, you have provided counseling and critiques to encourage me to be the best researcher I can be. In addition, you have been instrumental in ensuring that all research is conducted with the highest integrity and despite a desire to push forward faster, teaching me that research is an incremental process. Thank you for being exemplary in your dedication, hard work, and perseverance in the field.

I would also like to thank my committee members, Drs. Victoria Vieira-Potter, Jill Kanaley, and Shivendra Shukla. Without this team of intelligent, driven, and inspiring mentors it would have been impossible for me to finish my degree. They have all offered me insight on how to view my dilemmas in a new light and with a new perspective. Learning from and working with you all has fostered my passion for the pursuit of knowledge and research, which has been vital for this endeavor.

To the laboratory staff and my peers, this work could not have been completed without your assistance. Michelle Gastecki, Makenzie Woodford, Mariana Morales-Quinones, and Christopher Foote were instrumental in teaching me many techniques I learned in the lab. Thank you all for your patience and answering my endless questions. To my lab peers, Zachary Grunewald,

Francisco Ramirez-Perez, Gavin Power, James Smith, Neil McMillan, and Marc Augenreich, thank you for all the assistance with experiments, data analysis and jokes. Francisco, I would like to especially thank you for teaching me how to perform pressure myography and confocal microscopy. You were right, at some point, if it can go wrong, it will. Thank you for always being there to assist, even in the late hours of the evening when everyone else had already gone home. Additionally, I would like to thank the NEP faculty, staff, and fellow graduate students for all your help along the way. Together, you have all made Mizzou a second home, if not my primary residence.

# Table of Contents

<b>ACKNOWLEDGEMENTS</b> .....	<b>II</b>
<b>ABBREVIATIONS</b> .....	<b>VII</b>
<b>LIST OF FIGURES</b> .....	<b>X</b>
<b>LIST OF TABLES</b> .....	<b>XI</b>
<b>CHAPTER 1: Background</b> .....	<b>1</b>
<b>Adropin</b> .....	<b>2</b>
<b>Metabolic effects of adropin</b> .....	<b>2</b>
<b>Cardiovascular effects of adropin</b> .....	<b>5</b>
<b>Exercise-induced effects on adropin</b> .....	<b>7</b>
<b>Conclusion</b> .....	<b>8</b>
<b>Project hypothesis</b> .....	<b>8</b>
<b>Innovation</b> .....	<b>8</b>
<b>Impact</b> .....	<b>9</b>
<b>CHAPTER 2: Extended Literature Review</b> .....	<b>10</b>
<b>Obesity-associated arterial stiffening</b> .....	<b>10</b>
<b>Endothelium</b> .....	<b>11</b>
<b>VSMC stiffness and vascular function</b> .....	<b>17</b>

<b>ECM and arterial stiffness .....</b>	<b>19</b>
<b>Adropin.....</b>	<b>21</b>
<b>Hepatic <i>Enho</i> regulation .....</b>	<b>22</b>
<b>Circulating adropin .....</b>	<b>24</b>
<b>Weight loss and adropin.....</b>	<b>27</b>
<b>Exercise and adropin .....</b>	<b>27</b>
<b>Adropin-mediated regulation of adiposity, lipid and glucose metabolism..</b>	<b>30</b>
<b>Cardiovascular disease and adropin.....</b>	<b>33</b>
<b>Endothelial cell function and adropin .....</b>	<b>34</b>
<b>VSMCs and adropin .....</b>	<b>35</b>
<b><i>In vivo</i> cardiovascular effects of adropin .....</b>	<b>36</b>
<b>CHAPTER 3: Role of Adropin in Arterial Stiffening Associated with Obesity and Type 2 Diabetes.....</b>	<b>38</b>
<b>Tables and Figures.....</b>	<b>65</b>
<b>CHAPTER 4: Summary and Future Directions .....</b>	<b>120</b>
<b>Future directions .....</b>	<b>127</b>
<b>Bibliography .....</b>	<b>130</b>
<b>APPENDIX A: Curriculum Vitae .....</b>	<b>146</b>
<b>APPENDIX B: Abstracts of Published Manuscripts .....</b>	<b>154</b>

<b>VITA .....</b>	<b>167</b>
-------------------	------------



## ABBREVIATIONS

AdrHet – Heterozygote carriers of the adropin allele

AdrKO – Adropin knockout

AGEs – Advanced glycosylated end-products

Akt – Protein kinase b

Ang II – Angiotensin II

ApoEKO – Apoprotein E knockout

BAX – Bcl2-associated X protein 4

BCL2 – B-cell lymphoma 2

BH<sub>2</sub> – Dihydrobiopterin

BH<sub>4</sub> – Tetrahydrobiopterin

BMI – Body mass index

CVD – Cardiovascular disease

db/+ - Heterozygote for leptin receptor

db/db – Leptin receptor knockout

DIO – Diet-induced obese

ECM – Extracellular matrix

*Enho* – Energy homeostasis associated gene

eNOS – Endothelial nitric oxide synthase

Erk 1/2 – Extracellular-regulated kinase 1/2

ET-1 – Endothelin-1

F-actin – Filamentous actin

G-actin – Globular actin

H<sub>2</sub>O<sub>2</sub> – Hydrogen peroxide

HOMA-IR – Homeostatic model of assessment-insulin resistance

HR<sub>max</sub> – Maximum heart rate

HUVEC – Human umbilical vein endothelial cell

IP<sub>3</sub> – Inositol 1,4,5 phosphate

IRS-1 – Insulin receptor substrate-1

L-NAME - N $\omega$ -nitro-L-arginine methyl ester

LIMK – Lim kinase

LIMKi – LIMK inhibitor

LXR $\alpha$  - Liver X receptor- $\alpha$

MAPK – Mitogen-activated protein kinase

MLC2 – Myosin light chain 2

MMP – Matrix metalloproteinase

NADPH – Nicotinamide adenine dinucleotide

NO – Nitric oxide

NOX – NADPH oxidase

ONOO<sup>-</sup> - Peroxynitrite

PI3K – Phosphatidylinositol kinase

RER – Respiratory exchange ratio

ROCK – Rho-associated protein kinase

ROS – Reactive oxygen species

SAMP1 – Senescence-accelerated prone mouse 1

T2D – Type 2 diabetes

TG-2 – Tissue transglutaminase-2

TGF- $\beta$  - Transforming growth factor- $\beta$

TIMP- Tissue inhibitor of MMP

TNF- $\alpha$  - Tumor necrosis factor- $\alpha$

VEGFR2 – Vascular endothelial growth factor receptor 2

VO<sub>2max</sub> – Maximal volume oxygen consumption

VO<sub>2peak</sub> – Peak volume of oxygen consumption

VSMCs – Vascular smooth muscle cells

## LIST OF FIGURES

<b>Figure</b>	<b>Page</b>
<b>Figure 1.</b> Decreased adropin is associated with increased arterial stiffness. ..	110
<b>Figure 2.</b> Adropin reduces F-actin stress fibers and stiffness in endothelial cells (EC) and isolated mesenteric arteries of db/db male mice: role of NO. ....	113
<b>Figure 3.</b> Stimulation of vascular smooth muscle cells (VSMC) with sodium nitroprusside (SNP), an NO mimetic, reduces F-actin stress fibers and stiffness. ....	115
<b>Figure 4.</b> In vivo treatment of db/db male mice with adropin for four weeks reduces mesenteric arterial stiffness. ....	116
<b>Figure 5.</b> Proteomic analysis of endothelial cells treated with vehicle vs. adropin. ....	117
<b>Figure 6.</b> Schematic illustrating the interpretation of the results. ....	118

## LIST OF TABLES

<b>Table</b>	<b>Page</b>
<b>Table 1.</b> Circulating metabolic parameters of wild-type and adropin knockout littermates.....	65
<b>Table 2.</b> Circulating metabolic parameters of db/db mice after a four-week vehicle vs adropin administration. ....	66

ROLE OF ADROPIN IN ARTERIAL STIFFENING ASSOCIATED WITH  
OBESITY AND TYPE 2 DIABETES

Thomas Jurrissen

Dr. Jaume Padilla, Dissertation Supervisor

ABSTRACT

Adropin is a peptide largely secreted by the liver and known to regulate energy homeostasis; however, it also exerts cardiovascular effects. Herein, I tested the hypothesis that low circulating levels of adropin in obesity and type 2 diabetes (T2D) contribute to arterial stiffening. In support of this hypothesis, I report that obesity and T2D is associated with reduced levels of adropin expression in liver and plasma and increased arterial stiffness in mice and humans. Establishing causation, I showed that mesenteric arteries from adropin knockout mice are also stiffer relative to arteries from wild-type counterparts, thus recapitulating the stiffening phenotype observed in T2D db/db mice. Given the above, a series of follow-up experiments were performed that determined: 1) exposure of endothelial cells or isolated mesenteric arteries from db/db mice to adropin reduces filamentous actin (F-actin) stress fibers and stiffness; 2) adropin-induced reduction of F-actin and stiffness in endothelial cells and db/db mesenteric arteries is abrogated by inhibition of nitric oxide (NO) synthase; and 3) stimulation of smooth muscle cells or db/db mesenteric arteries with a NO mimetic reduces stiffness. Last, *in vivo* treatment of db/db mice with adropin for four weeks reduced stiffness in mesenteric arteries. Collectively, these findings

indicate that adropin can regulate arterial stiffness, likely via endothelial-derived NO, and thus support the notion that “hypoadropinemia” should be considered as a putative target for the prevention and treatment of arterial stiffening in obesity and T2D.

## CHAPTER 1: Background

Arterial stiffness is the result of functional and structural adaptations of the arterial wall in response to cardiometabolic dysfunction, injury and aging (1). Increased arterial stiffness is believed to occur early in cardiovascular disease progression and contribute to premature cardiovascular dysfunction, which leads to an increased risk of cardiovascular disease (CVD) morbidity and mortality. Indeed, the Framingham Heart Study confirmed that arterial stiffening is an independent risk factor of CVD morbidity and mortality in the general population, hypertensive patients, the elderly, and end-stage renal disease patients (2). Arterial stiffening is associated with natural aging, but obesity, insulin resistance and type 2 diabetes (T2D) accelerate its onset (3, 4). The development of arterial stiffening is a complex process affected by various endocrine factors, the interaction of cellular components, and the extracellular matrix composition. Adropin, a peptide hormone that is regulated by energy state and meal consumption, plays a role in energy homeostasis and metabolic regulation (5). Adropin has demonstrated systemic effects on insulin signaling in a variety of tissues including the liver, skeletal muscle, and heart (6, 7). Furthermore, adropin concentrations have been reported to have direct effects on the cardiovascular system (7-13) and is inversely correlated with arterial stiffness (14, 15). Therefore, adropin may provide a novel therapeutic approach in the treatment of obesity-induced vascular dysfunction.



## Adropin

Adropin, first discovered in 2008 as a secreted peptide, is encoded by the Energy Homeostasis Associated (*Enho*) gene and is mainly expressed in the liver and brain, but is also present in a variety of tissues including brown and white adipose tissue, aorta, heart, kidney, skeletal muscle, lung, spleen, and endothelial cells (5, 8, 16). Adropin is a highly conserved peptide, with identical sequences among mice, rats, and humans (17). The circulating concentration of adropin in healthy adults ranges from 3.0-6.0 ng/ml (16, 18). Currently, the half-life for adropin is unknown; however, it is posited to be as short as minutes (19). Circulating adropin concentrations are influenced by factors such as energy status and meal composition (5, 20), age (21, 22), and body mass index (BMI) (21, 23). Acutely, circulating adropin concentrations are increased by energy intake, with a high-fat meal increasing adropin concentrations more than a high-carbohydrate meal (5). In addition, circulating adropin concentrations have been reported to increase with exercise training (14, 15, 24, 25). Conversely, circulating adropin concentrations are negatively associated with increased BMI (21, 26, 27), age (21, 22), insulin resistance and T2D (27).

## Metabolic effects of adropin

Hepatic *Enho* expression is increased in a fed state compared to a fasted state (5). Upon refeeding after an overnight fast with a high-fat diet, *Enho* expression was increased nine-fold compared to a high-carbohydrate diet in lean male mice (5), suggesting that the meal composition is important for adropin secretion. Fasting adropin concentrations are correlated with fat intake in

normal-weight women, indicating that sex and diet composition may influence adropin concentrations (28). However, obese mice have decreased hepatic *Enho* expression (5, 29). Given that *Enho* expression is decreased with increased adiposity, adropin may play a role in regulating metabolic homeostasis. Indeed, adropin knockout (AdrKO) mice exhibit increased adiposity and insulin resistance despite no difference in body weight, food intake, or energy expenditure (20). Additionally, adropin AdrKO mice fed a high-fat diet had dyslipidemia, glucose intolerance, and insulin resistance (20). Collectively, these studies suggest that adropin plays a role in maintaining homeostasis following the consumption of a high-fat meal.

Given that adropin concentrations are altered due to energy status and meal composition, does adropin play a role in substrate utilization? In chow-fed adropin KO mice, respiratory exchange ratio (RER) was decreased throughout the day relative to wild-type mice, suggesting preferential utilization of fat over carbohydrates (30). Conversely, in adropin overexpression fasted mice, RER is elevated compared to their wild-type counterparts (30). This would indicate a preferential increase in glucose oxidation during fasting in these mice. Indeed, increased adropin concentrations induced an increase in glucose oxidizing enzymes in the liver and skeletal muscle (30, 31). Adropin improves hepatic and skeletal muscle insulin signaling in obese mice, therefore adropin may lead to improved glucose uptake in the liver and skeletal muscle (5, 31, 32). AdrKO mice exhibited fasting hyperinsulinemia, hyperglycemia, and increased fasting triglycerides (20). During a hyperglycemic-euglycemic clamp, AdrKO mice

glucose uptake was reduced by 30-35% in the gastrocnemius and diaphragm, but not in other skeletal muscles (20). However, endogenous glucose production was not suppressed during the hyperglycemic-euglycemic clamp in the AdrKO lean mice, suggesting hepatic insulin resistance (20). In diet-induced obese (DIO) AdrKO mice, fasting hyperinsulinemia and hyperglycemia were more severe than in wild-type DIO mice, with a genetic dose-effect being noted in the adropin heterozygous mice. Thapa et al. (33) reported decreased blood glucose concentrations due to reduced endogenous glucose production rather than increased uptake in either the gastrocnemius or quadriceps of high-fat diet-fed mice treated with adropin.

Adropin overexpression mice fed a high-fat diet exhibited protection against diet-induced obesity, specifically attenuated gain in adiposity (5). Elevated adropin concentrations, either genetically or injected, also resulted in decreased *de novo* fatty acid synthesis and fatty acid oxidation in skeletal muscle (5, 30, 31). It has been proposed that an accumulation of fatty acids in the mitochondria may result in insulin resistance (34), thus adropin may be mediating these effects by inhibiting fatty acid oxidation in skeletal muscle (30).

Collectively, adropin shifts preferential substrate utilization toward glucose. Additionally, adropin improves hepatic and skeletal muscle insulin signaling and decreases systemic insulin resistance. Therefore, adropin may be a promising therapeutic candidate for the treatment of insulin resistance and T2D.

## Cardiovascular effects of adropin

In addition to the metabolic effects, adropin also has cardiovascular effects. Given that obesity and insulin resistance are associated with increased risk of CVD and decreased adropin concentrations, it could be posited that adropin may also be decreased in patients with CVD. Indeed, patients with coronary artery disease (12, 35), atherosclerosis (27, 36), hypertension (37, 38), and endothelial dysfunction (10, 39) exhibit decreased adropin concentrations compared to their healthy counterparts.

In endothelial cells, adropin has a unique role in regulating the expression and modulates the activation of endothelial nitric oxide synthase (eNOS) and the production of nitric oxide (NO) (8). In human umbilical vein endothelial cells (HUVECs) adropin stimulates cell proliferation, tube formation, and decreased permeability (8). Furthermore, acute (within one hour) adropin treatment stimulated the production and release of NO via protein kinase b (Akt)- and mitogen-activated protein kinase (MAPK)-dependent phosphorylation of eNOS (8). HUVECs incubated in media containing adropin for up to 72 hours had elevated vascular endothelial growth factor receptor 2 (VEGFR2) gene and protein expression (8), suggesting that adropin mediates its effects via VEGFR2 signaling. Indeed, silencing and inhibition of VEGFR2 resulted in the abrogation of adropin-stimulated phosphorylation of Akt, eNOS, and MAPK (8).

In the setting of hindlimb ischemia, increased adropin enhanced hindlimb perfusion and capillary density (8). When this was repeated in eNOS knockout mice, blood flow was not restored (8), indicating adropin-induced increased

perfusion and capillary density are mediated through eNOS signaling. In addition to increased perfusion, adropin enhances endothelial-dependent vasodilation in *ex vivo* skeletal muscle resistance arteries of middle- and old-aged subjects (40).

Adropin also mitigated tumor necrosis factor-alpha (TNF- $\alpha$ )-induced activation of apoptotic regulators and inflammatory gene expression in HUVECs (8, 36), thus promoting an anti-inflammatory endothelial cell phenotype. In vascular smooth muscle cells (VSMCs), adropin decreased angiotensin II-induced migration and proliferation (36). Furthermore, exogenous adropin increased fibronectin and elastin protein expression in VSMCs, with these responses being adropin concentration-dependent (36). With low concentrations of exogenous adropin (10ng/ml), fibronectin protein expression was elevated (36). Meanwhile, at high concentrations of exogenous adropin (100ng/ml), elastin protein expression was increased, with no effect on fibronectin protein expression (36). In a model of atherosclerosis, apolipoprotein E knockout (ApoEKO) mice that were administered adropin had decreased the monocyte/macrophage and VSMC content within a plaque and atherosclerotic plaque size (36).

Circulating adropin concentrations are inversely correlated with arterial stiffness (14, 15); however, it has yet to be determined whether adropin directly decreases arterial or vascular cell cortical stiffness. Collectively, adropin mitigates proinflammatory signaling and augments endothelial function, promoting an anti-inflammatory endothelial cell phenotype. Given that arterial stiffening is also associated with a proinflammatory endothelial phenotype and

impaired endothelial function, it could be posited that adropin will be restorative for vascular health.

### Exercise-induced effects on adropin

It has been well documented that exercise improves glucose handling, insulin resistance, and endothelial health (41). Aerobic exercise training increases circulating adropin in obese adolescents (24) and obese elderly subjects (14), healthy middle- and old-aged subjects (15); however, this has not been a consistent finding (42). Zhang et al. (24) utilized a class structure to implement their exercise protocol, with 12 weeks of exercise consisting of aerobic activities with jogging as the preferential form of exercise. In this class setting, exercise intensity was set at 60-80% of maximum heart rate for 90 minutes per session, 3-5 times per week, obese adolescence increased adropin concentrations (24). Meanwhile, Fujie et al (14, 15) used an excise protocol that consisted of cycling for 45 minutes at 60-70% of  $VO_{2peak}$  and a 5-minute warm-up and cool-down period at 40%  $VO_{2peak}$ , for a total session time of 55 minutes, 3 days per week, for 8 weeks. In response to the exercise interventions, adropin concentrations significantly increased by ~1-1.5ng/ml (14, 15, 24). However, Ozbay et al. (42) did not find a difference in adropin concentrations with acute exercise or after 18 weeks of aerobic training in young healthy males.

Aerobic exercise improves many facets of health, including cardiometabolic health. The mechanisms associated with aerobic exercise-induced improvements in cardiometabolic health are multifactorial and not fully

understood. Increases in adropin concentrations may be partially responsible for beneficial cardiometabolic outcomes associated with aerobic exercise training.

### Conclusion

Although investigations into the effects of adropin are still in the early stages, there is increasing evidence that adropin may play a protective role in cardiometabolic health. Adropin has been beneficial in ameliorating endothelial dysfunction associated with increased oxidative stress, i.e. aging. Therefore, it could be posited that in other settings of oxidative stress, adropin may also play a protective role in vascular health. While adropin ameliorates insulin resistance systemically, largely without impacting body mass, the role of adropin has not been fully elucidated in the vascular system. Thus, it is the aim of this proposal to determine the acute and chronic effects of adropin on arterial stiffness.

### Project hypothesis

The hypothesis that adropin plays a direct role in the progression of arterial stiffening associated with obesity and T2D was tested. Specifically, that decreased adropin concentrations, which is associated with obesity and T2D, will induce increased arterial stiffness. Conversely, exogenous adropin will decrease stiffness of arteries of obese T2D mice.

### Innovation

This novel proposal seeks to determine the role that adropin plays in modulating arterial stiffness utilizing *in vitro*, *in vivo*, and *ex vivo* methodologies. Accordingly, this proposal sought to: 1) establish whether adropin decreases

vascular cell cortical stiffness and arterial stiffness; 2) determine if the loss of adropin increases arterial stiffness; and 3) determine if adropin administration can mitigate arterial stiffness associated with T2D in mice.

### Impact

Adropin may be essential for vascular health, with decreased concentrations of circulating adropin being a causal factor for the development of arterial stiffness. Therefore, restoring adropin concentrations may be critical for vascular health.



## CHAPTER 2: Extended Literature Review

### Obesity-associated arterial stiffening

Obesity and insulin resistance are associated with endothelial dysfunction, vascular remodeling, and arterial stiffening (43, 44). Relative to their nonobese counterparts, obese individuals exhibit increased arterial stiffness, and weight loss resulted in increased arterial compliance (45). Epidemiological studies indicate that insulin resistance is an independent risk factor for diabetic vasculopathies, including arterial stiffening (1, 46). Arterial stiffening, which occurs with aging, is accelerated in the setting of obesity and insulin resistance (3, 4, 43, 44) and increased arterial stiffness is an independent risk factor for the development and progression of CVD (1, 47). The non-invasive assessment of arterial stiffness is ascertained by using either 1) the analysis of pulse transit time, 2) the wave contour of the artery pulse, or 3) the direct measurement of arterial geometry and pressure that corresponds to the stiffness of large, conduit arteries (43). Meanwhile, in the presence of obesity and insulin resistance, small resistance arteries, which are  $<300\mu\text{m}$  in diameter and predominately responsible for the regulation of blood pressure and regional blood distribution (48), also exhibit increased arterial stiffening (49-51).

Arterial stiffening associated with obesity and insulin resistance is a multifactorial phenomenon driven by endocrine factors and cytokines that interact with vascular cell components, altering the individual components of arteries, the endothelium, VSMCs, and the extracellular matrix (ECM) (43, 44). This literature

review discusses some of the factors that lead to arterial stiffening and how adropin may play a role in improving vascular health and remodeling in the setting of obesity and insulin resistance.

### Endothelium

The endothelium consists of a single cell lining of endothelial cells along the lumen of blood vessels that plays a central role in the homeostasis of the vasculature by secreting numerous molecules that act in an autocrine, paracrine, and/or endocrine fashion to regulate vascular tone, the proliferation and growth of endothelial and VSMCs, inflammation, leukocyte-endothelial interactions, and permeability (52). Vascular tone is the degree of constriction relative to the maximal dilation and is mediated through vasoactive compounds that either induce vasodilation (e.g. NO, prostaglandins, endothelial-derived hyperpolarizing factor, and eicosatrienoic acids) or vasoconstriction (e.g. angiotensin II (Ang II), endothelin-1 (ET-1), prostanoids, and isoprostanes) (53). In addition to influencing vascular tone, vasodilators such as NO and prostacyclin are antiproliferative and anti-inflammatory. Meanwhile, vasoconstrictors such as Ang II and ET-1 are mitogenic and pro-inflammatory. The balance of these vasoactive molecules determines the vascular tone and endothelial function. In a healthy endothelium, the balance is shifted toward the anti-proliferative and anti-inflammatory. On the other hand, endothelial dysfunction is the maladaptive phenotype of the endothelium in the presence of noxious stimuli that is characterized by decreased NO bioavailability, increased production of adhesion

molecules, elevated expression of pro-inflammatory and pro-thrombotic factors, increased oxidative stress, and abnormal vasoreactivity (54).

Endothelial NO is produced from L-arginine and molecular oxygen ( $O_2$ ), in the presence of cofactors heme, tetrahydrobiopterin ( $BH_4$ ), flavin adenine mononucleotide, flavin adenine dinucleotide, and reduced nicotinamide adenine dinucleotide (NADPH), through the constitutively active enzyme endothelial nitric oxide synthase (eNOS) via  $Ca^{2+}$ -calmodulin-dependent signaling (55). In addition to  $Ca^{2+}$ -dependent activation, eNOS can also be stimulated to produce NO through the phosphorylation of Akt and eNOS Ser<sup>1177</sup>. NO, a soluble gas, diffuses from the endothelium and influences a myriad of cell signaling pathways, including the induction of vasodilation.

Under pathological conditions, eNOS becomes uncoupled from the production of NO and instead produces superoxide. Superoxide rapidly combines with NO to form the reactive nitrogen species peroxynitrite ( $ONOO^-$ ), thereby decreasing the bioavailability of NO. In addition, superoxide and  $ONOO^-$  can oxidize  $BH_4$  to dihydrobiopterin ( $BH_2$ ), limiting an essential cofactor for eNOS-induced NO production (55). Increased  $BH_4$ , either by genetic overexpression or exogenous administration, augments eNOS dimerization and endothelial-dependent vasodilation in conditions when  $BH_4$  concentrations are suboptimal. Therefore, in the dysregulated state eNOS activation produces reactive oxygen species (ROS) rather than NO, thus perpetuating the reduction in bioavailable NO.

In addition to the contributions from eNOS, ROS is produced from several other sources including NADPH oxidase (NOX) and the mitochondria. The four NOX isoforms in the vasculature are NOX1, 2, 4, and 5, all of which are capable of producing superoxide while only NOX4 can produce hydrogen peroxide (H<sub>2</sub>O<sub>2</sub>) (55). In models of insulin resistance, the upregulation of and activation of NOX1 and NOX2 have consistently been reported to be detrimental to vascular health (55). Recently, the role of NOX5 in the setting of insulin resistance has been posited as an emerging avenue of research given its expression in human vascular tissue (56, 57). In human endothelial cell culture models, Ang II, ET-1, and TNF- $\alpha$ , molecules associated with insulin resistance, induced increased mRNA expression of NOX5 (58). Given that rodents do not express NOX5, assessing its role in the endothelium has been challenging. In mice with selective endothelial and VSMC transfection of human NOX5, diabetes augmented NOX5 protein expression and increased extracellular matrix accumulation relative to control diabetic mice (59).

In cultured endothelial cells, NOX1 and NOX2 have been demonstrated to be the predominant isoforms responsible for increased ROS in the vasculature (55). In human aortic endothelial cells, high concentrations of glucose increased NOX2 and NOX4 protein expression (60, 61); while, cultured murine cerebral microvascular endothelial cells exposed to high glucose upregulated NOX1 mRNA and protein expression, but not NOX2 nor NOX4 (62). Thus, indicating that NOX isoform expression may vary throughout the vascular tree.

The predominately expressed NOX isoform in endothelial cells is NOX4 (63), which primarily produces H<sub>2</sub>O<sub>2</sub>. NOX4 is generally considered to be protective of vascular health since H<sub>2</sub>O<sub>2</sub> can promote endothelial-dependent vasodilation (64, 65). However, NOX4 has also been implicated with increased oxidative stress and eNOS uncoupling in response to Ang II (66). Furthermore, NOX4 is the only NOX isoform that is localized to the mitochondria and in the setting of hyperglycemia and diabetes has been associated with increased ROS production (67); which may contribute to ROS-induced ROS production that has been observed in obesity and insulin resistance (68).

#### *Endothelial insulin resistance and endothelin-1 signaling*

Endothelial health is critical in the regulation of stiffness of the vascular system. In healthy endothelial cells, insulin metabolic signaling stimulates the activation of endothelial nitric oxide synthase (eNOS) via insulin receptor substrate-1 (IRS-1)/phosphatidylinositol kinase (PI3K) signaling/Akt-mediated pathway. Concomitantly, the insulin-mediated growth signaling pathway stimulates the activation of mitogen-activated protein kinase (MAPK)/extracellular-regulated kinase 1/2 (Erk 1/2) and results in the production of ET-1. In a healthy endothelium, the net result of these signaling pathways is vasodilation. In the setting of insulin resistance and T2D, the insulin metabolic signaling pathway is diminished resulting in decreased phosphorylation of eNOS, while the insulin growth signaling pathway, i.e., the production of ET-1, is

increased resulting in increased pro-inflammatory and vasoconstriction signaling (69, 70).

In endothelial cells, ET-1 binds to the ET<sub>b</sub> receptors stimulating phospholipase C, which cleaves phosphatidylinositol 4,5-bisphosphate into diacylglycerol (38) and inositol 1,4,5 phosphate (IP<sub>3</sub>), where IP<sub>3</sub> binds to its receptor on the endoplasmic reticulum resulting in the release of Ca<sup>2+</sup>, inducing the Ca<sup>2+</sup>-dependent activation of eNOS and the production of NO (71).

Meanwhile, ET-1 also activates Rho kinase in endothelial cells, which inhibits eNOS activation (71). Furthermore, ET-1 induces the production of superoxide through the activation of NOX5 (72). Collectively, elevated ET-1 signaling associated with insulin resistance may result in decreased NO bioavailability.

#### *Endothelial cell cortical stiffness*

The biophysical properties of endothelial cells are largely due to the cell cortex and the cytoskeletal components. Directly underneath the plasma membrane, a dynamic network of fibers forms a cortical actin web (73) comprised of cross-linked F-actin that provides a supportive structure to the endothelial cell and its intracellular components (73). The regulation of this dynamic cytoskeleton, the assembly/disassembly of actin fibers, is regulated by a variety of actin-binding proteins (74). Actin formation is initiated by the Arp2/3 complex. Additionally, actin is polymerized by Cdc42 and Rac1, members of the Rho GTPase family, and stabilized via cross-linking with proteins such as cortactin, filamin, and fascin (73, 74). Meanwhile, disassembly of the cortical

actin network is induced by cofilin, gelsolin, or RhoA (73, 74). The Rho-Rho associated protein kinase (ROCK) pathway has been implicated in the pathogenesis of metabolic diseases and cardiovascular disease (75). Through the activation of the RhoA-ROCK-LIM kinase pathway, cofilin is phosphorylated, resulting in the inhibition of the cofilin-mediated actin disassembly (75), thereby increasing cortical stiffness (76).

In endothelial cells, a decrease in cell cortex stiffness is associated with increased NO production and release, likely resulting in the facilitation of vasodilation and tissue perfusion (77-79). The mechanism by which a more compliant endothelial cortical stiffness enhances eNOS activation remains to be fully elucidated, with two potential mechanisms posited (80). Firstly, eNOS activity is stimulated by an association with globular actin (G-actin), while it is inhibited by an association with F-actin (81). Increased F-actin depolymerization, thereby decreasing cortical stiffness, may increase the associations between G-actin and eNOS, resulting in the production of NO (82). Secondly, mechanosensitive calcium channels in a more compliant endothelial cell may be more responsive to shear stress, subsequently increasing intracellular  $Ca^{2+}$  concentrations (83-85), resulting in the activation of eNOS via  $Ca^{2+}$ -calmodulin.

In the setting of T2D, endothelial cells are exposed to elevated concentrations of glucose. High glucose concentrations induce increased cortical stiffness and F-actin expression in endothelial cells (86). In addition, high glucose concentrations decreased eNOS expression and thereby the synthesis of NO in endothelial cells (86). Furthermore, the Rho-ROCK pathway has been

implicated in the vascular pathogenesis of diabetes in rats (87-89), which may result in increased endothelial cell stiffness. Collectively, diabetes-induced increases in endothelial cell stiffness result in decreased NO production and bioavailability.

### VSMC stiffness and vascular function

VSMCs are the contractile component of arteries and make up ~25-35% of the arterial volume in large arteries (90). In conduit arteries, VSMCs are partially responsible for buffering the pulsatile pressure exerted on the vessel wall. Therefore, VSMCs play a critical role in the regulation of vascular tone and may contribute to overall vascular stiffness if they exhibit increased cortical stiffness. Indeed, VSMCs from models of arterial stiffness, i.e. hypertension (91, 92) and aging (93) exhibit increased cortical stress with increased F-actin (93, 94).

Similar to aging and hypertension, Western diet-fed and diabetic mice exhibit increased arterial stiffening (51, 95, 96). Furthermore, overnutrition is associated with increased ROCK activation (97), which subsequently stimulates the activation of LIM kinase (LIMK). LIMK regulates the phosphorylation of cofilin, where phosphorylated cofilin is inactive, therefore decreasing the cofilin-mediated severance of F-actin stress fibers. Morales-Quinones et al (76) have reported the inhibition of LIMK prevented the polymerization of actin and arterial stiffening induced by the coincubation of Ang II and norepinephrine in isolated arteries. Additionally, VSMCs treated with vasoconstrictors exhibited increased



F-actin and cortical stiffness, which was mitigated by the addition of a LIMK inhibitor (76). Given that ET-1 has been reported to increase F-actin in human airway smooth muscle cells (98), it could be posited that targeting actin polymerization could be an effective therapy for overnutrition-induced arterial stiffening.

In addition to regulating vascular tone and altering arterial stiffness through cortical stiffness, VSMCs interact with the extracellular matrix through the expression of cell-matrix anchoring proteins called integrins. Integrins are proteins that act as a physical connector between the cytoskeleton and the extracellular matrix, allowing for mechanotransduction of forces to be exerted from the VSMCs to the extracellular matrix and vice versa. Therefore, alterations in integrin expression may play a role in VSMC cortical stiffness, and thereby influence overall arterial stiffness. Indeed, in hypertensive rats, there is an increased protein expression of  $\alpha_5\beta_1$  integrins (99). Furthermore, VSMC treated with either high glucose or angiotensin II exhibited increased  $\alpha_5\beta_3$  integrin protein expression. Given that the  $\alpha_5$  subunit is responsible for the binding to fibronectin (99), increased fibronectin may be linked with increased arterial stiffening. Collectively, this would suggest that integrin protein concentration, specifically the  $\alpha_5$  subunit, plays a role in the progression of arterial stiffening observed in hypertension and diabetes.

## ECM and arterial stiffness

Within the vasculature, the ECM act as the scaffolding providing shape and structure for the artery. The ECM is essential for the arterial wall to withstand the changes in pulse pressure exerted throughout the cardiac cycle. Numerous proteins comprise the ECM, including collagen and elastin, providing rigidity and distensibility to the vessel. Under pathological conditions, the content and composition of these proteins are altered. The ECM from Western diet-fed animals exhibits increased collagen deposition (96, 100, 101). The accumulation of increased collagen deposition is partially mediated through elevated transforming growth factor beta (TGF- $\beta$ ) and increased connective tissue growth factor expression (102). Furthermore, advanced glycosylated end-products (AGEs), which are increased with overnutrition, enhance collagen content through a decreased rate of collagen degradation (3).

In addition to increased collagen content, the architecture of the collagen can influence the stiffness of the ECM (103). Thus, collagen structural composition, through increased cross-links via AGEs and tissue transglutaminase-2 (TG-2), may induce increased stiffness in the artery. AGEs induce collagen crosslinking and stimulate ROS production and decreased eNOS expression resulting in decreased NO bioavailability (104, 105). Moreover, TG-2, an enzyme expressed throughout the vasculature, can induce crosslinking within the ECM (106, 107). The regulation of secretion and function of TG-2 is largely mediated through NO (108). Furthermore, in models of obesity and insulin

resistance, TG-2 expression and activity is increased and plays a causal role in the development of increased arterial stiffening (96, 109, 110).

Concurrent with increased deposition and cross-linking of collagen, the breakdown of elastin content is associated with arterial stiffening (43). The elastic fibers in large, conduit arteries provide reversible deformations under applied hemodynamic loads thereby dampening the pulsatile flow exerted from the contraction of the left ventricle. The upregulation of enzymes associated with the breakdown of elastin, specifically matrix-metalloproteinase (MMP)-2 and MMP-9 are associated with arterial stiffening (43). Increased expression of MMP-9 and MMP-12 have been reported in diabetic models (51, 111), while MMP-2 is downregulated (112). In concert with altered expression of MMPs, tissue inhibitors of matrix metalloproteinases (TIMP) -1 and TIMP-2, which regulate the activity of MMPs, exhibit increased expression in diabetes (51, 113, 114). Therefore, the dysregulation of MMPs and TIMPs indicates dynamic turnover of the ECM in the setting of diabetes resulting in increased arterial stiffening.

Vascular cells are physically connected to the ECM via integrins that are formed at focal adhesions, which allows the forces exerted on one component of the vessel wall to be experienced and exerted on the others. Fibronectin, a critical component for the assembly of other proteins in the ECM, is directly involved in mechanotransduction through adhesions on VSMCs (90). VSMCs attachment to the ECM is partially regulated by vasoactive compounds (115-117), with attachments to fibronectin being mediated through the  $\alpha 5$  integrin

(118). In models of increased arterial stiffness, fibronectin and  $\alpha 5$  integrin expressions are increased (99, 119-121). Furthermore, the phenotype of increased fibronectin and  $\alpha 5$  integrin expression has been demonstrated in vascular tissue in the setting of diabetes and high glucose (122-125). The administration of antihypertensive drugs in hypertensive models has resulted in decreased stiffness in concert with a reduction in fibronectin (126, 127). Collectively, these data indicate that cells respond to mechanical and soluble cues from the local milieu, which impact VSMC mechanical and adhesive properties to the ECM (90).

#### Adropin

Adropin is a circulating peptide that is encoded by the *Enho* gene and expressed mainly in the brain and liver, with expression reported in various tissues including endothelial cells (8, 128). Adropin is a highly conserved peptide across many mammalian models, with homologous sequences present in humans, chimpanzees, macaques, rats, and mice (5). The half-life of circulating adropin has yet to be elucidated, but it has been posited to be within minutes to hours based on the half-life of other, similarly sized circulating peptides (129). Mean concentrations of circulating adropin in healthy adults range from approximately 3.0-6.0ng/ml (16, 99), which is inversely correlated with BMI and age. Circulating adropin concentrations have been reported to be higher in males (21, 29), however, this has not been universally confirmed (28). The receptor by which adropin mediates its biological effects is tissue-dependent and controversial (126, 130). Adropin has been reported to mediate effects via the G

protein-coupled receptor GPR19 in the brain (131), breast cancer cells (132), and cardiac cells (9), but this has not been found universally (133). In the brain, adropin has also been reported to be a membrane-bound protein (134), and signals through the Notch signaling pathway (134, 135). Meanwhile, VEGFR2 was required for adropin-mediated effects in endothelial cells (8). Collectively, the putative receptor for adropin has yet to be fully elucidated and may vary between cell types.

#### Hepatic *Enho* regulation

Hepatic *Enho* mRNA expression is influenced by body composition, energy status, and nutrient intake. In obese mouse models, *Enho* mRNA expression is reduced relative to their lean counterparts (5). Caloric restriction mitigated the reduction of *Enho* mRNA expression in mice prone to obesity (5). Meanwhile, ten-day fasted mice exhibited approximately an 80% reduction in *Enho* mRNA expression relative to chow-fed mice (5). Upon refeeding, there was an increase in *Enho* mRNA expression, with a delayed response corresponding with a low-fat diet (5). The onset of a high-fat diet in lean mice induced an initial increase in *Enho* mRNA expression, with decreased expression following several days on a high-fat diet (5). Interestingly, hepatic *Enho* mRNA expression was elevated following 28 days of high-fat feeding relative to their low-fat diet counterparts (5). Meanwhile, three months of high-fat feeding induced a reduction of hepatic *Enho* mRNA expression (5). Furthermore, a high-fat diet containing high-cholesterol for four months reduced hepatic *Enho* mRNA expression (29). Additionally, hepatic cells treated with cholesterol exhibited

decreased *Enho* mRNA expression (29). Given the initial induction of *Enho* mRNA expression by fat-enriched diets, Kumar et al (5) assessed whether activation of the energy sensor hepatic nuclear lipid nuclear liver X receptor  $\alpha$  (LXR $\alpha$ ) influenced *Enho* mRNA expression. Agonists of LXRs, which stimulate hepatic lipogenesis and storage of triglycerides in adipose tissue, decreased *Enho* mRNA expression in hepatic cells and *in vivo* (5) and therefore are not mediating the of increase *Enho* with acute high-fat diet administration. To date, if there is an energy sensor responsible for the regulation of hepatic *Enho* mRNA expression, it has yet to be elucidated. The temporal effects of consuming a high-fat diet inducing decreased hepatic *Enho* have yet to be determined. Subsequently, *Enho* mRNA expression was determined to fluctuate based on a circadian rhythm and thus may be regulated by the nuclear receptors retinoid-related orphan receptor-alpha/gamma  $\alpha/\gamma$  and Rev-erb (29). Collectively, acute high-fat diet elicits an increase in hepatic *Enho* expression, while cholesterol inhibits it.

Recently, hepatic *Enho* mRNA expression has been reported to be decreased with the loss of ovarian hormones via ovariectomy (136). Subsequently, estrogen-treated liver cells from mice and humans exhibited an increase in *Enho* mRNA expression (136). There is conflicting evidence on whether *Enho* has an estrogen response element near its promoter of *Enho* (136, 137). Given that Stokar et al. (136) intended on assessing biomarkers to alleviate metabolic derangement in postmenopausal women, the influence of estrogen signaling on hepatic *Enho* mRNA expression may be indicative of

differential regulation of *Enho* between the sexes. Interestingly, hepatocytes derived from male, but not female, mice exhibited elevated *Enho* mRNA expression (137). Meda et al. (137) did report an increase in *Enho* mRNA expression in estrogen-treated ovariectomized mice. Despite the role of estrogen signaling in the regulation of hepatic *Enho* mRNA expression, males have higher circulating concentrations of adropin (21, 29, 138), however, this has not been universally reported (28, 139-141). Moreover, Choi et al. (142) have reported that T2D females exhibit higher adropin concentrations than their male T2D counterparts. Collectively, the regulation of hepatic *Enho* mRNA expression mediated by estrogen exhibits a sexual dimorphic, with greater increases in males.

#### Circulating adropin

Circulating adropin concentrations have been reported to be affected by energy status, diet, metabolic health, and exercise training status. Acute low energy status, as seen with an overnight fast, resulted in decreased circulating adropin concentrations relative to chow-fed mice (20). In addition, dietary composition influences circulating adropin concentrations, where consumption of a high-fat diet for 48 hours increased circulating adropin concentrations more than the low-fat diet in mice (20), corroborating the hepatic *Enho* mRNA expression (5). In humans, the macronutrient composition of meals demonstrates similar effects on adropin concentration, with high-fat consumption correlated with an increase in adropin concentrations in women, but not men

(28). Subsequently, an investigation into meals with differing fat composition, medium-chain or long-chain triglycerides, resulted in no alterations in circulating adipon concentrations (143). However, when split into responders, i.e., subjects with a lower baseline concentration of circulating adipon, and non-responders, the responders exhibited an increase in adipon following the medium-chain triglyceride meal (143). Meanwhile, consumption of long-chain triglyceride meals induced a decline in adipon concentrations in the non-responders, i.e., those with a higher baseline adipon (143). Prolonged consumption of Western diet induced increased adiposity and body weight, along with reductions in circulating adipon in mice (144, 145). Given the decreased expression of hepatic *Enho* with cholesterol, it may be proposed that adipon concentrations may also decrease with cholesterol. Indeed, circulating cholesterol, specifically low-density lipoprotein-cholesterol in men, was inversely associated with adipon concentrations (29). Collectively, acute high-fat diet consumption may increase adipon, but the consequences of prolonged high-fat diet will result in decreased circulating adipon.

In addition to the impact of dietary fat on adipon, there is an inverse relationship between carbohydrate consumption and adipon concentrations (138). Moreover, Smith et al. (141) reported increased carbohydrate consumption coupled with decreased physical activity induced a reduction in circulating adipon in males, but not females. Upon further interrogation of the influence of carbohydrate consumption on circulating adipon demonstrated that glucose induced a reduction of circulating adipon, while fructose increased



circulating adipon (143). Moreover, fructose-induced upregulation of adipon was more pronounced in individuals with higher baseline triglyceride concentrations (143).

Several studies have found that adipon concentrations are inversely correlated with BMI and are affected by metabolic diseases (11, 21, 24, 29, 146-148). In line with this notion, patients with metabolic syndrome exhibit decreased adipon relative to their obese, metabolically healthy counterparts (39, 148). Interestingly, in subjects with non-alcoholic steatohepatitis, circulating concentrations of adipon were decreased, despite being classified as lean (149) or overweight (150). In diabetic subjects, adipon concentrations are decreased relative to their metabolically healthy counterparts (27, 146, 151-158). Moreover, lower circulating concentrations of adipon have also been reported with gestational diabetes, both in the mother (18, 26, 159) and in the infant (26, 160). It should be noted that studies assessing diabetes and adipon concentrations have some contradictory findings. While the majority of studies have reported decreased adipon with diabetes, adipon has also been reported to be increased with type I diabetes in rats (18), T2D (161, 162), and gestational diabetes (163). Therefore, despite adipon being posed as a marker of obesity, it may be more accurate to associate decreased adipon concentrations as a biomarker for metabolic impairment.

### Weight loss and adropin

Given that adropin is inversely associated with BMI, it could be posited that weight loss may induce an increase in adropin concentrations. Subjects that achieved a 6-8% reduction in body weight did not alter circulating adropin concentrations (138). Upon further analysis, baseline adropin concentrations were divided into quartiles of baseline adropin and assessed for changes post-intervention. Following weight loss, the subjects that had the highest concentrations of adropin exhibited a reduction in adropin after weight loss, while the three lower quartiles had no change in the weight-loss intervention (138). Similarly, mice that underwent weight loss due to caloric restriction for four weeks had decreased adropin concentrations (164). Meanwhile, lifelong caloric restriction increased adropin relative to *ad libitum*-fed mice (164). While a modest reduction in body weight did not alter adropin concentrations, subjects that had bariatric surgery exhibited increased adropin at three- and six-months post-operation (21, 23). It should be noted that one year after bariatric surgery adropin concentrations returned to baseline despite the continued reduction in BMI (21).

### Exercise and adropin

It has been well documented that exercise exerts significant physiological adaptations that improve cardiometabolic health. A single bout of aerobic exercise, at approximately 60-80% maximal heart rate for up to 90 minutes, did not elicit a significant alteration in adropin (24, 42, 165). Furthermore, seven

days of exercise training, 1 hour/day at 60% heart rate reserve, was not sufficient to impact adipon concentrations (138). It should be noted that seven days is not sufficient to alter body composition and training adaptations that occur with chronic exercise training (166).

In professional soccer players, adipon concentrations did not change throughout the year, regardless of whether they were in pre-season or in-season (167). Meanwhile, in young, healthy, male volleyball players, eight weeks of a combination of aerobic, plyometric, and resistance training increased adipon (168). Following six weeks of swimming, rats demonstrated an increase in hepatic and pancreatic *Enho* mRNA expression, however, no circulating adipon concentrations were reported (169). The controversial findings of the impact of exercise training on adipon concentrations may be explained in part by a ceiling effect in professional athletes, whereas collegiate athletes may still have some responsiveness to exercise training.

In sedentary and moderately active individuals, adipon concentrations were correlated with peak volume of oxygen consumption ( $VO_{2peak}$ ) (15), indicating that training status influences adipon concentration. In healthy, middle-aged and older subjects, eight-weeks of aerobic cycle ergometer training for 55 minutes 3 days/week at 60-70%  $VO_{2peak}$ , increased adipon concentrations, despite no influence on BMI (15). Subsequently, Fujie et al. (14, 170) utilized the same protocol in obese and elderly subjects to elicit a reduction in body fat percentage in concert with increased adipon concentrations. In aged, senescence-accelerated prone mice, voluntary wheel running was

sufficient to elevate adropin concentrations to levels comparable to young, mature counterparts (170). In old rats, aerobic exercise via 15-30 minutes of treadmill running at 65-70% maximal speed, elevated adropin concentrations (25). Furthermore, old rats that underwent high-intensity interval training of 5-8 two-minute intervals at 80-100% maximal speed separated by two-minutes of active recovery at 50-60% maximal speed, increased adropin relative to the control and continuous exercise counterparts (25). Collectively, aerobic exercise increases adropin in aged models.

In obese adolescents with reduced adropin, 12 weeks of aerobic training performed three-five days per week for 90 minutes per session with heart rate controlled to 60-80% of maximal heart rate ( $HR_{max}$ ) significantly decreased BMI and increased adropin concentrations (24). Furthermore, adropin was no longer different than the control group despite a higher BMI (24). Likewise, middle-aged T2D subjects also demonstrated an increase in adropin following 12 weeks of moderate-intensity continuous exercise intervention consisting of cycling for 42 minutes at 70%  $HR_{max}$  (140). While continuous moderate-intensity exercise elicited an increase in adropin, high-intensity interval training, consisting of 12 1.5-minute intervals of 85-90%  $HR_{max}$  separated by 2 minutes of active recovery at 55-60%  $HR_{max}$ , induced a more robust increase in adropin concentrations in T2D subjects (140). In diet-induced non-alcoholic steatohepatitis mice, aerobic exercise training via treadmill run at 75% maximal volume of  $O_2$  ( $VO_{2max}$ ) 5 days per week for either 8- or 12-weeks increased hepatic *Enho* expression and circulating adropin concentrations in concert with reduced body weight (145).

To date, the effects of resistance exercise training on adropin concentrations have not been assessed. Chen et al. (171) performed a 12-week stair walking protocol designed to compare concentric-focused vs eccentric-focused exercise, ascending stair walking vs descending stair walking, respectively. Older, obese women that ascended the stairs did not exhibit altered adropin concentrations, whereas subjects that descended the stairs increased adropin (171). Notably, eccentric contractions can undergo higher mechanical tension and promote skeletal muscle anabolic signaling to a greater extent than concentric contractions (172), however, the mechanism by which adropin is augmented during eccentric contractions remains to be elucidated. Collectively, aerobic exercise may be utilized as a therapeutic intervention to increase adropin concentrations.

#### Adropin-mediated regulation of adiposity, lipid and glucose metabolism

Alterations in adropin concentrations associated with decreased body weight and exercise would indicate that adropin may be playing a role in the regulation of metabolism. In mice fed a high-fat diet for 6 weeks, systemic transgenic overexpression of adropin protected against weight gain, specifically through decreasing accumulation of fat mass (5). Furthermore, there was less accumulation of liver triglycerides and decreased expression of fatty acid metabolizing genes in the liver and adipose tissue in mice with adropin overexpression (5). It should be noted that the protection against high-fat diet-induced weight gain in transgenic adropin mice was lost with the consumption of

a high-fat diet for 6-7 months. Meanwhile, in AdrKO mice, consumption of a high-fat diet for 9 weeks, but not 6-8 weeks, increased adiposity, despite not having differing body weights from their wild-type counterparts (20).

Consumption of a high-fat diet for 8 weeks was sufficient to induce increased fasting triglycerides in AdrKO mice, despite no change in body weight or composition (20). AdrKO mice also demonstrated increased hepatic lipid and triglyceride content following a high-fat diet, coinciding with an increase in hepatic lipogenic gene expression (20). In a fed state, AdrKO mice had an increase in whole-body substrate utilization that was shifted toward the preferential use of fats oxidation, with elevated fatty acid oxidation occurring in skeletal muscle lysates (30). Meanwhile, in a fasted state, the overexpression of adropin resulted in a whole-body substrate utilization shift toward increased carbohydrate utilization, with decreased fatty oxidation observed in skeletal muscle lysate (30). Taken together, adropin participates in the regulation of fat metabolism and storage.

In addition to the regulation of lipid metabolism, adropin influences glucose metabolism. Chow-fed, AdrKO mice exhibited hyperinsulinemia and hyperglycemia but were not glucose intolerant (20). Interestingly, following a hyperinsulinemic-euglycemic clamp, AdrKO chow-fed mice had a diminished glucose infusion rate, and attenuated suppression of endogenous rate of glucose appearance, despite intact hepatic insulin signaling (20). Furthermore, glucose uptake in AdrKO mice was not significantly different in the brain, adipose, or cardiac tissue, but was reduced in the gastrocnemius and diaphragm (20),

indicating that loss of adropin may be leading to impairments in skeletal muscle glucose uptake. When challenged with a high-fat diet, heterozygote carriers for the adropin allele (AdrHet) and AdrKO mice had a graded increase in fasting insulin and glucose concentrations, along with the homeostatic model of insulin resistance (HOMA-IR) relative to wild-type counterparts (20). Diminished adropin, regardless of expression, i.e., AdrHet and AdrKO mice, exhibited glucose and insulin intolerance (20). These results indicate that reductions in adropin concentrations exacerbate insulin resistance associated with diet-induced obesity. Therefore, exogenous adropin treatment may improve insulin and glucose tolerance in conditions associated with decreased adropin. Indeed, three days of adropin treatment in DIO mice resulted in improved fasting insulin and glucose concentrations, HOMA-IR, and insulin and glucose tolerance without altering body weight (32, 33). Furthermore, whole-body substrate carbohydrate utilization and skeletal muscle insulin sensitivity, specifically phosphorylation of Akt and translocation of glucose transporter 4 to the membrane, were augmented following adropin administration in DIO mice (32). Interestingly, Thapa et al. (33) found that during a hyperinsulinemic-euglycemic clamp that skeletal muscle, specifically the gastrocnemius and quadriceps, did not exhibit an increase in glucose uptake. Notably, adropin administration to high-fat diet-fed mice resulted in a reduction of whole-body glucose uptake due to decreased hepatic endogenous glucose production (33). This would indicate that adropin increases hepatic insulin sensitivity. In addition to improving skeletal muscle insulin sensitivity, adropin administration augments liver insulin sensitivity and

suppresses hepatic glucose production and endoplasmic reticulum stress (31). Furthermore, adropin administration increased cardiac insulin sensitivity and efficiency, and glucose oxidation (173, 174). Therefore, adropin administration presents an exciting potential therapeutic tool to improve obesity-associated insulin resistance and impaired glucose homeostasis.

### Cardiovascular disease and adropin

Circulating concentrations of adropin have been inversely related to age and metabolic dysfunction, which are causal factors in the development of endothelial dysfunction and cardiovascular disease. Adropin concentrations are related to endothelial function (10, 170), therefore adropin may represent an early biomarker for the progression of various cardiovascular diseases. Indeed, decreased adropin is associated with coronary artery disease (175), acute myocardial infarction (13, 176), coronary atherosclerosis (27), and cardiac syndrome x (177). Furthermore, adropin is inversely associated with increased arterial stiffness (14, 15, 170) and is reduced in patients with hypertension (38) and hypertensive pregnant women (178); however, this has not been universally reported (179). Taken together, decreased adropin may be utilized as a biomarker for the development of cardiovascular disease and cardiovascular-associated complications.



## Endothelial cell function and adropin

Adropin is inversely associated with many casual factors associated with the progression and development of cardiovascular disease, therefore it may mediate effects on vascular cells, specifically endothelial cells and vascular smooth muscle cells. Lovren et al. (8) were the first to report that adropin influenced endothelial function. Endothelial cells stimulated with adropin had increased proliferation, tube formation, and enhanced endothelial barrier (8). In addition, adropin attenuated monocyte adhesions (36, 180) and tumor necrosis factor- $\alpha$  induced apoptosis in endothelial cells (8), indicative of adropin promoting an anti-inflammatory role in the vasculature. Furthermore, adropin reduced endothelial cell permeability (181, 182), which is mediated through the ROCK-myosin light chain 2 (MLC2) pathway (182). Furthermore, adropin stimulates the activation of Akt, Erk1/2, and eNOS kinases through VEGFR2, resulting in the production of NO. Adropin, therefore, may help improve the function of the endothelium.

Due to the evidence that adropin exerts vasoactive effects, including the production of NO, adropin may also induce vasodilation. In isolated human skeletal muscle feed arteries, adropin protein content diminished with age (40). The presence of adropin restored flow-mediated as well as acetylcholine-induced, endothelial-dependent, vasodilation in arteries from middle-aged and old subjects, but not young arteries, in a NO-dependent manner (40). Interestingly, adropin increased the phosphorylation of eNOS in isolated middle-aged and old skeletal muscle feed arteries, but not in young arteries (40).

Despite the previously reported adropin-induced production of NO (8), Kwon et al. (40) did not assess whether adropin was a vasodilator in a pressurized artery. However, Fujie et al. (170) have reported adropin to be a vasodilator. Further, adropin induced approximately 50% vasodilation in the aorta of mature, male senescence-accelerated prone mouse 1 (SAMP1) mice. Adropin-induced vasodilation was blunted in aged mice, but the vasodilatory effects of adropin were restored with exercise training (170). The addition of N $\omega$ -nitro-L-arginine methyl ester (L-NAME) significantly decreased adropin-induced vasodilation regardless of age and exercise training. It should be noted that despite the addition of L-NAME, adropin provoked vasodilation of approximately 15% in the aorta, indicative of NO-independent vasodilation (170).

#### VSMCs and adropin

In addition to the role played in endothelial health, adropin has been reported to have direct effects on VSMCs. In VSMCs, adropin attenuated angiotensin II-induced cell migration and proliferation via regulation of the adenosine monophosphate-activated protein kinase/acetyl-CoA carboxylase signaling pathway (36, 183). Furthermore, adropin suppressed angiotensin II-induced phenotypic modulation of VSMCs. In VSMCs, adropin increased protein expression of fibronectin and elastin, likely through the activation of the Akt pathway, in concert with the downregulation of the Erk1/2 pathway (36). Sato et al. (36) posited that increased fibronectin and elastin may contribute to plaque stability and elasticity of arteries. Furthermore, adropin-induced increased B-cell

lymphoma 2 (BCL2) in concert with reductions in Bcl2-associated X protein 4 (BAX) protein content, which may reduce the apoptotic pathway in VSMCs (36). Notably, Sato et al. (36) did not report the ratio of BCL2/BAX, nor did they stimulate the apoptotic pathway to determine if adropin mitigates VSMC apoptosis. Therefore, adropin may play a role in limiting the phenotypic switching of VSMCs associated with increased inflammation.

#### *In vivo* cardiovascular effects of adropin

Cardiovascular diseases have been inversely associated with circulating concentrations of adropin, therefore providing an avenue to pursue a potential role of adropin within the cardiovascular system. Adropin, which increases endothelial cell proliferation and tube formation, was assessed for any physiological functions following unilateral hindlimb ischemia. Mice injected with an adropin plasmid following unilateral hindlimb ischemia had increased capillary density and leg blood flow relative to their untreated counterparts (8). When reassessed in mice lacking eNOS, there was no increase in leg blood flow following adropin administration (8), suggesting that adropin-mediated increases in capillarization and leg blood flow are eNOS dependent. In addition, adropin protects against vascular calcification in rats (183). The calcification of the vasculature is associated with the transdifferentiation of VSMCs into osteoblast-like cells and an increased risk of atherosclerotic plaque ruptures (180). Adropin inhibited the osteogenic transdifferentiation in VSMC (183). In ApoE knockout mice, a model of atherosclerosis, adropin decreased atherosclerotic lesion size,

reduced aortic monocyte/macrophage infiltration, and decreased VSMC proliferation (36). In healthy mice, three days of adropin administration exerted a moderate improvement on ex vivo cardiac work and output, in addition to increased coronary blood flow (173, 184); however, a high-fat diet inhibited adropin-induced cardiac function observed in the lean mice (184). Similar to skeletal muscle and the liver, adropin treatment improved insulin signaling and glucose utilization in cardiomyocytes from healthy mice and modulate substrate utilization (173, 184).

Given that adropin is associated with decreased endothelial cell permeability (181, 182), adropin may be utilized to augment the blood-brain barrier integrity. Indeed, adropin reduced the infarct size, oxidative damage, and neutrophil infiltration following an intracerebral ischemic event, in an eNOS-dependent manner (185). Meanwhile, in an intracerebral hemorrhage mouse model, adropin attenuated the hematoma volume via activation of the Notch 1 signaling pathway (135). Furthermore, a bolus of adropin induced a 30% increase in cerebral blood flow in healthy mice (185). Collectively, the vascular protective effects induced by adropin justify further investigations into its potential as a therapeutic intervention in the prevention of and in cardiovascular diseases.

# CHAPTER 3: Role of Adropin in Arterial Stiffening Associated with Obesity and Type 2 Diabetes

Thomas J. Jurrissen<sup>1,2</sup>, Francisco I. Ramirez-Perez<sup>3</sup>, Francisco J. Cabral-  
Amador<sup>3</sup>,

Rogério N. Soares<sup>3</sup>, Ryan J. Pettit-Mee<sup>1</sup>, Edgar E. Betancourt-Cortes<sup>3</sup>, Neil J.

McMillan<sup>1</sup>, Neekun Sharma<sup>3</sup>, Helena N. M. Rocha<sup>2,4</sup>, Shumpei Fujie<sup>2,5</sup>,

Mariana Morales-Quinones<sup>3</sup>, Yoskaly Lazo-Fernandez<sup>3</sup>, Andrew A. Butler<sup>6</sup>,

Subhashis Banerjee<sup>6</sup>, Harold S. Sacks<sup>7</sup>, Jamal A. Ibdah<sup>8,9</sup>, Elizabeth J. Parks<sup>1,9</sup>,

R. Scott Rector<sup>1,8,9</sup>, Camila Manrique-Acevedo<sup>2,8,10</sup>, Luis A. Martinez-Lemus<sup>2,3,11</sup>,

Jaume Padilla<sup>1,2,8</sup>

## **Affiliations:**

<sup>1</sup>Department of Nutrition and Exercise Physiology, University of Missouri,  
Columbia, MO, USA

<sup>2</sup>Dalton Cardiovascular Research Center, University of Missouri, Columbia, MO,  
USA

<sup>3</sup>Center for Precision Medicine, Department of Medicine, University of Missouri,  
Columbia, MO, USA

<sup>4</sup>Department of Physiology and Pharmacology, Fluminense Federal University,  
Niteroi, Brazil

<sup>5</sup>Faculty of Sport and Health Science, Ritsumeikan University, Shiga, Japan

<sup>6</sup>Department of Pharmacology and Physiological Sciences, Saint Louis University, Saint Louis, MO, USA

<sup>7</sup>Department of Medicine, David Geffen School of Medicine at UCLA, Los Angeles, CA, USA

<sup>8</sup>Harry S. Truman Memorial Veterans' Hospital, Columbia, MO, USA

<sup>9</sup>Division of Gastroenterology and Hepatology, Department of Medicine, University of Missouri, Columbia, MO, USA

<sup>10</sup>Division of Endocrinology and Metabolism, Department of Medicine, University of Missouri, Columbia, MO, USA

<sup>11</sup>Department of Medical Pharmacology and Physiology, University of Missouri, Columbia, MO, USA

**Running title:** Role of adropin in arterial stiffening

**Key words:** Adropin, nitric oxide, endothelial cells, smooth muscle cells, mesenteric arteries, liver

**Published in:** Jurrissen, Thomas J et al. "Role of adropin in arterial stiffening associated with obesity and type 2 diabetes." *American journal of physiology. Heart and circulatory physiology* vol. 323,5 (2022): H879-H891.

*Heart and circulatory physiology* vol. 323,5 (2022): H879-H891.

doi:10.1152/ajpheart.00385.2022

## INTRODUCTION

Stiffening of the vasculature, a feature of obesity and type 2 diabetes (T2D), is a causal factor and independent prognosticator of cardiovascular morbidity and mortality (47, 186, 187). Despite the indisputable recognition that arterial stiffening contributes to the pathogenesis of cardiovascular disease, the mechanisms underlying arterial stiffening remain largely unknown.

Adropin is a highly conserved 76-amino acid peptide encoded by the Energy Homeostasis Associated (*i.e.*, Enho) gene and is heavily expressed in the liver, where it was first identified approximately 15 years ago (5). Adropin plays a role in maintaining energy balance and regulating lipid and glucose metabolism (5, 20, 31). Beyond its well-established metabolic effects, increasing evidence indicates that adropin also exerts cardiovascular effects. For example, adropin has been shown to regulate cardiac energy substrate flexibility (9, 173, 174, 184), promote angiogenesis (8), decrease endothelial inflammation (8, 36), activate endothelial nitric oxide (NO) synthase (eNOS) (8), and cause endothelial-dependent vasodilation (170). All this suggests that adropin signaling may be beneficial to the cardiovascular system.

Data are also available indicating that circulating levels of adropin are depressed in various chronic diseases associated with arterial stiffening and cardiovascular disease, including obesity and T2D (10, 11, 21, 27, 39, 40, 148-150, 154, 158, 188-190) (reviewed in (16, 130, 191)). Herein, we first confirmed

that severity of obesity and T2D inversely associate with hepatic mRNA expression of adropin in a cohort of male and female patients that underwent liver tissue sampling during bariatric surgery. In a separate cohort, we also corroborated that low circulating levels of adropin in individuals with T2D are associated with increased arterial stiffness. The phenomenon that circulating levels of adropin are reduced in disease states characterized by arterial stiffening and are inversely correlated with indices of arterial stiffness prompted the hypothesis that diminished levels of adropin may contribute to the development of arterial stiffening in obesity and T2D. To begin to address this hypothesis, we tested whether adropin deficiency in mice causes arterial stiffening, thus phenocopying obesity and T2D. Furthermore, we posited that the converse is also true; that is, adropin exposure de-stiffens the vasculature in obese T2D mice. Mechanistically, we examined the role of NO signaling in mediating the vascular de-stiffening effects of adropin.

## **METHODS**

### **Ethics and approvals**

All human study procedures conformed to the Declaration of Helsinki and were approved by the University of Missouri Institutional Review Board (IRB, no. #2008181, #2012106, #2028142, and #2008258). Written informed consent was obtained from all subjects prior to any procedures. All animal study procedures received prior approval by the University of Missouri Institutional Animal Care



and Use Committee and were conducted in accordance with the National Institutes of Health Guide for the Care and Use of Laboratory Animals.

### **Cohort of bariatric surgery patients**

Forty-five female and male patients with clinical obesity (36F/9M,  $46.3 \pm 2.0$  years of age,  $BMI = 48.3 \pm 1.1 \text{ kg/m}^2$ ,  $HbA1c = 6.5 \pm 0.2\%$ ) that underwent elective bariatric surgery with liver tissue sampling at the University of Missouri Hospital, as part of a larger study (192), and from whom we had liver mRNA available, were included in this retrospective analysis. Specifically, subjects were segregated into fixed clusters according to their BMI and HbA1c values ( $\leq 40 \text{ kg/m}^2$  or  $> 40 \text{ kg/m}^2$  and  $< 6.5\%$  or  $\geq 6.5\%$ , respectively). A BMI above  $40 \text{ kg/m}^2$  is considered severe obesity and an HbA1c of 6.5% or higher is indicative of diabetes. Mean values of hepatic adropin mRNA expression are reported on the z-axis of a three-dimensional histogram.

### **Cohort of healthy and T2D individuals**

Forty-two individuals with a clinical diagnosis of T2D and confirmed  $HbA1c \geq 6.5\%$  (21F/21M,  $56.1 \pm 1.6$  years of age,  $BMI = 35.5 \pm 0.9 \text{ kg/m}^2$ ,  $HbA1c = 8.1 \pm 0.2\%$ ), along with thirty-three aged-matched healthy controls (20F/13M,  $51.8 \pm 1.9$  years of age,  $BMI = 23.3 \pm 0.4 \text{ kg/m}^2$ ,  $HbA1c = 5.2 \pm 0.1\%$ ), and from whom we either had fasting plasma available, data on carotid-to-femoral pulse wave velocity (PWV), or both, were included in this retrospective analysis.

Subjects were free of overt cardiovascular, hepatic, and autoimmune diseases, cancers, tobacco use, excessive alcohol consumption (>14 drinks/week for men, and >7 drinks/week for women), pregnancy, and uncontrolled hypertension ( $\geq 180$ mmHg systolic, or  $\geq 110$ mmHg diastolic). It should be noted that a small subset of these participants was included in a previous publication examining an unrelated question (*i.e.*, the effects of chronic heating on metabolic and vascular outcomes (193)). Participants were admitted to the laboratory after an overnight fast for a blood draw, anthropometric measures, and assessment of arterial stiffness. Participants rested supine for 15 minutes prior to the assessment of arterial stiffness via carotid-to-femoral PWV using the cuff-based SphygmoCor XCEL system (AtCor Medical, Itasca, IL), according to current recommendations (47, 194) and as previously described (195). The SphygmoCor XCEL device enables the simultaneous acquisition of carotid and femoral pulse waves, via tonometer and leg cuff, respectively. Transit time between carotid and femoral pressure waves was calculated with the foot-to-foot method. Wave foots were identified using intersecting tangent algorithms. PWV was calculated as distance traveled by the pulse wave divided by pulse transit time and reported as meters per second.

### **Mouse models**

Leptin receptor deficient homozygous (db/db) and heterozygous (db/+) male mice were purchased from The Jackson Laboratory (Bar Harbor, MA). Adropin knockout male mice and wild-type littermates were obtained from Saint

Louis University. This mouse model has been previously described in detail by Kumar *et al.* (20). All mice were group housed (n=2-5) with *ad libitum* access to chow (3.35 kcal/g food, Laboratory Rodent Diet 5001\*, Laboratory Diet (196)) and water. Mice were housed in an environmentally controlled animal facility maintained at 23°C on a 12:12-hour light:dark cycle from 0700 to 1900 hours.

### ***In vivo* adropin administration**

Nine-week-old db/db mice were assigned to two groups, using block randomization to balance initial body weight, and infused with either vehicle (phosphate-buffered saline, PBS, n=7) or adropin (63µg/kg/hour, n=12, NovoPro, #314322, Shanghai, China) for four weeks using an osmotic minipump (Alzet Model 2001; Durect, Cupertino, CA). Pumps were implanted subcutaneously into the dorsum and replaced after two weeks under isoflurane anesthesia, as previously described (197).

### ***Ex vivo* treatments in isolated mesenteric arteries**

Small mesenteric arteries were selected as the model of choice for this project because 1) they are considered resistance arteries and thus contribute to the regulation of blood pressure; 2) multiple arteries of the same size can be isolated from a single animal and exposed to different experimental conditions, thus allowing for paired analyses; 3) it is a non-sex specific vascular bed extensively utilized across animal models (48). To determine the impact of adropin on stiffness in diabetes, mesenteric arteries were excised from db/db

mice, cleaned of perivascular adipose and connective tissue, and flushed of blood. Two mesenteric arteries per animal were then incubated with VascuLife EnGS (Lifeline Cell Technology, Frederick, MD) culture media (2% FBS) under standard culture conditions (37°C, 5%CO<sub>2</sub>) and treated with vehicle (ddH<sub>2</sub>O) vs. adropin (10ng/mL, Phoenix Pharmaceuticals, Burlingame, CA) for 24 hours. To assess the role of NO in mediating adropin effects, the experiment above was repeated with co-treatment of NG-nitro-L-arginine methyl ester (L-NAME, 300μM) in mesenteric arteries isolated from separate db/db mice. L-NAME was added 30 minutes prior to vehicle or adropin. To examine the direct effect NO signaling on arterial stiffness, mesenteric arteries from db/db mice were cannulated in a pressure myography chamber (Living Systems Instruments, St. Albans City, VT). After corroborating that the vessels had no leaks, arteries were pressurized at 70mmHg and incubated in physiological salt solution (PSS) containing (in mM): 145.0 NaCl, 4.7 KCl, 2.0 CaCl<sub>2</sub>, 1.2 MgSO<sub>4</sub>, 1.0 NaH<sub>2</sub>PO<sub>4</sub>, 5.0 dextrose, 3.0 3-(N-morpholino) propanesulfonic acid (MOPS) buffer, 2.0 pyruvate and 0.02 EDTA at pH of 7.4 at 37°C containing either vehicle or sodium nitroprusside (SNP, 10μM, Sigma-Aldrich, BCCB2459) for four hours. After incubation, treated arteries underwent mechanical testing under passive conditions to assess arterial stiffness, as described below. As a point of clarification, isolated arteries treated with adropin for 24 hours were kept in the incubator under standard culture conditions to ensure viability. Given the shorter half-life of SNP (198), arteries were only treated with SNP for four hours and kept viable in the pressure

myography chamber set at the bench. Maintaining the vessels pressurized provides greater cytoskeletal dynamics.

### ***Ex vivo* assessment of arterial stiffness in isolated mesenteric arteries**

Mesenteric arteries were assessed for stiffness under passive conditions. Briefly, cleaned mesenteric arteries were cannulated and pressurized to 40mmHg for 40 minutes in PSS at 37°C to acclimate prior to mechanical testing. After the 40-minute acclimation period, the bath was replaced with Ca<sup>2+</sup>-free PSS and arteries were exposed to increasing intraluminal pressure from 5 to 120mmHg with a stepwise increase in intraluminal pressure maintained for two minutes to achieve diameter and wall thickness plateaus. Diameter and wall thickness curves were utilized to calculate the circumferential strain and stress, and from them the incremental modulus of elasticity ( $E_{inc}$ ), as previously reported (96). After mechanical testing, arteries were fixed with 4% paraformaldehyde (PFA) at 70mmHg for 30 minutes for further wall composition experiments.

### **Confocal microscopy imaging of isolated mesenteric arteries**

The amount of nuclear material and filamentous-actin (F-actin) were measured in fixed db/db mesenteric resistance arteries after mechanical testing. Briefly, fixed mesenteric arteries were cannulated, permeabilized, and incubated in Syto 63 (250nM, Thermo Fisher Scientific, Cat. No. S11345) and Alexa Fluor 546 phalloidin (200nM, Thermo Fisher Scientific, Cat. No. A22283) for one hour at room temperature in PBS and subsequently washed with PBS. Images of

nuclei and F-actin were obtained using a Leica SP5 confocal-multiphoton microscope with a 63X water immersion and 1.2 numerical aperture objective (Leica Microsystems, Inc., Morrisville, NC). Imaris software (Bitplane, Inc., Concord, MA) was used to render three-dimensional reconstructions. An unbiased Matlab script was utilized to quantify the volume of the molecules of interest (76). Volumetric data were normalized to the volume of nuclei.

### **Whole blood and plasma analysis**

Assessment of HbA1c in humans was performed at the University of Missouri Diabetes Diagnostic Lab or at Quest Diagnostics, Columbia MO. Mouse HbA1c and plasma concentrations of glucose, insulin, total cholesterol, non-esterified fatty acids (NEFAs), were assessed at the University of California Davis Mouse Metabolic Phenotyping Center. Human and mouse plasma adropin concentrations were determined via a commercially available enzyme immunoassay per the manufacturer instructions (Phoenix Pharmaceuticals, Burlingame, CA).

### **Cell culture experiments**

Human aortic endothelial cells (Lonza: #CC-2535, Morristown, NJ) were obtained and cultured under standard culture conditions in Vasculife EnGS culture media (2% FBS) and treated with vehicle (ddH<sub>2</sub>O) vs. adropin (10ng/mL) for 24 hours in the presence or absence of L-NAME (300μM). L-NAME was added 30 minutes prior to vehicle or adropin. Endothelial cells used for

immunohistochemical imaging were seeded on 15-well-ibidi plates (Ibidi, Cat No. 81506, Fitchburg, WI). Cells used for Western blotting and atomic force microscopy (AFM) analyses were seeded on 60-mm cell culture dishes. Cells used for nitrite analysis were seeded on 6-well cell culture dishes.

Human coronary artery smooth muscle cells (Thermo Fisher Scientific, #C0175C, Waltham, MA) were obtained and cultured under standard culture conditions in Medium 231 (Thermo Fisher Scientific, #M231500), with 5% FBS; with smooth muscle cell supplements (Thermo Fisher Scientific, #S-007-25) and treated with vehicle (ddH<sub>2</sub>O) vs. SNP (10 $\mu$ M) for one hour. To further examine the effects of NO signaling on actin polymerization, the experiment above was repeated with co-treatment of LIM kinase inhibitor 3 (10 $\mu$ M, LIMKi, Calbiochem, #435930, San Diego, CA) or jasplakinolide (100nM, Thermo Fisher Scientific). LIMKi and jasplakinolide were used to inhibit and force actin polymerization, respectively. LIMKi and jasplakinolide were added 30 minutes prior to vehicle or SNP. Cells used for immunohistochemical imaging were seeded on 15-well-ibidi plates. Cells used for AFM were seeded on either 40-mm or 60-mm cell culture dishes.

### **Measurement of nitrite in cell culture supernatant**

Nitrite, a by-product of NO, was assessed using the gold-standard method of ozone-based reductive chemiluminescence (CLD88, Eco Physics, Ann Arbor, MI) according to the manufacturer recommendations and as previously described (199-201). Briefly, endothelial cell supernatant samples (50 $\mu$ L) were injected in

duplicate into a purge vessel containing an acidified iodide solution serving as a nitrite reducing agent (50mg potassium iodide dissolved in 1mL filtered ddH<sub>2</sub>O with 4mL glacial acetic acid), which was then purged with pure nitrogen in line with the CLD88 gas-phase NO analyzer. The chemiluminescence signal was captured using eDAQ Chart™ v5.5.27 and NO<sub>2</sub>- was quantified using the Flow Injection Analysis (FIA) software extension (ADInstruments, Australia). The FIA software calculated area under the curve for each sample peak which was then converted to a concentration using a calibrated standard curve of known sodium nitrite (NaNO<sub>2</sub>) and normalized to protein content using the bicinchoninic acid protein assay.

### **Vascular cell cortical stiffness**

Cultured endothelial and smooth muscle cells were assessed for cortical stiffness via AFM. Briefly, individual cells were exposed to nano-indentation at room temperature using a silicon nitride cantilever (Bruker, #MLCT, Billerica, MA) on either a MFP-3D Atomic Force Microscope (Asylum Research Inc., Goleta, CA) mounted on an Olympus IX81 microscope (Olympus Ins., Tokyo, Japan) or a NanoWizard IV Atomic Force Microscope (Bruker, JPK) mounted on a Leica DMI8 automated microscope (Leica Microsystems, Inc., Morrisville, NC). At least 40 force curves were obtained from each cell at a location of approximated 1/3 the distance from the edge of the cell to the nucleus, with seven cells assessed per dish. Elastic moduli were calculated from the force curves using a custom-made Python script that, in an unbiased manner, identifies and removes curves



with excessive noise and the remaining curves are fitted to the Hertz model, as previously described (76).

### **Immunohistochemical imaging of endothelial and smooth muscle cells**

Immunohistochemical images of endothelial and smooth muscle cells were obtained from cells plated on 15-well-ibidi plates. After incubation with the respective treatments, cells were fixed in 4% PFA at room temperature for 30 minutes and permeabilized with 0.5% Triton X-100 for 15 minutes. Cells were incubated for one hour in 1.5nM 4',6-diamidino-2-phenylindole (DAPI) and 200nM Alexa Fluor 563 phalloidin (Thermo Fisher Scientific, A12380) to stain for nuclei and F-actin, respectively. Images were acquired with either a Leica SPE confocal microscope (endothelial cells, Leica Microsystems, Inc.) or Leica THUNDER Imager 3D Cell Culture microscope (smooth muscle cells, Leica Microsystems, Inc.). Fluorescence intensity was quantified using Imaris software (Bitplane Inc. Concord, MA) and normalized by the total number of cells. Values are expressed as fold difference.

### **Adropin mRNA expression via RT-PCR**

Samples from mice and humans were processed to assess expression of *Enho*, the gene encoding adropin. Tissues were homogenized in TRIzol reagent (TissueLyser LT, Qiagen, Valencia, CA) and total RNA was isolated using Qiagen's RNeasy lipid tissue protocol and assayed using a Nanodrop spectrophotometer (Thermo Fisher Scientific) to assess purity and concentration.

First strand cDNA was synthesized from total RNA by using the High-Capacity cDNA Reverse Transcription kit (Agilent Technologies, Salt Lake City, UT). mRNA expression was analyzed by RT-PCR using either the CFX96 real time PCR system (C1000 thermocycler, Bio-Rad Laboratories, Hercules, CA) or Quant Studio 5 applied biosystems (Thermo Fisher Scientific). The *Enho* sequences were as follows: human: forward: 5'-ATTGAGGCAGCTCCACTGTC-3'; reverse: 5'-CTGGAGTTGGGACTGGATTC-3'; mouse: forward: 5'-CTCAACTCAGGCCAGGA-3'; reverse: 5'-GCTGTCCTGTCCACACAC-3'. The *glyceraldehyde-3-phosphate dehydrogenase (GAPDH)* sequences were as follows: human: forward: 5'-CACCCAGGGCTGCTTTTAACTCTGGTA-3'; reverse: 5'-CCTTGACGGTGCCATGGAATTGC-3'; mouse: forward: 5'-GGAGAAACCTGCCAAGTATGA-3'; reverse: 5'-TCCTCAGTGTAGCCCAAGA-3'. All data were normalized to the corresponding *GAPDH* mRNA and analyzed using the  $2^{-\Delta\Delta C_t}$  method, where  $C_t$  is threshold cycle.

### **Western blot analysis**

Specific protein content was assessed in endothelial cell lysates prepared in RIPA buffer (Invitrogen, Cat. No. 1861278, Waltham, MA) and phosphatase inhibitors (Invitrogen, Cat. No. 1862495). Proteins within samples were separated in Criterion Tris-Glycine eXtended-PAGE precast gels (Bio-Rad) and transferred onto polyvinylidene difluoride membranes. Specific proteins were probed using the following antibodies: anti-phospho-eNOS (Ser1177) (1:500, #9570, Cell Signaling Technology, Danvers, MA) and anti-eNOS (1:500, #32027,

Cell Signaling). The individual protein band intensities were quantified via densitometry via Bio-Rad ChemiDoc XRS+ System (Bio-Rad). Phosphorylated eNOS was normalized to total eNOS. Values are expressed as fold difference.

## **Proteomics**

Proteomics analysis of adropin-treated endothelial cells was performed at Charles W. Gehrke Proteomics Center, a research core facility at the University of Missouri. Briefly, following a 24-hour incubation with either vehicle or adropin (10ng/mL), endothelial samples were homogenized in 100ul RIPA buffer and sonicated. Samples were then heated to 65°C for 20 minutes and finally centrifuged for 10 minutes at 16,000 g. The supernatant was transferred to a new tube and protein was precipitated overnight at -20°C with 4 volumes of cold acetone added to each sample. Each protein sample was centrifuged and washed with 80% acetone twice, and protein pellets were then resuspended with 6M urea, 2M thiourea, and 100mM ammonium bicarbonate. Protein was quantified using Pierce 660nm protein assay method following manufacturer instructions. Details on spectral library built-up, DIA data, statistical analysis, and full list of proteins that showed to be significantly changed with adropin are described in the supplemental material.

## **Statistical Analysis**

Statistical analyses were performed using GraphPad Prism version 9 (GraphPad Prism Software, La Jolla, CA). The Shapiro-Wilk test was used to

determine if data were normally distributed. The ROUT test was used to determine if data had outliers based on a false discovery rate, with Q set to 5%. The Mann-Whitney  $U$  nonparametric test was used to compare data not normally distributed. Two-tailed, unpaired Student's  $t$ -test was used to compare independent samples, while the two-tailed, paired Student's  $t$ -test was used to compare paired samples. The  $E_{inc}$  slopes were calculated for each artery and was compared to its respective control via Student's unpaired and paired  $t$ -test, according to experimental design. The  $E_{inc}$  data are represented as a simple linear regression to represent the group mean slopes. A two-way repeated measure analysis of variance (ANOVA) was performed to assess group by time effects of glucose tolerance. In addition, Pearson's correlation or partial correlation analyses were performed to examine the relationship between adropin, PWV, and other cardiovascular risk factors when appropriate (SPSS Statistics software version 26, IBM Corporation, Armonk, NY). Data are represented as mean  $\pm$  standard error of the mean (202). The results were considered significant when  $P < 0.05$ . Whenever possible, investigators were blinded to the treatment conditions. However, it should be acknowledged that for several of the protocols, the investigator administering the treatments was the same one performing the measurements and thus blinding could not be ensured. Data analysis was performed by a single investigator and repeated by a second independent investigator for confirmation.

## RESULTS

**Obesity and T2D are associated with reduced adropin levels and increased arterial stiffness in humans.**

As displayed in **Figure 1A**, levels of BMI and HbA1c inversely associate with hepatic adropin mRNA expression in a cohort of male and female patients that underwent liver tissue sampling during bariatric surgery. That is, those individuals with a BMI $>40\text{kg/m}^2$  and HbA1c $\geq 6.5\%$  had lower adropin mRNA expression in the liver relative to those with a BMI $\leq 40\text{kg/m}^2$  and HbA1c $< 6.5\%$  ( $P < 0.05$ ). In **Figure 1B**, in a separate cohort, we show that individuals with T2D exhibited lower plasma concentrations of adropin, relative to healthy subjects ( $P < 0.05$ ), and that this was associated with increased arterial stiffness as assessed by carotid-to-femoral PWV ( $P < 0.05$ ). Sex did not influence the differences between healthy subjects and T2D in plasma adropin or PWV (*i.e.*, sex by group interactions were not significant;  $P > 0.05$ ).

There was a significant correlation between adropin and PWV ( $R = -0.26$ ,  $P = 0.033$ , **Figure 1B**), and further adjusted for BMI, HbA1c, age, and mean arterial pressure (MAP). Adjusting for BMI or HbA1c eliminated the significance of the correlation between adropin and PWV (BMI-adjusted:  $R = -0.131$ ,  $P = 0.285$ ; HbA1c-adjusted:  $R = -0.139$ ,  $P = 0.315$ ); whereas adjusting for age or MAP did not (age-adjusted:  $R = -0.26$ ,  $P = 0.032$ ; MAP-adjusted:  $R = -0.297$ ,  $P = 0.016$ ). There was no significant correlation between adropin and MAP ( $R = -0.06$ ,  $P = 0.583$ ). Age and PWV ( $R = 0.458$ ,  $P < 0.01$ ) as well as BMI and PWV ( $R = 0.675$ ,  $P < 0.01$ ) were significantly correlated.

**Mesenteric arteries from adropin knockout mice are stiffer, thus recapitulating the stiffening phenotype observed in db/db mice.**

As shown in **Figure 1C**, db/db mice exhibited lower mRNA expression of adropin in the liver and lower adropin concentrations in plasma relative to db/+ littermates ( $P<0.05$ ). Db/db mice also displayed increased stiffness in isolated mesenteric arteries as assessed by pressure myography ( $P<0.05$ ). In **Figure 1D**, as confirmation of the adropin knockout mouse model, we show that knockout mice demonstrated reduced levels of adropin mRNA across tissues, relative to wild-type littermates ( $P<0.05$ ). Plasma insulin concentrations were reduced in adropin knockout mice ( $P<0.05$ ), but no significant differences in body weight, glucose tolerance, or other metabolic parameters were noted between knockout and wild-type mice ( $P>0.05$ , **Table 1, Figure 1D**). Despite the overall similar metabolic phenotype between genotypes, mesenteric arteries from adropin knockout mice were stiffer compared to arteries from wild-type counterparts ( $P<0.05$ ).

**Exposure of endothelial cells or isolated mesenteric arteries from db/db male mice to adropin reduces F-actin stress fibers and stiffness: Role of NO**

In **Figure 2A**, we report that adropin stimulation increased phosphorylation of eNOS in endothelial cells as well as nitrite concentration, a by-product of NO, in the cell culture supernatant ( $P<0.05$ ). **Figure 2B** shows that prolonged exposure of endothelial cells to adropin reduced F-actin stress fibers

and cellular stiffness, as assessed by AFM ( $P < 0.05$ ). Notably, these effects of adropin were abrogated when cells were co-treated with L-NAME, a NOS inhibitor ( $P > 0.05$ ). Similarly, as illustrated in **Figure 2C**, prolonged exposure of isolated mesenteric arteries from db/db mice to adropin reduced F-actin stress fibers and stiffness ( $P < 0.05$ ); effects that were also abrogated by L-NAME ( $P > 0.05$ ).

**Stimulation of smooth muscle cells or isolated mesenteric arteries from db/db male mice with SNP, an NO mimetic, reduces F-actin stress fibers and stiffness.**

As shown in **Figure 3A**, stimulation of smooth muscle cells with SNP decreased F-actin stress fibers ( $P < 0.05$ ). This effect of SNP was abrogated by co-treatment of cells with LIMK inhibitor or jasplakinolide ( $P > 0.05$ ). Congruently, as displayed in **Figure 3B**, stimulation of smooth muscle cells or db/db mesenteric arteries with SNP reduced stiffness as assessed by AFM and pressure myography, respectively ( $P < 0.05$ ).

***In vivo* treatment of db/db mice with adropin reduced stiffness in mesenteric arteries.**

As illustrated in **Figure 4**, treatment of db/db mice with adropin for four weeks via osmotic minipumps increased plasma concentrations of adropin, compared to mice treated with vehicle. Adropin treatment did not cause significant changes in body weight or other circulating indices of metabolic

function (**Table 2**) ( $P>0.05$ ). Despite the lack of adropin effect on metabolic function, mesenteric arteries from adropin-treated mice were less stiff compared to arteries from vehicle-treated mice ( $P<0.05$ ).

### **Molecular signature of endothelial cells treated with adropin**

The proteomic analysis identified 421 differentially expressed proteins, of which 404 increased while 17 decreased, in endothelial cells treated with adropin for 24 hours. Unbiased ingenuity pathway analysis revealed that organization of the cytoskeleton was one of the top activated networks associated with disease and biological function (**Figure 5, Tables S1-3**,  $P=7.92E-5$ , Z-score 2.708). The top upstream translational regulator, also linked with the cytoskeletal organization, was switch/sucrose non-fermentable related (SWI/SNF), matrix associated, actin dependent regulator of chromatin subfamily A, member 4 (SMARCA4, **Figure 5**,  $P=8.18E-3$ , Z-score 3.341). Additionally, the unbiased ingenuity pathway analysis revealed an activation of the cell survival network in concert with a downregulation of apoptotic network (**Supplemental Figure 1, Table S4-7**,  $P=0.00197$  and  $P=7.28E-4$ , and Z-scores 4.456 and -3.551, respectively).

### **DISCUSSION**

Increased arterial stiffness contributes to the pathogenesis of cardiovascular disease and represents an independent predictor of adverse cardiovascular events, morbidity, and mortality (2, 3, 43, 44, 47, 186, 187). A



better understanding of factors regulating arterial stiffness in obesity and T2D is critical for the identification of novel therapeutic targets to reduce cardiovascular disease burden. In this work, we further establish that adropin is decreased in obesity and T2D in humans and preclinical animal models, as well as provide evidence that reduced adropin may directly contribute to arterial stiffening.

Specifically, in liver samples from male and female patients that underwent bariatric surgery, we show that levels of BMI and HbA1c inversely associate with hepatic mRNA expression of adropin, corroborating previous findings (149). In a separate cohort, we show that individuals with T2D also exhibit lower plasma concentrations of adropin, relative to healthy subjects, and that this is associated with increased arterial stiffness. Subsequently, we provide several lines of evidence which collectively support the role of adropin in regulating arterial stiffness, as elaborated below.

First, we report that increased stiffness in mesenteric arteries of db/db mice, a genetic mouse model of obesity and T2D, is accompanied with reduced mRNA expression of adropin in the liver and lower adropin concentrations in plasma. Notably, we show that mesenteric arteries from adropin knockout mice are also stiffer, relative to arteries from wild-type counterparts, thus recapitulating the stiffening phenotype we and others (51) observed in db/db mice. Of note, the stiffening effect caused by adropin ablation appears to be independent of obesity and metabolic dysfunction because metabolic derangements in this mouse model are primarily or only manifested when animals are subjected to another insult (*e.g.*, an obesogenic diet) (20, 152).

Next, we provide evidence that overnight exposure of isolated mesenteric arteries from db/db mice to adropin has a de-stiffening effect. To examine the role of NO in mediating this beneficial effect of adropin, first we documented that adropin does indeed activate eNOS and increase NO production in endothelial cells, a finding that is consistent with prior work by others (8). Importantly, we show that the de-stiffening effect of adropin in db/db mesenteric arteries is abolished when arteries are co-treated with the NOS inhibitor L-NAME, suggesting that the stiffness-reducing effect of adropin is at least in part mediated by NO.

While collagen deposition and crosslinking are important determinants of arterial stiffness, another important driver of stiffness at the cellular level is cytoskeletal actin polymerization (43, 44, 76, 203). Here we show that the de-stiffening effect of adropin in db/db mesenteric arteries is accompanied by reduced content of F-actin stress fibers and that the actin depolymerization effects of adropin are also abolished by NOS inhibition. Similarly, endothelial cells treated with adropin become less stiff, as assessed by AFM, and this de-stiffening effect is paralleled with reduced F-actin stress fibers, as well as abrogated by NOS inhibition. These findings indicate that the actin depolymerization and stiffness-reducing effects of adropin, in both isolated arteries and endothelial cells, are NO-dependent. Notably, we are not asserting that reduced endothelial rigidity with adropin physically contributes to the lowering of whole artery stiffness. Rather, based on previous evidence that reduced endothelial cell stiffness promotes eNOS activation (80), a more

conceivable scenario is that adropin-induced de-stiffening of endothelial cells potentiates NO production and that, subsequently, NO signaling in smooth muscle cells promotes actin depolymerization and reduced stiffening. Consistent with this proposition, we show that stimulation of smooth muscle cells with SNP, an NO mimetic, reduces F-actin stress fibers and cellular stiffness. As proof-of-concept, we also confirmed that prolonged treatment of db/db mesenteric arteries with SNP results in a de-stiffening effect. Because LIMK inactivates cofilin to favor formation of actin networks and stress fibers (76, 96), and earlier work indicates that NO signaling can act upstream of LIMK and reduce its activity (e.g., by inhibiting tissue transglutaminase activity and the RhoA-ROCK pathway) (96, 108, 110, 204), here we reasoned that inhibition of LIMK would prevent SNP-induced actin depolymerization. Indeed, this is what we observed. Reciprocally, we show that treatment of smooth muscle cells with jasplakinolide, an approach to experimentally force actin polymerization and stabilization, also prevents SNP-induced actin depolymerization. Collectively, these findings are consistent with a scenario in which adropin-induced endothelial-derived NO drives smooth muscle cell actin depolymerization and consequently reduce cellular stiffness (**Figure 6**). In this regard, there is precedence in the literature demonstrating that changes in smooth muscle cell stiffness can substantially contribute to changes in whole-artery stiffness (90, 93).

To further examine the role of adropin as a potential therapeutic target for vascular de-stiffening in obesity and T2D, we chronically treated db/db mice with adropin using surgically implanted subcutaneous osmotic minipumps. In concert

with the hypothesis, we found that *in vivo* treatment of db/db mice with adropin reduced stiffness in mesenteric arteries. No significant changes in body weight or circulating metabolic parameters were observed after the four weeks of adropin treatment, suggesting that the de-stiffening effects of adropin in obesity and T2D are likely independent of changes in metabolic function.

Finally, as an approach to provide a better understanding of signaling pathways and molecules modulated by adropin and thus stimulate future research, we performed a proteomic analysis in adropin-treated vs. untreated endothelial cells. We found that a total of 421 proteins were differentially expressed in response to adropin treatment. An unbiased ingenuity pathway analysis revealed that a large fraction of differentially expressed proteins were associated with organization of the cytoskeleton. In response to the adropin treatment, the most upregulated transcriptional regulator linked to the organization of the cytoskeleton was SMARCA4 (gene encoding for SWI/SNF complex containing Brahma-related gene 1 (BRG1), a transcriptional activator associated with angiogenesis (205, 206). The observation that adropin induces an endothelial molecular signature indicative of cytoskeletal organization is in alignment with the abovementioned finding that adropin reduced cytoskeletal actin polymerization and cortical stiffness in endothelial cells. Furthermore, in corroboration of previous reports that adropin decreases apoptosis in vascular tissues (8, 36), ingenuity pathway analysis also revealed that treatment of endothelial cells with adropin stimulated the activation of cell survival pathways and repression of apoptotic pathways.

Several aspects of this investigation warrant further consideration. First, the reason for including carotid-to-femoral PWV in humans was to add greater translational relevance to the project; however, it should be acknowledged that carotid-to-femoral PWV reflects large elastic artery stiffness, whereas stiffness in our mouse models was examined in small (more muscular) arteries. Even though the mechanisms driving stiffening are likely not the same across the arterial tree, smooth muscle cytoskeletal remodeling is a determinant of arterial wall stiffening in both large and small vessels (93, 207-209). Also, while most data supporting the clinical relevance of aortic stiffening comes from human studies in which measures of carotid-to-femoral PWV were obtained (210-212), data are also available indicating that stiffening of more peripheral and small arteries leads to poor perfusion and impaired blood pressure control (76, 213-218). Another disconnect between the human and mouse arterial stiffness outcomes of the current study is the *in vivo* vs. *ex vivo* nature of the measures. Measures of PWV are impacted by physiological factors such as sympathetic activity and blood pressure (219, 220), whereas in our *ex vivo* preparation, isolated arteries are kept in  $\text{Ca}^{2+}$ -free conditions thus removing any active tone and allowing for the assessment of stiffness of the wall material. For mechanistic studies, this could be considered a strength of the *ex vivo* measurement. Second, identification of adropin receptors in the vasculature remain largely elusive. While elucidation of the receptor responsible for adropin signaling in the endothelium was outside the scope of this work, a prior study showed that in vascular endothelial growth factor receptor 2 (VEGFR2)-silenced endothelial

cells, adropin-induced activation of eNOS was abrogated, suggesting that VEGFR2 may be an upstream mediator of adropin-induced eNOS activation [11]. Third, while other studies have examined and reported the effects of adropin on endothelium-dependent dilation (40, 170), and have served as the impetus for the current work focused on arterial stiffness, the lack of endothelial function outcomes in the present report can be considered a limitation. Fourth, findings from the *ex vivo* treatment of arteries or cells with adropin for 24 hours suggest that adropin-induced de-stiffening effects can occur rather quickly. The acute nature of these adropin effects is consistent with the idea that cytoskeletal remodeling can occur rapidly (*i.e.*, within minutes/hours) (207, 221-223); nevertheless, time course studies are needed to establish the kinetics of these changes. Fifth, follow-up telemetry studies are needed to determine if the observed changes in arterial stiffness in our mouse model of adropin deficiency and/or adropin treatment are associated with, or independent of, changes in blood pressure. Lastly, while data from men and women were used for establishing the inverse association between magnitude of BMI/HbA1c and adropin expression in the liver, as well as the inverse relationship plasma adropin and arterial stiffness, it should be acknowledged that only male mice were included in the present studies. Accordingly, the extent to which findings from our preclinical models can be translated to females requires further investigation.

In aggregate, herein we extend prior work on cardiovascular effects of adropin by providing the first evidence that loss of adropin alone causes an increase in arterial stiffness that recapitulates the effects of obesity and T2D.

Conversely, we show that adropin exposure reduces obesity and T2D-associated arterial stiffening, likely through a pathway involving NO. The significance of these observations is notable in that arterial stiffening is a strong and independent predictor of life-threatening cardiovascular events. Accordingly, this work supports that consideration should be given to “hyoadropinemia” as a potential target for the prevention and treatment of arterial stiffening in obesity and T2D.

### **Funding**

This work was supported, in part, by the National Institutes of Health Grants R01 HL137769 (to JP), R21 DK116081 (to CM-A), R01 HL088105 (to LAM-L), R01 DK113701 (to EJP, RSR, and JAI), as well as funds from the Cardiometabolic Disease Research Foundation (to JP).

### **Disclosures**

No conflicts of interest, financial or otherwise, are declared by the authors.

## Tables and Figures

**Table 1.** Circulating metabolic parameters of wild-type and adropin knockout littermates.

	Wild-type (n=9) (Mean $\pm$ SEM)	Adropin knockout (n=13) (Mean $\pm$ SEM)
Glucose (mg/dL)	246.5 $\pm$ 18.4	243.0 $\pm$ 8.7
Insulin (pg/mL)	1117.2 $\pm$ 264.7	659.7 $\pm$ 121.7*
Free glycerol (mg/dL)	25.1 $\pm$ 1.3	22.7 $\pm$ 1.5
Triglycerides (mg/dL)	63.5 $\pm$ 7.1	64.9 $\pm$ 6.7
Free-fatty acids (mEq/L)	0.4 $\pm$ 0.1	0.4 $\pm$ 0.0
Total cholesterol (mg/dL)	90.2 $\pm$ 5.0	84.8 $\pm$ 2.4
HbA1c (%)	4.8 $\pm$ 0.1	4.8 $\pm$ 0.3

\* $P < 0.05$  compared to wild-type.



**Table 2.** Circulating metabolic parameters of db/db mice after a four-week vehicle vs adropin administration.

	Vehicle (n=7) (Mean $\pm$ SEM)	Adropin (n=12) (Mean $\pm$ SEM)
Glucose (mg/dL)	798.1 $\pm$ 48.3	843.2 $\pm$ 32.0
Insulin (pg/mL)	8736.2 $\pm$ 1277.8	8038.9 $\pm$ 735.8
Free glycerol (mg/dL)	47.6 $\pm$ 6.1	38.8 $\pm$ 2.4
Triglycerides (mg/dL)	164.4 $\pm$ 34.7	151.3 $\pm$ 15.6
Free-fatty acids (mEq/L)	0.4 $\pm$ 0.0	0.5 $\pm$ 0.0
Total cholesterol (mg/dL)	129.7 $\pm$ 6.9	124.1 $\pm$ 5.9
HbA1c (%)	7.6 $\pm$ 0.4	7.8 $\pm$ 0.2

**Supplemental Table 1.** Proteomics in endothelial cells treated with vehicle vs. adropin for 24 hours: Proteins represented on left side of Figure 5.

Genes	Protein Descriptions	AVG Log2 Ratio	<i>P</i> value
CKM	Creatine kinase M-type	2.70	3.75E-03
NECTIN3	Nectin-3	1.70	7.80E-03
ANK2	Ankyrin-2	1.61	1.77E-04
UGCG	Ceramide glucosyltransferase	1.53	7.98E-08
ACAP1	Arf-GAP with coiled-coil, ANK repeat and PH domain-containing protein 1	1.24	1.92E-04
CFAP58	Cilia- and flagella-associated protein 58	1.18	2.22E-02
CD47	Leukocyte surface antigen CD47	1.17	1.04E-04
MAP1A	Microtubule-associated protein 1A	1.15	6.73E-04
TMEM67	Meckelin	1.13	2.32E-03
CLCN4	H(+)/Cl(-) exchange transporter 4	1.11	1.62E-03
GPRIN1	G protein-regulated inducer of neurite outgrowth 1	1.11	4.47E-03
ATF6	Cyclic AMP-dependent transcription factor ATF-6 alpha	1.09	7.23E-05
LOX	Protein-lysine 6-oxidase	1.03	1.21E-06
PLXNA3	Plexin-A3	1.03	1.53E-05

EFNB2	Ephrin-B2	1.02	5.28E-05
EIF4EBP2	Eukaryotic translation initiation factor 4E-binding protein 2	1.00	2.63E-04
PRUNE1	Exopolyphosphatase PRUNE1	1.00	1.84E-06
AKT2	RAC-beta serine/threonine-protein kinase	1.00	3.30E-04
MAD2L1	Mitotic spindle assembly checkpoint protein MAD2A	0.96	1.94E-03
KIF2C	Kinesin-like protein KIF2C	0.94	6.80E-04
FARP2	FERM, ARHGEF and pleckstrin domain-containing protein 2	0.94	7.09E-03
SP3	Transcription factor Sp3	0.93	1.23E-04
CPEB4	Cytoplasmic polyadenylation element-binding protein 4	0.91	1.55E-06
ERBB2	Receptor tyrosine-protein kinase erbB-2	0.90	3.92E-04
FGF2	Fibroblast growth factor 2	0.86	1.57E-08
CHN1	N-chimaerin	0.82	2.85E-04
SEMA3F	Semaphorin-3F	0.82	7.19E-04
ROR1	Inactive tyrosine-protein kinase transmembrane receptor ROR1	0.82	5.79E-08
HTR1B	5-hydroxytryptamine receptor 1B	0.81	4.97E-03

IFT80	Intraflagellar transport protein 80 homolog	0.80	2.69E-05
ATE1	Arginyl-tRNA--protein transferase 1	0.78	9.64E-04
FOXC2	Forkhead box protein C2	0.78	1.12E-05
TNR	Tenascin-R	0.76	3.28E-07
CTSS	Cathepsin S	0.76	1.45E-05
PLS1	Plastin-1	0.74	1.10E-05
ANK3	Ankyrin-3	0.73	9.08E-03
HDAC8	Histone deacetylase 8	0.72	4.61E-03
MAP2K5	Dual specificity mitogen-activated protein kinase kinase 5	0.72	3.38E-03
STX3	Syntaxin-3	0.71	1.94E-03
NCKIPSD	NCK-interacting protein with SH3 domain	0.69	2.68E-03
TUBB4A	Tubulin beta-4A chain	0.69	1.99E-04
MYLK	Myosin light chain kinase, smooth muscle	0.69	2.30E-03
EPS8	Epidermal growth factor receptor kinase substrate 8	0.68	7.46E-04
ZMYM3	Zinc finger MYM-type protein 3	0.67	7.61E-05
SLC11A2	Natural resistance-associated macrophage protein 2	0.66	9.29E-04

TRPV4	Transient receptor potential cation channel subfamily V member 4	0.64	1.80E-03
WWP1	NEDD4-like E3 ubiquitin-protein ligase WWP1	0.63	7.73E-05
TACC2	Transforming acidic coiled-coil-containing protein 2	0.63	1.51E-04
NRG1	Pro-neuregulin-1, membrane-bound isoform	0.62	2.76E-04
DYRK1A	Dual specificity tyrosine-phosphorylation-regulated kinase 1A	0.62	2.57E-04
KIF21A	Kinesin-like protein KIF21A	0.62	1.28E-03
TTC26	Intraflagellar transport protein 56	0.61	1.16E-04
NDEL1	Nuclear distribution protein nudE-like 1	0.61	2.23E-04
GNAI1	Guanine nucleotide-binding protein G(i) subunit alpha-1	0.61	2.38E-05
TTC21B	Tetratricopeptide repeat protein 21B	0.61	2.73E-03
IFT81	Intraflagellar transport protein 81 homolog	0.60	8.39E-06
GSTM1	Glutathione S-transferase Mu 1	0.59	9.94E-05

NINJ1	Ninjurin-1	0.59	4.54E-04
FBXW5	F-box/WD repeat-containing protein 5	0.59	1.65E-04
PITPNM1	Membrane-associated phosphatidylinositol transfer protein 1	0.59	1.11E-04
TBCK	TBC domain-containing protein kinase-like protein	0.59	9.17E-04
MBP	Myelin basic protein	0.58	1.22E-02
TMEM138	Transmembrane protein 138	-0.68	8.35E-05
B9D1	B9 domain-containing protein 1	-0.75	3.04E-06
KRT17	Keratin, type I cytoskeletal 17	-1.34	1.80E-02

---

**Supplemental Table 2.** Proteomics in endothelial cells treated with vehicle vs. adropin for 24 hours: Proteomic data for right side of Figure 5.

Genes	Protein Descriptions	AVG Log2 Ratio	<i>P</i> value
CKM	Creatine kinase M-type	2.70	3.75E-03
SOX17	Transcription factor SOX-17	1.50	7.99E-04
MYL1	Myosin light chain 1/3, skeletal muscle isoform	1.43	2.39E-03
SERPINB7	Serpin B7	1.41	1.78E-02
CD47	Leukocyte surface antigen CD47	1.17	1.04E-04
ST6GALNA C4	Alpha-N-acetyl-neuraminyl-2,3-beta-galactosyl-1,3-N-acetyl-galactosaminide alpha-2,6-sialyltransferase	1.14	4.90E-07
PLEKHG2	Pleckstrin homology domain-containing family G member 2	1.10	1.37E-03
LOX	Protein-lysine 6-oxidase	1.03	1.21E-06
LDB1	LIM domain-binding protein 1	0.85	4.49E-04
TIMP2	Metalloproteinase inhibitor 2	0.83	1.44E-06
HLA-B	HLA class I histocompatibility antigen, B alpha chain	0.81	7.81E-08
CTSS	Cathepsin S	0.76	1.45E-05
WDR45	WD repeat domain phosphoinositide-	0.75	7.09E-09

	interacting protein 4		
MEIS1	Homeobox protein Meis1	0.74	2.83E-05
PLS1	Plastin-1	0.74	1.10E-05
APOA1	Apolipoprotein A-I	0.73	9.45E-05
MYLK	Myosin light chain kinase, smooth muscle	0.69	2.30E-03
SERPINE2	Glia-derived nexin	0.68	2.36E-02
CORO6	Coronin-6	0.61	2.08E-04
SLC43A3	Equilibrative nucleobase transporter 1	0.60	6.42E-04
MBP	Myelin basic protein	0.58	1.22E-02

---



**Supplemental Table 3.** Proteomics in endothelial cells treated with vehicle vs. adropin for 24 hours: All proteins in Figure 5.

Genes	Protein Descriptions	AVG Log2 Ratio	<i>P</i> value
CKM	Creatine kinase M-type	6.52	3.75E-03
NECTIN3	Nectin-3	3.26	7.80E-03
ANK2	Ankyrin-2	3.05	1.77E-04
UGCG	Ceramide glucosyltransferase	2.88	7.98E-08
SOX17	Transcription factor SOX-17	2.82	7.99E-04
MYL1	Myosin light chain 1/3, skeletal muscle isoform	2.70	2.39E-03
SERPINB7	Serpin B7	2.65	1.78E-02
ACAP1	Arf-GAP with coiled-coil, ANK repeat and PH domain-containing protein 1	2.36	1.92E-04
CFAP58	Cilia- and flagella-associated protein 58	2.27	2.22E-02
CD47	Leukocyte surface antigen CD47	2.24	1.04E-04
MAP1A	Microtubule-associated protein 1A	2.23	6.73E-04
ST6GALNAC4	Alpha-N-acetyl-neuraminy-2,3-beta-galactosyl-1,3-N-acetyl-galactosaminide alpha-2,6-	2.20	4.90E-07

	sialyltransferase		
TMEM67	Meckelin	2.19	2.32E-03
CLCN4	H(+)/Cl(-) exchange transporter 4	2.16	1.62E-03
GPRIN1	G protein-regulated inducer of neurite outgrowth 1	2.16	4.47E-03
PLEKHG2	Pleckstrin homology domain-containing family G member 2	2.14	1.37E-03
ATF6	Cyclic AMP-dependent transcription factor ATF-6 alpha	2.12	7.23E-05
LOX	Protein-lysine 6-oxidase	2.04	1.21E-06
PLXNA3	Plexin-A3	2.04	1.53E-05
EFNB2	Ephrin-B2	2.03	5.28E-05
EIF4EBP2	Eukaryotic translation initiation factor 4E-binding protein 2	2.00	2.63E-04
PRUNE1	Exopolyphosphatase PRUNE1	2.00	1.84E-06
AKT2	RAC-beta serine/threonine-protein kinase	2.00	3.30E-04
MAD2L1	Mitotic spindle assembly checkpoint protein MAD2A	1.94	1.94E-03
KIF2C	Kinesin-like protein KIF2C	1.91	6.80E-04
FARP2	FERM, ARHGEF and pleckstrin domain-containing protein 2	1.91	7.09E-03

SP3	Transcription factor Sp3	1.91	1.23E-04
CPEB4	Cytoplasmic polyadenylation element-binding protein 4	1.88	1.55E-06
ERBB2	Receptor tyrosine-protein kinase erbB-2	1.87	3.92E-04
FGF2	Fibroblast growth factor 2	1.81	1.57E-08
LDB1	LIM domain-binding protein 1	1.81	4.49E-04
TIMP2	Metalloproteinase inhibitor 2	1.77	1.44E-06
CHN1	N-chimaerin	1.77	2.85E-04
SEMA3F	Semaphorin-3F	1.77	7.19E-04
ROR1	Inactive tyrosine-protein kinase transmembrane receptor ROR1	1.76	5.79E-08
HLA-B	HLA class I histocompatibility antigen, B alpha chain	1.76	7.81E-08
HTR1B	5-hydroxytryptamine receptor 1B	1.75	4.97E-03
IFT80	Intraflagellar transport protein 80 homolog	1.74	2.69E-05
ATE1	Arginyl-tRNA--protein transferase 1	1.72	9.64E-04
FOXC2	Forkhead box protein C2	1.72	1.12E-05
TNR	Tenascin-R	1.70	3.28E-07
CTSS	Cathepsin S	1.69	1.45E-05

WDR45	WD repeat domain phosphoinositide-interacting protein 4	1.69	7.09E-09
MEIS1	Homeobox protein Meis1	1.67	2.83E-05
PLS1	Plastin-1	1.66	1.10E-05
ANK3	Ankyrin-3	1.65	9.08E-03
APOA1	Apolipoprotein A-I	1.65	9.45E-05
HDAC8	Histone deacetylase 8	1.65	4.61E-03
MAP2K5	Dual specificity mitogen-activated protein kinase kinase 5	1.64	3.38E-03
STX3	Syntaxin-3	1.64	1.94E-03
NCKIPSD	NCK-interacting protein with SH3 domain	1.62	2.68E-03
TUBB4A	Tubulin beta-4A chain	1.61	1.99E-04
MYLK	Myosin light chain kinase, smooth muscle	1.61	2.30E-03
EPS8	Epidermal growth factor receptor kinase substrate 8	1.60	7.46E-04
SERPINE2	Glia-derived nexin	1.60	2.36E-02
ZMYM3	Zinc finger MYM-type protein 3	1.59	7.61E-05
SLC11A2	Natural resistance-associated macrophage protein 2	1.58	9.29E-04

TRPV4	Transient receptor potential cation channel subfamily V member 4	1.55	1.80E-03
WWP1	NEDD4-like E3 ubiquitin-protein ligase WWP1	1.55	7.73E-05
TACC2	Transforming acidic coiled-coil- containing protein 2	1.55	1.51E-04
NRG1	Pro-neuregulin-1, membrane- bound isoform	1.54	2.76E-04
DYRK1A	Dual specificity tyrosine- phosphorylation-regulated kinase 1A	1.54	2.57E-04
KIF21A	Kinesin-like protein KIF21A	1.53	1.28E-03
TTC26	Intraflagellar transport protein 56	1.53	1.16E-04
NDEL1	Nuclear distribution protein nudE- like 1	1.53	2.23E-04
GNAI1	Guanine nucleotide-binding protein G(i) subunit alpha-1	1.53	2.38E-05
TTC21B	Tetratricopeptide repeat protein 21B	1.52	2.73E-03
CORO6	Coronin-6	1.52	2.08E-04
SLC43A3	Equilibrative nucleobase	1.52	6.42E-04

	transporter 1		
IFT81	Intraflagellar transport protein 81 homolog	1.51	8.39E-06
GSTM1	Glutathione S-transferase Mu 1	1.51	9.94E-05
NINJ1	Ninjurin-1	1.51	4.54E-04
FBXW5	F-box/WD repeat-containing protein 5	1.51	1.65E-04
PITPNM1	Membrane-associated phosphatidylinositol transfer protein 1	1.50	1.11E-04
TBCK	TBC domain-containing protein kinase-like protein	1.50	9.17E-04
MBP	Myelin basic protein	1.50	1.22E-02
TMEM138	Transmembrane protein 138	0.62	8.35E-05
B9D1	B9 domain-containing protein 1	0.60	3.04E-06
KRT17	Keratin, type I cytoskeletal 17	0.39	1.80E-02

---

**Supplemental Table 4.** Proteomics in endothelial cells treated with vehicle vs. adropin for 24 hours: All proteins in apoptotic and cell survival networks.

Genes	Protein Descriptions	AVG Log2 Ratio	<i>P</i> value
PPT2	Lysosomal thioesterase PPT2	2.46	2.38E-03
ATP13A2	Polyamine-transporting ATPase 13A2	2.18	1.52E-03
H2AX	Histone H2AX	1.60	2.54E-02
MCUR1	Mitochondrial calcium uniporter regulator 1	1.54	2.28E-06
UGCG	Ceramide glucosyltransferase	1.53	7.98E-08
DCD	Dermcidin	1.51	2.12E-04
SOX17	Transcription factor SOX- 17	1.50	7.99E-04
HABP2	Hyaluronan-binding protein 2	1.48	4.19E-03
RAMAC	RNA guanine-N7 methyltransferase activating subunit	1.44	5.11E-06
TNIP1	TNFAIP3-interacting protein 1	1.38	8.25E-04

PIK3R2	Phosphatidylinositol 3-kinase regulatory subunit beta	1.38	1.17E-07
ADARB1	Double-stranded RNA-specific editase 1	1.34	7.45E-05
SLC7A11	Cystine/glutamate transporter	1.31	3.39E-06
PUS10	tRNA pseudouridine synthase Pus10	1.24	1.16E-03
NRGN	Neurogranin	1.22	2.20E-06
TOMM20	Mitochondrial import receptor subunit TOM20 homolog	1.21	9.71E-05
NR2C2	Nuclear receptor subfamily 2 group C member 2	1.20	6.90E-06
CD47	Leukocyte surface antigen CD47	1.17	1.04E-04
RAD9A	Cell cycle checkpoint control protein RAD9A	1.14	4.38E-08
GPS2	G protein pathway suppressor 2	1.13	6.36E-05



CLCN4	H(+)/Cl(-) exchange transporter 4	1.11	1.62E-03
HHEX	Hematopoietically- expressed homeobox protein HHEX	1.10	2.91E-06
HIGD1A	HIG1 domain family member 1A, mitochondrial	1.10	5.84E-06
PLEKHG2	Pleckstrin homology domain-containing family G member 2	1.10	1.37E-03
PCDHGB6	Protocadherin gamma-B6	1.09	2.46E-04
ATF6	Cyclic AMP-dependent transcription factor ATF-6 alpha	1.09	7.23E-05
DAP	Death-associated protein 1	1.07	1.17E-03
ST6GAL1	Beta-galactoside alpha- 2,6-sialyltransferase 1	1.07	3.59E-04
LOX	Protein-lysine 6-oxidase	1.03	1.21E-06
PLXNA3	Plexin-A3	1.03	1.53E-05
SIRT3	NAD-dependent protein	1.03	3.91E-04

	deacetylase sirtuin-3, mitochondrial		
EFNB2	Ephrin-B2	1.02	5.28E-05
HMG5	High mobility group nucleosome-binding domain-containing protein 5	1.02	2.98E-02
UBE2V2	Ubiquitin-conjugating enzyme E2 variant 2	1.00	1.35E-08
AKT2	RAC-beta serine/threonine-protein kinase	1.00	3.30E-04
STEAP3	Metalloreductase STEAP3	0.98	2.02E-04
MTFP1	Mitochondrial fission process protein 1	0.97	4.34E-05
MAD2L1	Mitotic spindle assembly checkpoint protein MAD2A	0.96	1.94E-03
NCAPG2	Condensin-2 complex subunit G2	0.96	8.92E-04
INPP5A	Inositol polyphosphate-5-	0.95	7.96E-05

	phosphatase A		
PPP2R3A	Serine/threonine-protein	0.94	8.63E-03
	phosphatase 2A		
	regulatory subunit B"		
	subunit alpha		
SCD	Stearoyl-CoA desaturase	0.92	8.45E-03
DCAF1	DDB1- and CUL4-	0.92	1.02E-03
	associated factor 1		
CPEB4	Cytoplasmic	0.91	1.55E-06
	polyadenylation element-		
	binding protein 4		
CA3	Carbonic anhydrase 3	0.90	1.07E-02
ERBB2	Receptor tyrosine-protein	0.90	3.92E-04
	kinase erbB-2		
ENPP1	Ectonucleotide	0.90	1.03E-04
	pyrophosphatase/phosph		
	odiesterase family		
	member 1		
TUSC2	Tumor suppressor	0.89	5.17E-06
	candidate 2		
NOMO1	Nodal modulator 1	0.88	5.02E-08
SMARCAL1	SWI/SNF-related matrix-	0.88	6.46E-06

	associated actin- dependent regulator of chromatin subfamily A- like protein 1		
SNX33	Sorting nexin-33	0.88	5.57E-03
CREG1	Protein CREG1	0.88	2.74E-08
RNASEH2A	Ribonuclease H2 subunit A	0.88	2.48E-05
A4GALT	Lactosylceramide 4- alpha- galactosyltransferase	0.87	2.40E-05
PHKA2	Phosphorylase b kinase regulatory subunit alpha, liver isoform	0.87	1.50E-05
SPIN1	Spindlin-1	0.86	9.16E-06
FGF2	Fibroblast growth factor 2	0.86	1.57E-08
FOXK2	Forkhead box protein K2	0.86	3.13E-04
CDK2AP1	Cyclin-dependent kinase 2-associated protein 1	0.85	1.78E-04
ATP6V1G2	V-type proton ATPase subunit G 2	0.84	4.69E-03
TIMP2	Metalloproteinase	0.83	1.44E-06

	inhibitor 2		
SEMA3F	Semaphorin-3F	0.82	7.19E-04
ROR1	Inactive tyrosine-protein kinase transmembrane receptor ROR1	0.82	5.79E-08
HLA-B	HLA class I histocompatibility antigen, B alpha chain	0.81	7.81E-08
TRMT11	tRNA (guanine(10)-N2)- methyltransferase homolog	0.80	1.08E-04
AGA	N(4)-(beta-N- acetylglucosaminy)-L- asparaginase	0.79	1.74E-04
AKTIP	AKT-interacting protein	0.78	2.82E-04
TAF10	Transcription initiation factor TFIID subunit 10	0.78	3.97E-03
MGMT	Methylated-DNA--protein- cysteine methyltransferase	0.78	1.56E-05
ATE1	Arginyl-tRNA--protein transferase 1	0.78	9.64E-04

FOXC2	Forkhead box protein C2	0.78	1.12E-05
PIK3CB	Phosphatidylinositol 4,5- bisphosphate 3-kinase catalytic subunit beta isoform	0.78	2.01E-04
NAA38	N-alpha-acetyltransferase 38, NatC auxiliary subunit	0.77	2.61E-03
RTKN	Rhotekin	0.77	2.99E-04
CTSS	Cathepsin S	0.76	1.45E-05
ANKZF1	Ankyrin repeat and zinc finger domain-containing protein 1	0.75	4.19E-05
DDX19A	ATP-dependent RNA helicase DDX19A	0.74	8.71E-03
DYNC111	Cytoplasmic dynein 1 intermediate chain 1	0.74	2.32E-05
PLS1	Plastin-1	0.74	1.10E-05
SENP8	Sentrin-specific protease 8	0.73	8.02E-05
APOA1	Apolipoprotein A-I	0.73	9.45E-05
HDAC8	Histone deacetylase 8	0.72	4.61E-03
CKS2	Cyclin-dependent kinases	0.72	2.07E-03

	regulatory subunit 2		
MAP2K5	Dual specificity mitogen- activated protein kinase kinase 5	0.72	3.38E-03
STX3	Syntaxin-3	0.71	1.94E-03
RPS6KB2	Ribosomal protein S6 kinase beta-2	0.70	5.13E-03
SGK3	Serine/threonine-protein kinase Sgk3	0.70	1.27E-03
PAXIP1	PAX-interacting protein 1	0.70	2.89E-04
MRM1	rRNA methyltransferase 1, mitochondrial	0.70	1.77E-06
ANAPC11	Anaphase-promoting complex subunit 11	0.70	7.43E-04
TICAM1	TIR domain-containing adapter molecule 1	0.70	2.22E-06
CERK	Ceramide kinase	0.69	1.45E-04
MAP3K4	Mitogen-activated protein kinase kinase kinase 4	0.69	1.07E-03
MADD	MAP kinase-activating death domain protein	0.69	1.54E-02
TUBB4A	Tubulin beta-4A chain	0.69	1.99E-04

MYLK	Myosin light chain kinase, smooth muscle	0.69	2.30E-03
SEC61G	Protein transport protein Sec61 subunit gamma	0.69	9.90E-04
SERPINE2	Glia-derived nexin	0.68	2.36E-02
TNRC6A	Trinucleotide repeat- containing gene 6A protein	0.67	9.18E-04
STK11	Serine/threonine-protein kinase STK11	0.67	5.65E-05
TLE4	Transducin-like enhancer protein 4	0.66	1.03E-03
SLC11A2	Natural resistance- associated macrophage protein 2	0.66	9.29E-04
NSMCE1	Non-structural maintenance of chromosomes element 1 homolog	0.65	2.77E-03
ZNF830	Zinc finger protein 830	0.65	7.60E-06
ABCB6	ATP-binding cassette sub-family B member 6	0.65	1.55E-03



APOC3	Apolipoprotein C-III	0.64	5.39E-04
TRPV4	Transient receptor potential cation channel subfamily V member 4	0.64	1.80E-03
FANCD2	Fanconi anemia group D2 protein	0.64	4.38E-05
SPRY4	Protein sprouty homolog 4	0.63	2.59E-06
NHEJ1	Non-homologous end- joining factor 1	0.63	1.16E-05
CDK8;CDK19	Cyclin-dependent kinase 8;Cyclin-dependent kinase 19	0.63	5.16E-06
XPA	DNA repair protein complementing XP-A cells	0.63	1.83E-05
NRG1	Pro-neuregulin-1, membrane-bound isoform	0.62	2.76E-04
DYRK1A	Dual specificity tyrosine- phosphorylation- regulated kinase 1A	0.62	2.57E-04
NDEL1	Nuclear distribution	0.61	2.23E-04

	protein nudE-like 1		
ANKRD1	Ankyrin repeat domain- containing protein 1	0.61	5.63E-05
NOL3	Nucleolar protein 3	0.61	1.56E-04
HTRA3	Serine protease HTRA3	0.60	2.10E-02
TRIM24	Transcription intermediary factor 1- alpha	0.60	1.75E-03
LIPA	Lysosomal acid lipase/cholesteryl ester hydrolase	0.60	2.59E-04
FURIN	Furin	0.60	1.30E-02
GSTM1	Glutathione S-transferase Mu 1	0.59	9.94E-05
NINJ1	Ninjurin-1	0.59	4.54E-04
NSD2	Histone-lysine N- methyltransferase NSD2	0.59	1.88E-03
NR3C1	Glucocorticoid receptor	0.59	2.27E-05
PLEKHF1	Pleckstrin homology domain-containing family F member 1	0.59	1.31E-02
PCBP4	Poly(rC)-binding protein 4	0.58	3.46E-06

MBP	Myelin basic protein	0.58	1.22E-02
USP53	Inactive ubiquitin carboxyl-terminal hydrolase 53	0.58	5.79E-04
MACROH2A1	Core histone macro- H2A.1	-0.60	6.47E-03
CASP14	Caspase-14	-0.63	8.94E-03
SRCAP	Helicase SRCAP	-0.64	1.32E-02
PHLDA3	Pleckstrin homology-like domain family A member 3	-0.69	2.14E-04
ATG12	Ubiquitin-like protein ATG12	-0.77	1.46E-04
NABP2	SOSS complex subunit B1	-1.35	6.21E-03

---

**Supplemental Table 5.** Proteomics in endothelial cells treated with vehicle vs. adropin for 24 hours: Proteins associated with the apoptotic network.

Genes	Protein Descriptions	AVG Log2 Ratio	<i>P</i> value
PPT2	Lysosomal thioesterase PPT2	2.46	2.38E-03
H2AX	Histone H2AX	1.60	2.54E-02
UGCG	Ceramide glucosyltransferase	1.53	7.98E-08
SOX17	Transcription factor SOX-17	1.50	7.99E-04
HABP2	Hyaluronan-binding protein 2	1.48	4.19E-03
TNIP1	TNFAIP3-interacting protein 1	1.38	8.25E-04
ADARB1	Double-stranded RNA-specific editase 1	1.34	7.45E-05
SLC7A11	Cystine/glutamate transporter	1.31	3.39E-06
PUS10	tRNA pseudouridine synthase Pus10	1.24	1.16E-03
NRGN	Neurogranin	1.22	2.20E-06
TOMM20	Mitochondrial import receptor subunit TOM20 homolog	1.21	9.71E-05
CD47	Leukocyte surface antigen CD47	1.17	1.04E-04
RAD9A	Cell cycle checkpoint control protein RAD9A	1.14	4.38E-08
GPS2	G protein pathway suppressor	1.13	6.36E-05

	2		
HIGD1A	HIG1 domain family member 1A, mitochondrial	1.10	5.84E-06
PCDHGB6	Protocadherin gamma-B6	1.09	2.46E-04
ATF6	Cyclic AMP-dependent transcription factor ATF-6 alpha	1.09	7.23E-05
DAP	Death-associated protein 1	1.07	1.17E-03
ST6GAL1	Beta-galactoside alpha-2,6- sialyltransferase 1	1.07	3.59E-04
LOX	Protein-lysine 6-oxidase	1.03	1.21E-06
PLXNA3	Plexin-A3	1.03	1.53E-05
SIRT3	NAD-dependent protein deacetylase sirtuin-3, mitochondrial	1.03	3.91E-04
EFNB2	Ephrin-B2	1.02	5.28E-05
HMG5	High mobility group nucleosome-binding domain- containing protein 5	1.02	2.98E-02
UBE2V2	Ubiquitin-conjugating enzyme E2 variant 2	1.00	1.35E-08
AKT2	RAC-beta serine/threonine-	1.00	3.30E-04

	protein kinase		
STEAP3	Metalloreductase STEAP3	0.98	2.02E-04
MTFP1	Mitochondrial fission process protein 1	0.97	4.34E-05
MAD2L1	Mitotic spindle assembly checkpoint protein MAD2A	0.96	1.94E-03
NCAPG2	Condensin-2 complex subunit G2	0.96	8.92E-04
SCD	Stearoyl-CoA desaturase	0.92	8.45E-03
DCAF1	DDB1- and CUL4-associated factor 1	0.92	1.02E-03
CPEB4	Cytoplasmic polyadenylation element-binding protein 4	0.91	1.55E-06
CA3	Carbonic anhydrase 3	0.90	1.07E-02
ERBB2	Receptor tyrosine-protein kinase erbB-2	0.90	3.92E-04
ENPP1	Ectonucleotide pyrophosphatase/phosphodies terase family member 1	0.90	1.03E-04
SMARCAL1	SWI/SNF-related matrix- associated actin-dependent regulator of chromatin	0.88	6.46E-06

	subfamily A-like protein 1		
SNX33	Sorting nexin-33	0.88	5.57E-03
CREG1	Protein CREG1	0.88	2.74E-08
A4GALT	Lactosylceramide 4-alpha- galactosyltransferase	0.87	2.40E-05
SPIN1	Spindlin-1	0.86	9.16E-06
FGF2	Fibroblast growth factor 2	0.86	1.57E-08
FO XK2	Forkhead box protein K2	0.86	3.13E-04
CDK2AP1	Cyclin-dependent kinase 2- associated protein 1	0.85	1.78E-04
ATP6V1G2	V-type proton ATPase subunit G 2	0.84	4.69E-03
TIMP2	Metalloproteinase inhibitor 2	0.83	1.44E-06
SEMA3F	Semaphorin-3F	0.82	7.19E-04
ROR1	Inactive tyrosine-protein kinase transmembrane receptor ROR1	0.82	5.79E-08
HLA-B	HLA class I histocompatibility antigen, B alpha chain	0.81	7.81E-08
TRMT11	tRNA (guanine(10)-N2)- methyltransferase homolog	0.80	1.08E-04
AGA	N(4)-(beta-N-	0.79	1.74E-04

	acetylglucosaminyl)-L- asparaginase		
AKTIP	AKT-interacting protein	0.78	2.82E-04
TAF10	Transcription initiation factor TFIID subunit 10	0.78	3.97E-03
MGMT	Methylated-DNA--protein- cysteine methyltransferase	0.78	1.56E-05
ATE1	Arginyl-tRNA--protein transferase 1	0.78	9.64E-04
FOXC2	Forkhead box protein C2	0.78	1.12E-05
PIK3CB	Phosphatidylinositol 4,5- bisphosphate 3-kinase catalytic subunit beta isoform	0.78	2.01E-04
NAA38	N-alpha-acetyltransferase 38, NatC auxiliary subunit	0.77	2.61E-03
RTKN	Rhotekin	0.77	2.99E-04
CTSS	Cathepsin S	0.76	1.45E-05
ANKZF1	Ankyrin repeat and zinc finger domain-containing protein 1	0.75	4.19E-05
DDX19A	ATP-dependent RNA helicase DDX19A	0.74	8.71E-03
PLS1	Plastin-1	0.74	1.10E-05



SENP8	Sentrin-specific protease 8	0.73	8.02E-05
APOA1	Apolipoprotein A-I	0.73	9.45E-05
HDAC8	Histone deacetylase 8	0.72	4.61E-03
CKS2	Cyclin-dependent kinases regulatory subunit 2	0.72	2.07E-03
MAP2K5	Dual specificity mitogen- activated protein kinase kinase 5	0.72	3.38E-03
RPS6KB2	Ribosomal protein S6 kinase beta-2	0.70	5.13E-03
SGK3	Serine/threonine-protein kinase Sgk3	0.70	1.27E-03
TICAM1	TIR domain-containing adapter molecule 1	0.70	2.22E-06
MAP3K4	Mitogen-activated protein kinase kinase kinase 4	0.69	1.07E-03
MADD	MAP kinase-activating death domain protein	0.69	1.54E-02
MYLK	Myosin light chain kinase, smooth muscle	0.69	2.30E-03
SEC61G	Protein transport protein Sec61 subunit gamma	0.69	9.90E-04

SERPINE2	Glia-derived nexin	0.68	2.36E-02
TNRC6A	Trinucleotide repeat-containing gene 6A protein	0.67	9.18E-04
STK11	Serine/threonine-protein kinase STK11	0.67	5.65E-05
TLE4	Transducin-like enhancer protein 4	0.66	1.03E-03
ZNF830	Zinc finger protein 830	0.65	7.60E-06
APOC3	Apolipoprotein C-III	0.64	5.39E-04
TRPV4	Transient receptor potential cation channel subfamily V member 4	0.64	1.80E-03
SPRY4	Protein sprouty homolog 4	0.63	2.59E-06
NHEJ1	Non-homologous end-joining factor 1	0.63	1.16E-05
CDK8;CDK19	Cyclin-dependent kinase 8;Cyclin-dependent kinase 19	0.63	5.16E-06
XPA	DNA repair protein complementing XP-A cells	0.63	1.83E-05
NRG1	Pro-neuregulin-1, membrane-bound isoform	0.62	2.76E-04
NDEL1	Nuclear distribution protein	0.61	2.23E-04

	nudE-like 1		
NOL3	Nucleolar protein 3	0.61	1.56E-04
TRIM24	Transcription intermediary factor 1-alpha	0.60	1.75E-03
LIPA	Lysosomal acid lipase/cholesteryl ester hydrolase	0.60	2.59E-04
FURIN	Furin	0.60	1.30E-02
NINJ1	Ninjurin-1	0.59	4.54E-04
NSD2	Histone-lysine N- methyltransferase NSD2	0.59	1.88E-03
NR3C1	Glucocorticoid receptor	0.59	2.27E-05
PLEKHF1	Pleckstrin homology domain- containing family F member 1	0.59	1.31E-02
PCBP4	Poly(rC)-binding protein 4	0.58	3.46E-06
USP53	Inactive ubiquitin carboxyl- terminal hydrolase 53	0.58	5.79E-04
CASP14	Caspase-14	-0.63	8.94E-03
SRCAP	Helicase SRCAP	-0.64	1.32E-02
PHLDA3	Pleckstrin homology-like domain family A member 3	-0.69	2.14E-04
ATG12	Ubiquitin-like protein ATG12	-0.77	1.46E-04

NABP2	SOSS complex subunit B1	-1.35	6.21E-03
-------	-------------------------	-------	----------

---

**Supplemental Table 6.** Proteomics in endothelial cells treated with vehicle vs. adropin for 24 hours: All proteins associated with cell survival network.

Genes	Protein Descriptions	AVG Log2 Ratio	<i>P</i> value
ATP13A2	Polyamine-transporting ATPase 13A2	2.18	1.52E-03
H2AX	Histone H2AX	1.60	2.54E-02
MCUR1	Mitochondrial calcium uniporter regulator 1	1.54	2.28E-06
UGCG	Ceramide glucosyltransferase	1.53	7.98E-08
DCD	Dermcidin	1.51	2.12E-04
RAMAC	RNA guanine-N7 methyltransferase activating subunit	1.44	5.11E-06
PIK3R2	Phosphatidylinositol 3-kinase regulatory subunit beta	1.38	1.17E-07
NR2C2	Nuclear receptor subfamily 2 group C member 2	1.20	6.90E-06
CD47	Leukocyte surface antigen CD47	1.17	1.04E-04
RAD9A	Cell cycle checkpoint control protein RAD9A	1.14	4.38E-08
CLCN4	H(+)/Cl(-) exchange transporter 4	1.11	1.62E-03
HHEX	Hematopoietically-expressed	1.10	2.91E-06

	homeobox protein HHEX		
PLEKHG2	Pleckstrin homology domain- containing family G member 2	1.10	1.37E-03
PCDHGB6	Protocadherin gamma-B6	1.09	2.46E-04
ATF6	Cyclic AMP-dependent transcription factor ATF-6 alpha	1.09	7.23E-05
ST6GAL1	Beta-galactoside alpha-2,6- sialyltransferase 1	1.07	3.59E-04
EFNB2	Ephrin-B2	1.02	5.28E-05
AKT2	RAC-beta serine/threonine- protein kinase	1.00	3.30E-04
MAD2L1	Mitotic spindle assembly checkpoint protein MAD2A	0.96	1.94E-03
INPP5A	Inositol polyphosphate-5- phosphatase A	0.95	7.96E-05
PPP2R3A	Serine/threonine-protein phosphatase 2A regulatory subunit B" subunit alpha	0.94	8.63E-03
SCD	Stearoyl-CoA desaturase	0.92	8.45E-03
ERBB2	Receptor tyrosine-protein kinase erbB-2	0.90	3.92E-04
TUSC2	Tumor suppressor candidate 2	0.89	5.17E-06

NOMO1	Nodal modulator 1	0.88	5.02E-08
SMARCAL1	SWI/SNF-related matrix-associated actin-dependent regulator of chromatin subfamily A-like protein 1	0.88	6.46E-06
RNASEH2A	Ribonuclease H2 subunit A	0.88	2.48E-05
PHKA2	Phosphorylase b kinase regulatory subunit alpha, liver isoform	0.87	1.50E-05
FGF2	Fibroblast growth factor 2	0.86	1.57E-08
CDK2AP1	Cyclin-dependent kinase 2-associated protein 1	0.85	1.78E-04
TIMP2	Metalloproteinase inhibitor 2	0.83	1.44E-06
ROR1	Inactive tyrosine-protein kinase transmembrane receptor ROR1	0.82	5.79E-08
AGA	N(4)-(beta-N-acetylglucosaminyl)-L-asparaginase	0.79	1.74E-04
MGMT	Methylated-DNA--protein-cysteine methyltransferase	0.78	1.56E-05
PIK3CB	Phosphatidylinositol 4,5-bisphosphate 3-kinase catalytic	0.78	2.01E-04

	subunit beta isoform		
DYNC111	Cytoplasmic dynein 1	0.74	2.32E-05
	intermediate chain 1		
APOA1	Apolipoprotein A-I	0.73	9.45E-05
MAP2K5	Dual specificity mitogen-activated protein kinase kinase 5	0.72	3.38E-03
STX3	Syntaxin-3	0.71	1.94E-03
RPS6KB2	Ribosomal protein S6 kinase beta-2	0.70	5.13E-03
SGK3	Serine/threonine-protein kinase Sgk3	0.70	1.27E-03
PAXIP1	PAX-interacting protein 1	0.70	2.89E-04
MRM1	rRNA methyltransferase 1, mitochondrial	0.70	1.77E-06
ANAPC11	Anaphase-promoting complex subunit 11	0.70	7.43E-04
TICAM1	TIR domain-containing adapter molecule 1	0.70	2.22E-06
CERK	Ceramide kinase	0.69	1.45E-04
MAP3K4	Mitogen-activated protein kinase kinase kinase 4	0.69	1.07E-03
TUBB4A	Tubulin beta-4A chain	0.69	1.99E-04



STK11	Serine/threonine-protein kinase STK11	0.67	5.65E-05
SLC11A2	Natural resistance-associated macrophage protein 2	0.66	9.29E-04
NSMCE1	Non-structural maintenance of chromosomes element 1 homolog	0.65	2.77E-03
ABCB6	ATP-binding cassette sub-family B member 6	0.65	1.55E-03
FANCD2	Fanconi anemia group D2 protein	0.64	4.38E-05
CDK8;CDK19	Cyclin-dependent kinase 8;Cyclin-dependent kinase 19	0.63	5.16E-06
XPA	DNA repair protein complementing XP-A cells	0.63	1.83E-05
NRG1	Pro-neuregulin-1, membrane- bound isoform	0.62	2.76E-04
DYRK1A	Dual specificity tyrosine- phosphorylation-regulated kinase 1A	0.62	2.57E-04
ANKRD1	Ankyrin repeat domain- containing protein 1	0.61	5.63E-05
NOL3	Nucleolar protein 3	0.61	1.56E-04

HTRA3	Serine protease HTRA3	0.60	2.10E-02
GSTM1	Glutathione S-transferase Mu 1	0.59	9.94E-05
NSD2	Histone-lysine N- methyltransferase NSD2	0.59	1.88E-03
NR3C1	Glucocorticoid receptor	0.59	2.27E-05
MBP	Myelin basic protein	0.58	1.22E-02
MACROH2A1	Core histone macro-H2A.1	-0.60	6.47E-03
ATG12	Ubiquitin-like protein ATG12	-0.77	1.46E-04
NABP2	SOSS complex subunit B1	-1.35	6.21E-03

---

**Supplemental Table 7.** Proteomics in endothelial cells treated with vehicle vs. adropin for 24 hours: Top 15 positive and negative regulated proteins.

Genes	Protein Descriptions	AVG Log2 Ratio	<i>P</i> value
NUDT15	Nucleotide triphosphate diphosphatase NUDT15	5.37	9.40E-05
GAPDHS	Glyceraldehyde-3-phosphate dehydrogenase, testis-specific	2.87	6.76E-07
CKM	Creatine kinase M-type	2.70	3.75E-03
LSM3	U6 snRNA-associated Sm-like protein LSm3	2.56	1.81E-07
SNX14	Sorting nexin-14	2.51	1.79E-04
NUP42	Nucleoporin NUP42	2.48	8.31E-04
PPT2	Lysosomal thioesterase PPT2	2.46	2.38E-03
INO80C	INO80 complex subunit C	2.23	2.36E-03
ATP13A2	Polyamine-transporting ATPase 13A2	2.18	1.52E-03
ZDHHC7	Palmitoyltransferase ZDHHC7	2.02	4.52E-06
CYB5R4	Cytochrome b5 reductase 4	1.97	4.66E-06
NSUN4	5-methylcytosine rRNA methyltransferase NSUN4	1.91	1.86E-05
MT1L	Metallothionein-1L	1.86	7.27E-05
CCDC126	Coiled-coil domain-containing protein 126	1.76	9.04E-03

IQSEC1	IQ motif and SEC7 domain-containing protein 1	1.74	1.42E-03
NES	Nestin	-0.61	1.14E-03
SLC7A7	Y+L amino acid transporter 1	-0.61	1.01E-02
CASP14	Caspase-14	-0.63	8.94E-03
SRCAP	Helicase SRCAP	-0.64	1.32E-02
RRP7A	Ribosomal RNA-processing protein 7 homolog A	-0.64	2.94E-05
TMEM138	Transmembrane protein 138	-0.68	8.35E-05
PHLDA3	Pleckstrin homology-like domain family A member 3	-0.69	2.14E-04
B9D1	B9 domain-containing protein 1	-0.75	3.04E-06
PZP	Pregnancy zone protein	-0.77	7.64E-04
ATG12	Ubiquitin-like protein ATG12	-0.77	1.46E-04
MT-ND3	NADH-ubiquinone oxidoreductase chain 3	-0.88	5.24E-07
KRT5	Keratin, type II cytoskeletal 5	-1.30	1.77E-02
KRT17	Keratin, type I cytoskeletal 17	-1.34	1.80E-02
NABP2	SOSS complex subunit B1	-1.35	6.21E-03
IL17RA	Interleukin-17 receptor A	-2.03	1.92E-03

---

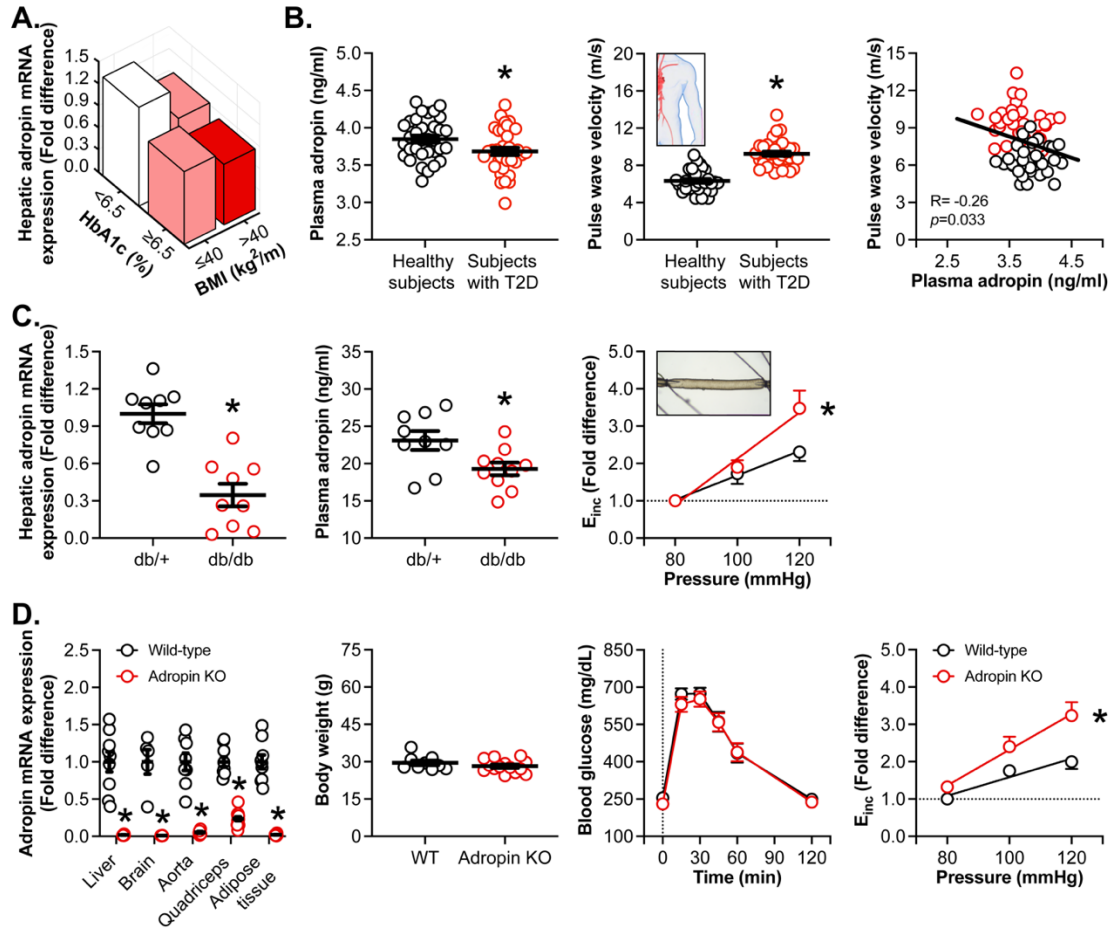
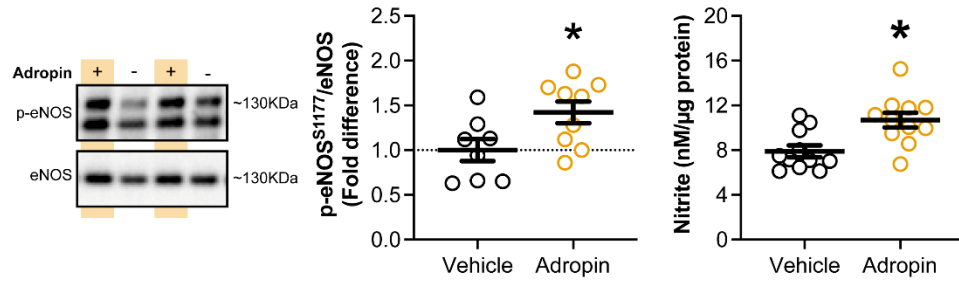


**Figure 1.** Decreased adropin is associated with increased arterial stiffness.

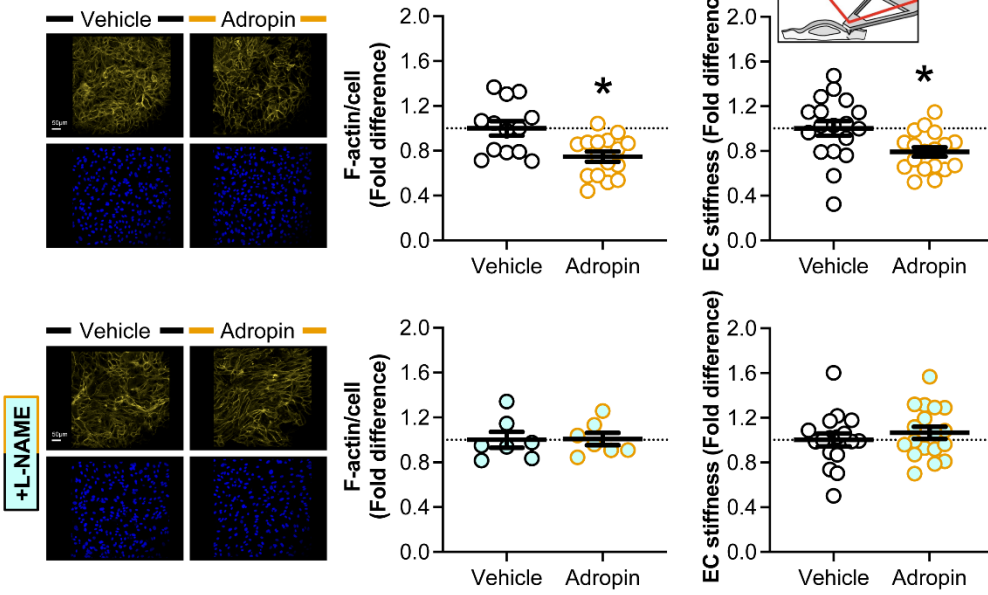
**(A)** Human hepatic adropin mRNA expression is inversely associated with glycosylated hemoglobin (HbA1c) and body mass index (BMI) in subjects that underwent a liver biopsy during bariatric surgery (n=45, F=36, M=9, n=3-24/per cluster). **(B)** Plasma adropin concentrations of healthy subjects (n=33, F=20, M=13) and subjects with type 2 diabetes (T2D) (n=42, F=21, M=21). Carotid-to-femoral pulse wave velocity in healthy subjects (n=33, F=20, M=13) and subjects with T2D (n=36, F=19, M=17). Pearson correlation between plasma adropin concentration and pulse wave velocity in healthy subjects (n= 33, F=20, M=13) and subjects with T2D (n=36, F=19, M=17). **(C)** Hepatic adropin mRNA expression in db/db and db/+ male mice (n=9/genotype). Plasma adropin concentrations in db/db and db/+ male mice (n=9-10/genotype). Incremental modulus of elasticity ( $E_{inc}$ ) of mesenteric arteries of db/db and db/+ male mice (n=9-

10/genotype). **(D)** Adropin mRNA expression in various tissues harvested from adropin knockout and wild-type littermate male mice (n=5-14/genotype). Final body weight of adropin knockout and wild-type littermate male mice (n=9-14/genotype). Blood glucose concentration during a glucose tolerance test in adropin knockout and wild-type littermate male mice (n=10-14/genotype).  $E_{inc}$  of mesenteric arteries from adropin knockout and wild-type littermate male mice (n=9-14/genotype). Student's unpaired *t*-tests were performed in all panels.  $E_{inc}$  data (panels C-D) are represented using simple linear regression. Mann-Whitney test was performed for the comparison of adropin mRNA expression in the brain (panel D). A two-way, repeated measures ANOVA was performed to assess glucose tolerance (panel D). \* $P$ <0.05 compared to control.

**A.**



**B.**



**C.**

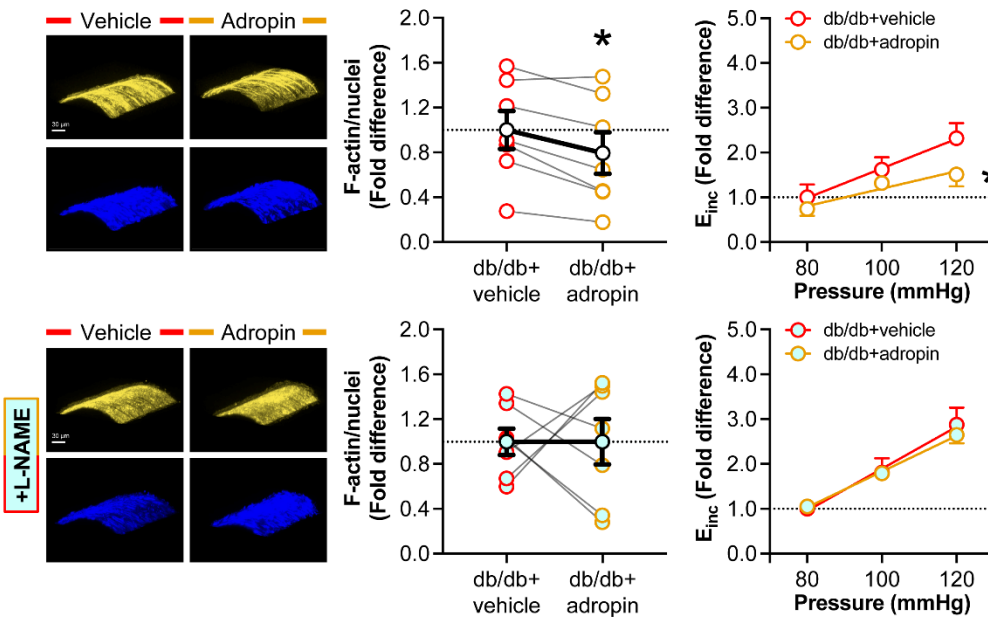
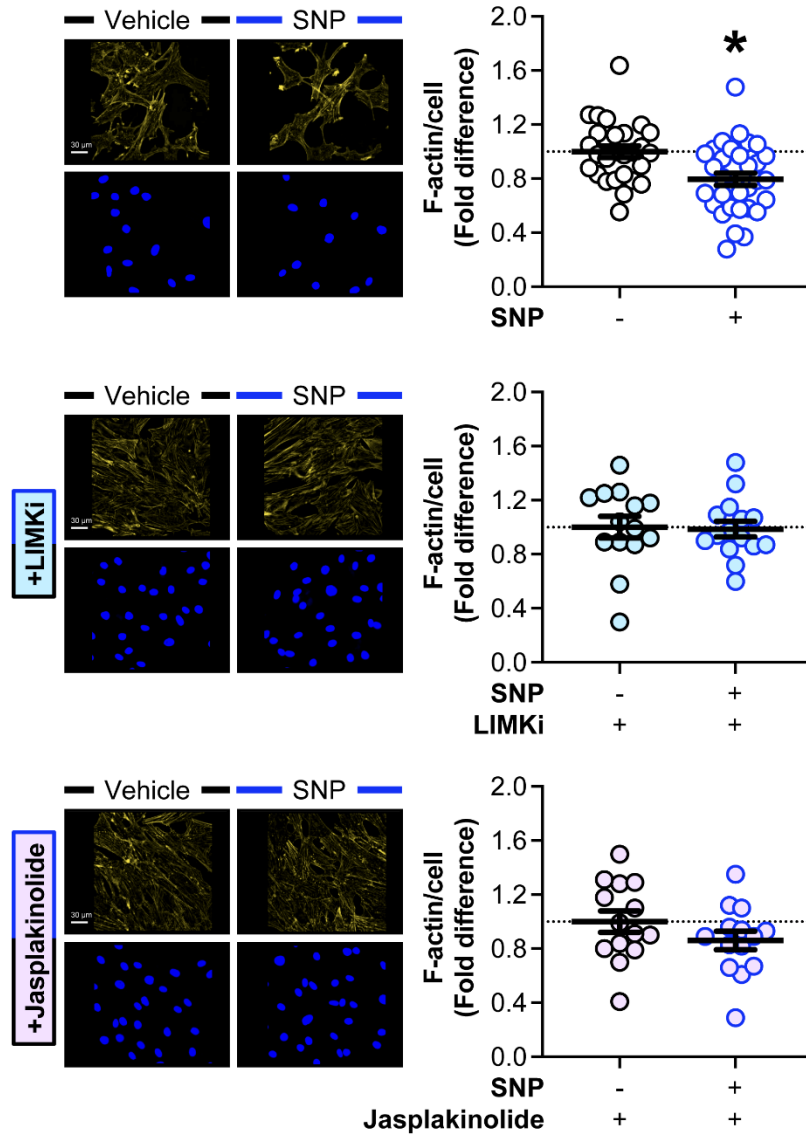


**Figure 2.** Adropin reduces F-actin stress fibers and stiffness in endothelial cells (EC) and isolated mesenteric arteries of db/db male mice: role of NO.

**(A)** Phosphorylation of eNOS Ser 1177 relative to total eNOS in human aortic EC treated with vehicle vs. adropin (10ng/mL) for 30 minutes (n=8-9/condition); representative Western blot images are also included. Only the top band was responsive to adropin and selected for quantification and analysis. Nitrate concentrations in the supernatant of human aortic EC treated with vehicle vs. adropin (10ng/mL) for 24 hours (n=11/condition). **(B)** Volume of F-actin stress fibers in human aortic EC treated with vehicle vs. adropin (10ng/mL) for 24 hours (n=20-24/condition); representative confocal microscope images of F-actin (yellow) and nuclei (blue) are also included (scale bar 30 $\mu$ m). Cortical stiffness of human aortic EC treated with vehicle vs. adropin (10ng/mL) for 24 hours (n=18/condition). Below panels are repeat experiments in the presence of L-NAME (added 30 minutes prior to adropin) (n=17-18/condition). **(C)** Volume of F-actin content and incremental modulus of elasticity ( $E_{inc}$ ) of isolated mesenteric arteries from db/db male mice treated with vehicle vs. adropin (10ng/mL) for 24 hours (n=8/condition); representative images of confocal microscope images of F-actin (yellow) and nuclei (blue) are also included (scale 30 $\mu$ m). Below panels are repeat experiments in the presence of L-NAME (added 30 minutes prior to adropin) (n=7-8/group). Student's unpaired (panels A, B) and paired *t*-tests (panel C) were performed, according to experimental design.  $E_{inc}$  data (panel C) are represented using simple linear regression. \* $P$ <0.05 compared to control.



**A.**



**B.**

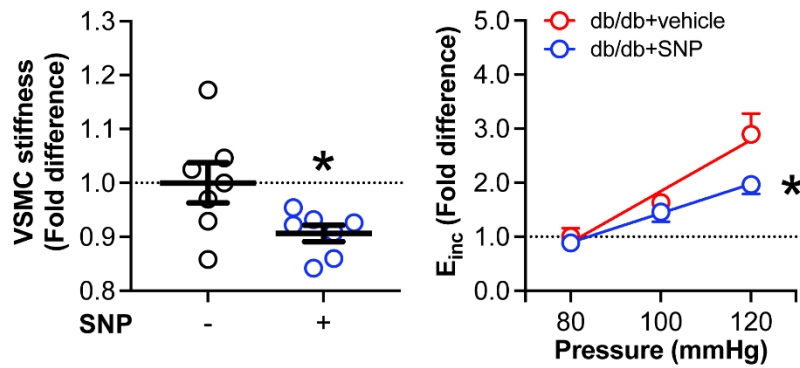


**Figure 3.** Stimulation of vascular smooth muscle cells (VSMC) with sodium nitroprusside (SNP), an NO mimetic, reduces F-actin stress fibers and stiffness.

**(A)** Volume of F-actin stress fibers in human coronary artery VSMC treated with vehicle vs. SNP (10 $\mu$ M) for 1 hour (n=28-32/condition); representative fluorescent images of F-actin (yellow) and nuclei (blue) are also included (scale bar 30 $\mu$ m). Below panels are repeat experiments in the presence of LIMKi or jasplakinolide (added 30 minutes prior to SNP) (n=14-16/condition). **(B)** Cortical stiffness of human coronary artery VSMC treated with vehicle vs. SNP (10 $\mu$ M) for 1 hour (n=6=7/condition). Incremental modulus of elasticity ( $E_{inc}$ ) of mesenteric arteries from db/db male mice treated with vehicle vs. SNP (10 $\mu$ M) for 4 hours (n=14-16/condition). Student's unpaired (panels A, B) and paired (panel B) *t*-tests were performed, according to experimental design.  $E_{inc}$  data are represented using simple linear regression. \* $P$ <0.05 compared to control.

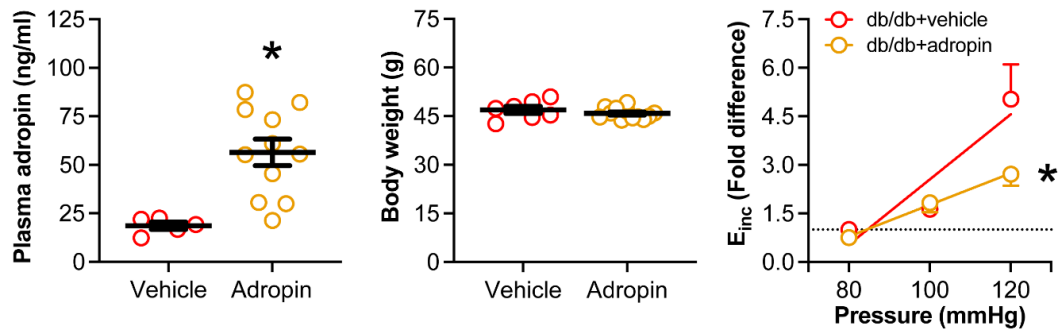


**Figure 4.** *In vivo* treatment of db/db male mice with adropin for four weeks reduces mesenteric arterial stiffness.

Plasma adropin concentration in db/db male mice implanted with osmotic minipumps containing either vehicle or adropin (63 $\mu$ g/kg/hour, n=5-11/group). Final body weight of db/db male mice after four weeks of vehicle or adropin administration (n=7-12/group). Incremental modulus of elasticity (E<sub>inc</sub>) of mesenteric arteries after four weeks of vehicle or adropin administration (n=6-12/group). Student's unpaired and paired *t*-tests were performed, as appropriate. E<sub>inc</sub> data are represented using simple linear regression. \**P*<0.05 compared to control.

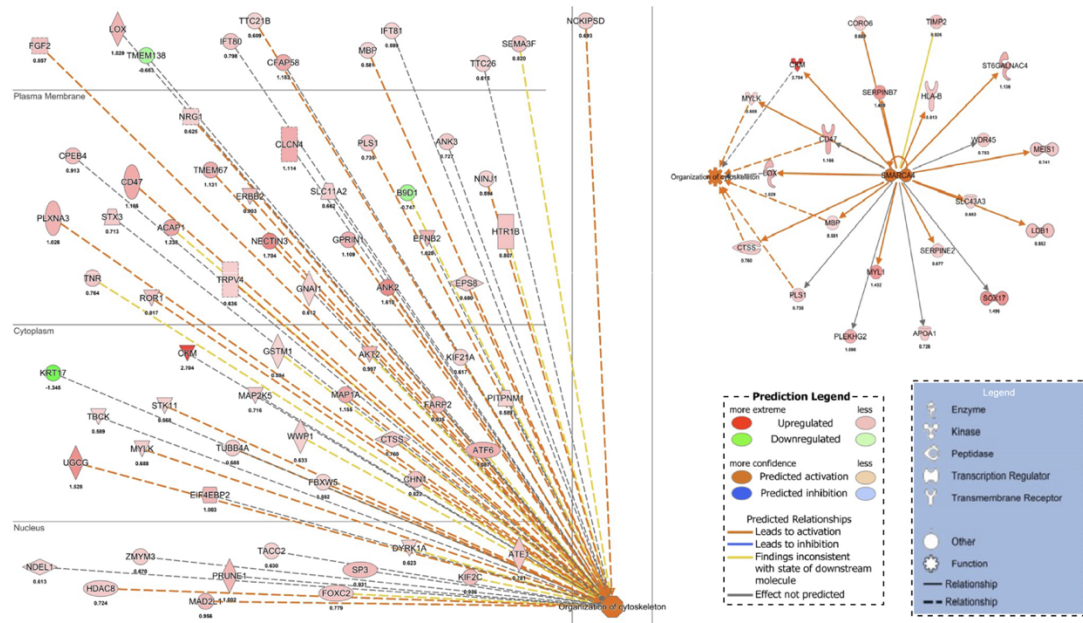


**Figure 5.** Proteomic analysis of endothelial cells treated with vehicle vs. adropin.

Upregulation of pathways linked to organization of the cytoskeleton in human aortic endothelial cells treated with vehicle vs. adropin (10ng/mL) for 24 hours (n=10/condition). Data expressed as average log<sub>2</sub> ratio relative to vehicle. Student's unpaired *t*-test was performed for all protein comparisons (see supplementary material for further description of the statistical analysis and individual proteins within figure).

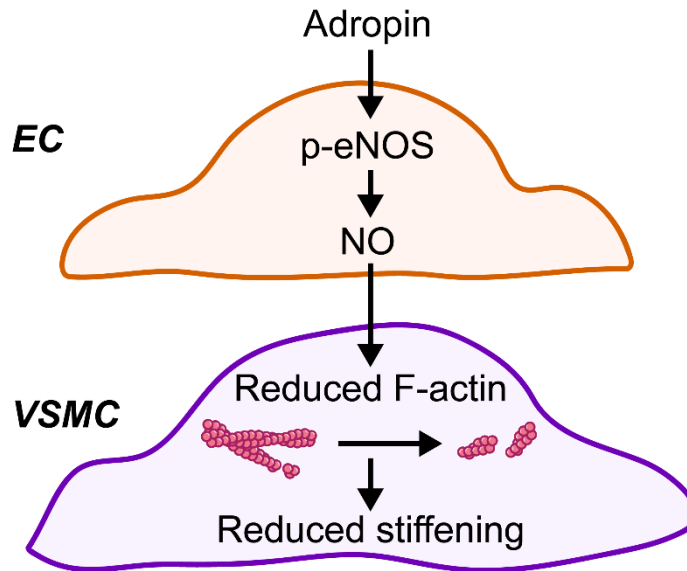
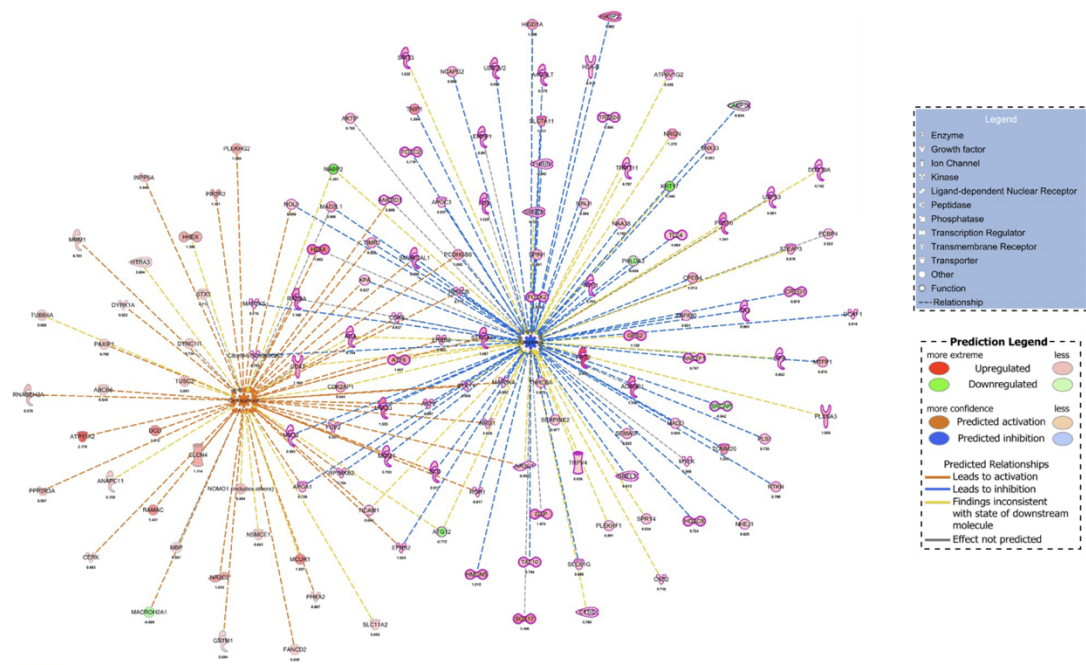


**Figure 6.** Schematic illustrating the interpretation of the results.

Adropin-induced NO production in endothelial cells (EC) promotes vascular smooth muscle cell (VSMC) actin depolymerization and reduced stiffness. De-stiffening of VSMC likely contributes to reduced whole-artery stiffness. Not depicted here, adropin also causes actin depolymerization and reduced stiffness in EC. While endothelial rigidity does not physically contribute to whole-artery stiffness, it is possible that decreased EC stiffness augments endothelial nitric oxide synthase activation and, consequently, increased nitric oxide signaling in VSMC.



**Supplemental Figure 1.** Proteomic analysis of endothelial cells treated with vehicle vs. adropin.

Upregulation of pathways linked to cell survival (left) and suppression of apoptosis (224) in human aortic endothelial cells treated with vehicle vs. adropin (10ng/mL) for 24 hours (n=10/condition). Data expressed as average log<sub>2</sub> ratio relative to vehicle. Student's unpaired *t*-test was performed for all protein comparisons

## CHAPTER 4: Summary and Future Directions

Increased arterial stiffening contributes to the development of cardiovascular disease and is an independent predictor of cardiovascular morbidity and mortality (47, 186, 187). Elucidating the factors that regulate the onset of obesity and T2D-mediated arterial stiffening is vital for the synthesis of new therapeutic targets to reduce the burden of cardiovascular disease. Herein, adropin, a metabolic peptide that is inversely associated with insulin resistance and arterial stiffening, directly contributes to the regulation of arterial stiffening in a NO-mediated manner.

In liver samples isolated from bariatric surgery patients, we report that hepatic *Enho* mRNA expression is decreased in individuals that exhibit an increased BMI in concert with elevated HbA1c. This evidence provides support that circulating adropin concentrations are related to metabolic function and further supports the notion that adropin concentrations are a potential biomarker of metabolic health (6). Moreover, we report that reduced hepatic expression of *Enho* and circulating concentrations of adropin were associated with increased arterial stiffening in T2D, supporting previous findings that adropin is inversely correlated with arterial stiffness. In addition, male db/db mice, a genetic mouse model of obesity and insulin resistance, exhibited decreased hepatic *Enho* mRNA expression and circulating adropin, which was accompanied by increased mesenteric arterial stiffness. Given the relationship surrounding metabolic

dysfunction, arterial stiffness and adropin, we sought to interrogate the direct effects of adropin on arterial stiffening.

In order to determine the role of adropin on arterial stiffness, first we determined that mesenteric arteries isolated from whole-body AdrKO mice demonstrated increased stiffness relative to their wild-type controls. The increased arterial stiffness observed in the AdrKO mice was independent of increased obesity or metabolic dysfunction. This is the first evidence to support that the loss of adropin alone can induce stiffness. Given that previous studies report that the loss of adropin exacerbates the adiposity and insulin resistance (20, 152), it would be intriguing to interrogate whether a similar phenomenon would occur in the stiffening of arteries.

Second, our findings corroborate that adropin stimulated the phosphorylation of eNOS and increased nitrite production (8), a surrogate measure of NO production. Subsequently, endothelial cells treated with adropin had a reduction in F-actin stress fibers, thereby inducing a decrease in cortical stiffness. Decreased F-actin stress fibers and cortical stiffness was abrogated in the presence of L-NAME, indicating that these effects are mediated by adropin-induced NO. Furthermore, 24 hours of adropin incubation reduced arterial stiffness in concert with decreased F-actin, which was abolished with L-NAME co-treatment. It should be noted that decreased endothelial cell cortical stiffness induces NO production via two posited mechanisms (73): 1) increased G-actin associated activation of eNOS (81) and 2) mechanosensitive  $Ca^{2+}$  channels in the membrane which are susceptible to shear stress (84, 85). While G-actin



interacts with eNOS to induce the production of NO (81), adropin did not increase G-actin in either endothelial cells or isolated arteries (data not shown). Furthermore, the 24-hour adropin-treatment protocol was performed on unpressurized arteries and stiffness was determined without flow, indicating adropin mediating these effects through an independent mechanism, i.e., adropin mediated production of NO. Moreover, collagen content, a major contributing factor in the progression obesity associated arterial stiffening (43), was unaltered post adropin treatment (data not shown). Importantly, we are not suggesting that decreased endothelial cell stiffness alone is inducing reductions in whole arterial stiffness, but rather that the reduced arterial stiffness is likely due to increased NO production mediated by adropin.

Given the increased appreciation for the role of the cytoskeleton plays in arterial stiffening (90), VSMCs were treated with adropin to interrogate any endothelial-independent alteration in cytoskeletal stiffness. Unlike endothelial cells, adropin did not decrease VSMC cortical stiffness (data not shown), further suggesting that the adropin-induced decreases in arterial stiffness are NO mediated. Subsequently, treatment with an NO-mimetic, SNP, induced a reduction in polymerized actin and VSMC cortical stiffness. Furthermore, we recapitulated the SNP-induced reduced arterial stiffness in mesenteric arteries of db/db mice. Since NO regulates enzymes associated with cytoskeletal remodeling upstream of LIMK through inhibition of the RhoA-ROCK pathway and TG-2 activity resulting in the increased cofilin-mediated actin depolymerization (96, 108, 110, 204), we reasoned that the addition of a LIMK inhibitor would not

augment SNP-induced reductions in polymerized actin and VSMC stiffness. Indeed, the co-incubation of SNP and the LIMK inhibitor 3 (LIMKi) did not result in an augmentation in actin depolymerization, likely due to SNP and LIMKi mediating their effects through the RhoA-ROCK pathway (96, 108, 110, 204). Conversely, we hypothesized if actin polymerization and stabilization was induced via jasplakinolide-incubation (225), then SNP-induced decreases in F-actin in VSMCs would be abolished. Here, we report SNP-induced actin depolymerization did not overcome jasplakinolide-induced actin polymerization. Collectively, these findings support the notion that adropin-induced reductions in arterial stiffening is mediated through the production of NO and depolymerization of actin.

To date, adropin signaling in endothelial cells is linked with activation of VEGFR2 (8). In order to elucidate a better understanding of the effects of adropin on the endothelium a proteomic data analysis was performed. Herein, we report that a total of 421 proteins were differentially expressed in endothelial cells treated with adropin for 24 hours relative to vehicle-treated endothelial cells. Following an unbiased ingenuity pathway analysis, the most upregulated upstream regulator was SMARCA4, which was linked with organization of the cytoskeleton. SMARCA4 encodes for SWI/SNF complex containing brahma-related gene 1, a transcription activator associated with angiogenesis (205, 206), which supports previous findings of adropin-induced angiogenesis (8). Furthermore, reorganization of the cytoskeleton was one of the most activated molecular networks following adropin incubation. In addition, adropin augmented

the cell survival molecular pathways in concert with suppression of the apoptotic pathways in endothelial cells, corroborating previous findings (8). The results of the proteomic analysis indicate that adropin promotes the cytoskeletal remodeling and cell survival, potentially through increased NO bioavailability and thereby promoting endothelial health.

Subsequently, to investigate the physiological effects of adropin as a potential therapeutic target to decreased arterial stiffening associated with obesity and insulin resistance, we chronically treated db/db mice with adropin at a pharmacological dose using surgically implanted, subcutaneous osmotic minipumps. Adropin administration did not significantly influence body weight or circulating metabolic markers. However, adropin reduced arterial stiffening of mesenteric arteries in db/db mice, indicating that the effects of adropin on arterial stiffness were independent of metabolic function.

Several aspects of the current work necessitate further consideration. First, the inverse relationship of human carotid-to-femoral PWV and adropin provides clinical relevance considering the relationship between aortic arterial stiffness and the risk for a major cardiovascular event (2). In the current study, mesenteric resistance arteries were utilized to assess arterial stiffness in our mouse models. Previous research has posited remodeling of resistance arteries may occur prior to conduit arterial stiffening (226), which may account for the adropin-induced effects on resistance arteries independent of effects on aortic stiffening (data not shown). In addition to the considerations of the arteries studied, the age of the db/db mice used in this study should be noted.

Previously, db/db mice at 12-weeks-of-age do not to exhibit increase arterial stiffness relative to db/+ mice (51). Souza-Smith et al. compared arterial remodeling between db/db mice and db/+ littermates, and reported they are phenotypically similar to wild-type mice. In a subsequent study, db/+ mice are glucose intolerant compared to their wild-type littermates (227), suggesting that there may be some metabolic alterations that are similar to those observed with early insulin resistance and therefore a better control may be a C57BK6 mouse. Given that a significant reduction in mesenteric arterial stiffness of C57BK6 following adropin treatment was not detected (data not shown), the observed reduction in arterial stiffness in db/db mice following adropin treatment would indicate that some arterial remodeling has taken place. Furthermore, even though the progression of arterial stiffening is not universal throughout the arterial tree, smooth muscle cytoskeletal remodeling is an important causal factor in the development of arterial stiffening in small and large arteries (76, 90, 91, 96). Therefore, the observation that adropin-induced reduction in arterial stiffness through NO-mediated actin depolymerization further supports the role of the cytoskeletal regulation on arterial stiffening. Second, while previous studies have reported that exogenous adropin augments (40) and induces endothelial-dependent vasodilation (170), we do not report those findings here despite this being the initial motivator for this work. Kwon et al. (40) reported an improvement in endothelial function of aged arteries with adropin present during the vascular assessments, but did not assess whether adropin induced vasodilation in a pressurized artery. In our hands, adropin did not impact

endothelial-dependent vasodilation in the AdrKO or the 4-week adropin-treated mice (data not shown). This would indicate that presence of adropin may be required for priming the phosphorylation of eNOS and the production of NO through Akt activation, which is Ca<sup>2+</sup>-independent, to elicit augmented endothelial-dependent vasodilation. Alternatively, adropin has been reported to decrease reactive oxygen species (228), which could result in the increased bioavailability of NO and endothelial function of aged arteries. Third, the receptor for adropin-mediated effects on endothelial cells remains to be fully elucidated and controversial. Several studies have indicated that the receptor for adropin is tissue specific but has mostly centered around GPR19 (9, 131, 132), however there is some dispute here (133). Moreover, Lovren et al. (8) demonstrated that silencing of the VEGFR2 receptor abrogated adropin-mediated activation of eNOS and Erk1/2 in endothelial cells, suggesting that adropin effects mediated through VEGFR2 is endothelial cell specific. Therefore, determining the receptor the adropin in the vasculature could result in novel therapeutics for arterial stiffening. Finally, while data from men and women were used to establish the inverse correlation between circulating concentrations of adropin and arterial stiffness, only male mice were utilized in the project. Given that estrogen regulates adropin expression in the liver (136, 137), and that estrogens play a protective role in the vasculature, it could be posited that adropin production in endothelial cells may also be regulated in part by estrogen. Collectively, this would suggest that adropin is likely playing a similar role between the sexes, specifically in the vasculature, but this needs to be verified in future studies.

Taken together, the current study expands upon previous work that adropin exerts effects on the cardiovascular system, specifically in regulating arterial stiffening. For the first time we report that the lack of adropin alone is sufficient to induce arterial stiffening. Conversely, adropin induced a reduction in arterial stiffening in obesity and T2D, which is likely through an NO-dependent reduction in cytoskeletal actin polymerization. Given that arterial stiffening is an independent predictor of cardiovascular morbidity and mortality, augmenting adropin concentration provides a novel therapeutic target for the prevention of arterial stiffening associated with obesity and T2D.

#### Future directions

The current study provides evidence that adropin is directly associated with the regulation of arterial stiffening. While not presented in the current study, four-weeks of adropin administration resulted in a nonsignificant trend toward decreased collagen content in mesenteric arteries (data not presented). Furthermore, we concluded that adropin-mediated reductions in arterial stiffening were likely due to NO-mediated reductions in cytosolic stress fiber accumulation. In addition to being a vasodilator, NO regulates proteins associated with arterial remodeling, like TG-2. TG-2, predominately a cytosolic protein, when in the extracellular space is capable of increasing actin polymerization via activation of the RhoA-Rock pathway and induce collagen crosslinking, thereby increasing arterial stiffness (96, 106). Therefore, understanding whether adropin may regulate collagen content and/or crosslinking remains to be explored and could

provide further mechanistic insight into how adropin may be mediating reductions in arterial stiffness.

Given the age of the mice that underwent adropin administration, it could be argued that the reduction in arterial stiffening was in fact a mitigation of the progression of arterial stiffening rather than decreased stiffening. In other words, adropin may prevent the development of arterial stiffening and therefore it remains unclear whether it can restore arteries after a prolonged period of obesity and insulin resistance-induced arterial stiffening. It should be noted that the adropin treated db/db mice were sacrificed at 13 weeks of age, which is earlier than the previously reported onset of arterial stiffening that occurs by 16 weeks of age (51), therefore supporting this notion. Thus, it would be interesting to see whether the current findings are recapitulated in the setting of more severe arterial stiffening associated with prolonged age and duration of insulin resistance.

In addition to being negatively associated with metabolic dysfunction, adropin is inversely associated with age. Increased age is a risk factor for the development of cardiovascular disease, as well as neural cognitive decline. Alzheimer's disease and vascular dementia are the most common forms of cognitive impairments in the elderly. Adropin has been reported to be neuroprotective in the setting of intracerebral ischemia and hemorrhage, decreasing infarct volume and lesion volume, respectively (135, 185). Furthermore, adropin administration mitigated cognitive deficits associated with stroke and hemorrhage (135, 185). Given that Alzheimer's disease and

dementia appear to be influenced by arterial stiffening (229), elucidating the role of adropin on cerebral arterial stiffening could result in novel and exciting findings.



## Bibliography

1. Aroor AR, Demarco VG, Jia G, Sun Z, Nistala R, Meininger GA, et al. The role of tissue Renin-Angiotensin-aldosterone system in the development of endothelial dysfunction and arterial stiffness. *Front Endocrinol (Lausanne)*. 2013;4:161.
2. Mitchell GF, Hwang SJ, Vasan RS, Larson MG, Pencina MJ, Hamburg NM, et al. Arterial stiffness and cardiovascular events: the Framingham Heart Study. *Circulation*. 2010;121(4):505-11.
3. Jia G, Aroor AR, Sowers JR. Arterial Stiffness: A Nexus between Cardiac and Renal Disease. *Cardiorenal Med*. 2014;4(1):60-71.
4. Liao J, Farmer J. Arterial stiffness as a risk factor for coronary artery disease. *Curr Atheroscler Rep*. 2014;16(2):387.
5. Kumar KG, Trevaskis JL, Lam DD, Sutton GM, Koza RA, Chouljenko VN, et al. Identification of adropin as a secreted factor linking dietary macronutrient intake with energy homeostasis and lipid metabolism. *Cell metabolism*. 2008;8(6):468-81.
6. Jasaszwili M, Billert M, Strowski MZ, Nowak KW, Skrzypski M. Adropin as A Fat-Burning Hormone with Multiple Functions-Review of a Decade of Research. *Molecules*. 2020;25(3).
7. Mushala BA, Scott I. ADROPIN: A HEPATOKINE MODULATOR OF VASCULAR FUNCTION AND CARDIAC FUEL METABOLISM. *American journal of physiology Heart and circulatory physiology*. 2020.
8. Lovren F, Pan Y, Quan A, Singh KK, Shukla PC, Gupta M, et al. Adropin is a novel regulator of endothelial function. *Circulation*. 2010;122(11 Suppl):S185-S92.
9. Thapa D, Stoner MW, Zhang M, Xie B, Manning JR, Guimaraes D, et al. Adropin regulates pyruvate dehydrogenase in cardiac cells via a novel GPCR-MAPK-PDK4 signaling pathway. *Redox Biol*. 2018;18:25-32.
10. Topuz M, Celik A, Aslantas T, Demir AK, Aydin S, Aydin S. Plasma adropin levels predict endothelial dysfunction like flow-mediated dilatation in patients with type 2 diabetes mellitus. *J Investig Med*. 2013;61(8):1161-4.
11. Yu H-y, Zhao P, Wu M-c, Liu J, Yin W. Serum adropin levels are decreased in patients with acute myocardial infarction. *Regul Pept*. 2014;190-191:46-9.
12. Zhao L-P, Xu W-T, Wang L, You T, Chan S-P, Zhao X, et al. Serum adropin level in patients with stable coronary artery disease. *Heart Lung Circ*. 2015;24(10):975-9.
13. Zheng J, Liu M, Chen L, Yin F, Zhu X, Gou J, et al. Association between serum adropin level and coronary artery disease: a systematic review and meta-analysis. *Cardiovasc Diagn Ther*. 2019;9(1):1-7.
14. Fujie S, Hasegawa N, Kurihara T, Sanada K, Hamaoka T, Iemitsu M. Association between aerobic exercise training effects of serum adropin level, arterial stiffness, and adiposity in obese elderly adults. *Appl Physiol Nutr Metab*. 2017;42(1):8-14.
15. Fujie S, Hasegawa N, Sato K, Fujita S, Sanada K, Hamaoka T, et al. Aerobic exercise training-induced changes in serum adropin level are associated with reduced

- arterial stiffness in middle-aged and older adults. *American journal of physiology Heart and circulatory physiology*. 2015;309(10):H1642-H7.
16. Marczuk N, Cecerska-Heryć E, Jesionowska A, Dołęgowska B. Adropin - physiological and pathophysiological role. *Postepy Hig Med Dosw (Online)*. 2016;70(0):981-8.
  17. Wang S-p, Gao Y-l, Liu G, Deng D, Chen R-j, Zhang Y-z, et al. Molecular cloning, characterization and expression of the energy homeostasis-associated gene in piglet. *J Zhejiang Univ Sci B*. 2015;16(6):524-32.
  18. Aydin S, Kuloglu T, Aydin S. Copeptin, adropin and irisin concentrations in breast milk and plasma of healthy women and those with gestational diabetes mellitus. *Peptides*. 2013;47:66-70.
  19. Aydin S. Three new players in energy regulation: preptin, adropin and irisin. *Peptides*. 2014;56:94-110.
  20. Ganesh Kumar K, Zhang J, Gao S, Rossi J, McGuinness OP, Halem HH, et al. Adropin deficiency is associated with increased adiposity and insulin resistance. *Obesity (Silver Spring, Md)*. 2012;20(7):1394-402.
  21. Butler AA, Tam CS, Stanhope KL, Wolfe BM, Ali MR, O'Keeffe M, et al. Low circulating adropin concentrations with obesity and aging correlate with risk factors for metabolic disease and increase after gastric bypass surgery in humans. *The Journal of Clinical Endocrinology & Metabolism*. 2012;97(10):3783-91.
  22. Yang C, DeMars KM, Candelario-Jalil E. Age-Dependent Decrease in Adropin is Associated with Reduced Levels of Endothelial Nitric Oxide Synthase and Increased Oxidative Stress in the Rat Brain. *Aging and disease*. 2018;9(2):322-30.
  23. Glück M, Glück J, Wiewióra M, Rogala B, Piecuch J. Serum Irisin, Adropin, and Preptin in Obese Patients 6 Months After Bariatric Surgery. *Obes Surg*. 2019;29(10):3334-41.
  24. Zhang H, Jiang L, Yang Y-J, Ge R-K, Zhou M, Hu H, et al. Aerobic exercise improves endothelial function and serum adropin levels in obese adolescents independent of body weight loss. *Scientific Reports*. 2017;7(1):17717-.
  25. Soori R, Amini AA, Choobineh S, Eskandari A, Behjat A, Ghram A, et al. Exercise attenuates myocardial fibrosis and increases angiogenesis-related molecules in the myocardium of aged rats. *Arch Physiol Biochem*. 2019:1-6.
  26. Celik E, Yilmaz E, Celik O, Ulas M, Turkuoglu I, Karaer A, et al. Maternal and fetal adropin levels in gestational diabetes mellitus. *Journal of Perinatal Medicine* 2013. p. 375.
  27. Wu L, Fang J, Chen L, Zhao Z, Luo Y, Lin C, et al. Low serum adropin is associated with coronary atherosclerosis in type 2 diabetic and non-diabetic patients. *Clin Chem Lab Med*. 2014;52(5):751-8.
  28. St-Onge M-P, Shechter A, Shlisky J, Tam CS, Gao S, Ravussin E, et al. Fasting plasma adropin concentrations correlate with fat consumption in human females. *Obesity (Silver Spring, Md)*. 2014;22(4):1056-63.
  29. Ghoshal S, Stevens JR, Billon C, Girardet C, Sitaula S, Leon AS, et al. Adropin: An endocrine link between the biological clock and cholesterol homeostasis. *Molecular metabolism*. 2018;8:51-64.

30. Gao S, McMillan RP, Jacas J, Zhu Q, Li X, Kumar GK, et al. Regulation of substrate oxidation preferences in muscle by the peptide hormone adropin. *Diabetes*. 2014;63(10):3242-52.
31. Gao S, Ghoshal S, Zhang L, Stevens JR, McCommis KS, Finck BN, et al. The peptide hormone adropin regulates signal transduction pathways controlling hepatic glucose metabolism in a mouse model of diet-induced obesity. *J Biol Chem*. 2019;294(36):13366-77.
32. Gao S, McMillan RP, Zhu Q, Lopaschuk GD, Hulver MW, Butler AA. Therapeutic effects of adropin on glucose tolerance and substrate utilization in diet-induced obese mice with insulin resistance. *Molecular metabolism*. 2015;4(4):310-24.
33. Thapa D, Xie B, Manning JR, Zhang M, Stoner MW, Huckestein BR, et al. Adropin reduces blood glucose levels in mice by limiting hepatic glucose production. *Physiological reports*. 2019;7(8):e14043-e.
34. Koves TR, Ussher JR, Noland RC, Slentz D, Mosedale M, Ilkayeva O, et al. Mitochondrial overload and incomplete fatty acid oxidation contribute to skeletal muscle insulin resistance. *Cell metabolism*. 2008;7(1):45-56.
35. Erdol M, Ertem S, Ertem AG, Demirtas K, Unal S, Karanfil M, et al. Adropin: Connection between Nonalcoholic Fatty Liver Disease and Coronary Artery Disease. *Med Princ Pract*. 2019;10.1159/000502039.
36. Sato K, Yamashita T, Shirai R, Shibata K, Okano T, Yamaguchi M, et al. Adropin Contributes to Anti-Atherosclerosis by Suppressing Monocyte-Endothelial Cell Adhesion and Smooth Muscle Cell Proliferation. *Int J Mol Sci*. 2018;19(5):1293.
37. Bolayır HA, Kivrak T, Gunes H, Bolayır A, Karaca I. Adropin and circadian variation of blood pressure. *Kardiol Pol*. 2018;76(4):776-82.
38. Gulen B, Eken C, Kucukdagli OT, Serinken M, Kocyigit A, Kılıc E, et al. Adropin levels and target organ damage secondary to high blood pressure in the ED. *Am J Emerg Med*. 2016;34(11):2061-4.
39. Oruc CU, Akpınar YE, Dervisoglu E, Amikishiyev S, Salmaslioglu A, Gurdol F, et al. Low concentrations of adropin are associated with endothelial dysfunction as assessed by flow-mediated dilatation in patients with metabolic syndrome. *Clin Chem Lab Med*. 2017;55(1):139-44.
40. Kwon OS, Andtbacka RHI, Hyngstrom JR, Richardson RS. Vasodilatory function in human skeletal muscle feed arteries with advancing age: the role of adropin. *The Journal of physiology*. 2019;597(7):1791-804.
41. Padilla J, Olver TD, Thyfault JP, Fadel PJ. Role of habitual physical activity in modulating vascular actions of insulin. *Experimental physiology*. 2015;100(7):759-71.
42. Ozbay S, Ulupınar S, Şebin E, Altınkaynak K. Acute and chronic effects of aerobic exercise on serum irisin, adropin, and cholesterol levels in the winter season: Indoor training versus outdoor training. *Chin J Physiol*. 2020;63(1):21-6.
43. Aroor AR, Jia G, Sowers JR. Cellular mechanisms underlying obesity-induced arterial stiffness. *American journal of physiology Regulatory, integrative and comparative physiology*. 2018;314(3):R387-r98.
44. Jia G, Aroor AR, DeMarco VG, Martinez-Lemus LA, Meininger GA, Sowers JR. Vascular stiffness in insulin resistance and obesity. *Front Physiol*. 2015;6:231.

45. Seifalian AM, Filippatos TD, Joshi J, Mikhailidis DP. Obesity and arterial compliance alterations. *Current vascular pharmacology*. 2010;8(2):155-68.
46. Padilla J, Vieira-Potter VJ, Jia G, Sowers JR. Role of perivascular adipose tissue on vascular reactive oxygen species in type 2 diabetes: a give-and-take relationship. *Diabetes*. 2015;64(6):1904-6.
47. Townsend RR, Wilkinson IB, Schiffrin EL, Avolio AP, Chirinos JA, Cockcroft JR, et al. Recommendations for Improving and Standardizing Vascular Research on Arterial Stiffness: A Scientific Statement From the American Heart Association. *Hypertension (Dallas, Tex : 1979)*. 2015;66(3):698-722.
48. Martinez-Lemus LA, Hill MA, Meininger GA. The plastic nature of the vascular wall: a continuum of remodeling events contributing to control of arteriolar diameter and structure. *Physiology (Bethesda)*. 2009;24:45-57.
49. Bender SB, Castorena-Gonzalez JA, Garro M, Reyes-Aldasoro CC, Sowers JR, DeMarco VG, et al. Regional variation in arterial stiffening and dysfunction in Western diet-induced obesity. *American journal of physiology Heart and circulatory physiology*. 2015;309(4):H574-82.
50. Foote CA, Castorena-Gonzalez JA, Ramirez-Perez FI, Jia G, Hill MA, Reyes-Aldasoro CC, et al. Arterial Stiffening in Western Diet-Fed Mice Is Associated with Increased Vascular Elastin, Transforming Growth Factor- $\beta$ , and Plasma Neuraminidase. *Front Physiol*. 2016;7:285.
51. Souza-Smith FM, Katz PS, Trask AJ, Stewart JA, Jr., Lord KC, Varner KJ, et al. Mesenteric resistance arteries in type 2 diabetic db/db mice undergo outward remodeling. *PloS one*. 2011;6(8):e23337.
52. Rajendran P, Rengarajan T, Thangavel J, Nishigaki Y, Sakthisekaran D, Sethi G, et al. The vascular endothelium and human diseases. *Int J Biol Sci*. 2013;9(10):1057-69.
53. Sandoo A, van Zanten JJ, Metsios GS, Carroll D, Kitis GD. The endothelium and its role in regulating vascular tone. *Open Cardiovasc Med J*. 2010;4:302-12.
54. Barac A, Campia U, Panza JA. Methods for evaluating endothelial function in humans. *Hypertension (Dallas, Tex : 1979)*. 2007;49(4):748-60.
55. Meza CA, La Favor JD, Kim DH, Hickner RC. Endothelial Dysfunction: Is There a Hyperglycemia-Induced Imbalance of NOX and NOS? *Int J Mol Sci*. 2019;20(15).
56. BelAiba RS, Djordjevic T, Petry A, Diemer K, Bonello S, Banfi B, et al. NOX5 variants are functionally active in endothelial cells. *Free Radic Biol Med*. 2007;42(4):446-59.
57. Jay DB, Papaharalambus CA, Seidel-Rogol B, Dikalova AE, Lassègue B, Griendling KK. Nox5 mediates PDGF-induced proliferation in human aortic smooth muscle cells. *Free Radic Biol Med*. 2008;45(3):329-35.
58. Pandey D, Patel A, Patel V, Chen F, Qian J, Wang Y, et al. Expression and functional significance of NADPH oxidase 5 (Nox5) and its splice variants in human blood vessels. *American journal of physiology Heart and circulatory physiology*. 2012;302(10):H1919-28.
59. Jha JC, Dai A, Holterman CE, Cooper ME, Touyz RM, Kennedy CR, et al. Endothelial or vascular smooth muscle cell-specific expression of human NOX5 exacerbates renal inflammation, fibrosis and albuminuria in the Akita mouse. *Diabetologia*. 2019;62(9):1712-26.

60. Taye A, Saad AH, Kumar AH, Morawietz H. Effect of apocynin on NADPH oxidase-mediated oxidative stress-LOX-1-eNOS pathway in human endothelial cells exposed to high glucose. *European journal of pharmacology*. 2010;627(1-3):42-8.
61. Williams CR, Lu X, Sutliff RL, Hart CM. Rosiglitazone attenuates NF- $\kappa$ B-mediated Nox4 upregulation in hyperglycemia-activated endothelial cells. *Am J Physiol Cell Physiol*. 2012;303(2):C213-23.
62. Chen F, Qian LH, Deng B, Liu ZM, Zhao Y, Le YY. Resveratrol protects vascular endothelial cells from high glucose-induced apoptosis through inhibition of NADPH oxidase activation-driven oxidative stress. *CNS Neurosci Ther*. 2013;19(9):675-81.
63. Wang H, Yang Z, Jiang Y, Hartnett ME. Endothelial NADPH oxidase 4 mediates vascular endothelial growth factor receptor 2-induced intravitreal neovascularization in a rat model of retinopathy of prematurity. *Mol Vis*. 2014;20:231-41.
64. Craige SM, Chen K, Pei Y, Li C, Huang X, Chen C, et al. NADPH oxidase 4 promotes endothelial angiogenesis through endothelial nitric oxide synthase activation. *Circulation*. 2011;124(6):731-40.
65. Ray R, Murdoch CE, Wang M, Santos CX, Zhang M, Alom-Ruiz S, et al. Endothelial Nox4 NADPH oxidase enhances vasodilatation and reduces blood pressure in vivo. *Arteriosclerosis, thrombosis, and vascular biology*. 2011;31(6):1368-76.
66. Lee DY, Wauquier F, Eid AA, Roman LJ, Ghosh-Choudhury G, Khazim K, et al. Nox4 NADPH oxidase mediates peroxynitrite-dependent uncoupling of endothelial nitric-oxide synthase and fibronectin expression in response to angiotensin II: role of mitochondrial reactive oxygen species. *J Biol Chem*. 2013;288(40):28668-86.
67. Block K, Gorin Y, Abboud HE. Subcellular localization of Nox4 and regulation in diabetes. *Proceedings of the National Academy of Sciences of the United States of America*. 2009;106(34):14385-90.
68. Zorov DB, Juhaszova M, Sollott SJ. Mitochondrial reactive oxygen species (ROS) and ROS-induced ROS release. *Physiological reviews*. 2014;94(3):909-50.
69. Schneider JG, Tilly N, Hierl T, Sommer U, Hamann A, Dugi K, et al. Elevated plasma endothelin-1 levels in diabetes mellitus. *American journal of hypertension*. 2002;15(11):967-72.
70. Takahashi K, Ghatei MA, Lam HC, O'Halloran DJ, Bloom SR. Elevated plasma endothelin in patients with diabetes mellitus. *Diabetologia*. 1990;33(5):306-10.
71. Houde M, Desbiens L, D'Orléans-Juste P. Endothelin-1: Biosynthesis, Signaling and Vasoreactivity. *Adv Pharmacol*. 2016;77:143-75.
72. Montezano AC, Burger D, Paravicini TM, Chignalia AZ, Yusuf H, Almasri M, et al. Nicotinamide adenine dinucleotide phosphate reduced oxidase 5 (Nox5) regulation by angiotensin II and endothelin-1 is mediated via calcium/calmodulin-dependent, rac-1-independent pathways in human endothelial cells. *Circulation research*. 2010;106(8):1363-73.
73. Fels J, Jeggle P, Liashkovich I, Peters W, Oberleithner H. Nanomechanics of vascular endothelium. *Cell Tissue Res*. 2014;355(3):727-37.
74. dos Remedios CG, Chhabra D, Kekic M, Dedova IV, Tsubakihara M, Berry DA, et al. Actin binding proteins: regulation of cytoskeletal microfilaments. *Physiological reviews*. 2003;83(2):433-73.

75. Amin E, Dubey BN, Zhang SC, Gremer L, Dvorsky R, Moll JM, et al. Rho-kinase: regulation, (dys)function, and inhibition. *Biol Chem*. 2013;394(11):1399-410.
76. Morales-Quinones M, Ramirez-Perez FI, Foote CA, Ghiarone T, Ferreira-Santos L, Bloksgaard M, et al. LIMK (LIM Kinase) Inhibition Prevents Vasoconstriction- and Hypertension-Induced Arterial Stiffening and Remodeling. *Hypertension (Dallas, Tex : 1979)*. 2020;76(2):393-403.
77. Oberleithner H, Callies C, Kusche-Vihrog K, Schillers H, Shahin V, Riethmüller C, et al. Potassium softens vascular endothelium and increases nitric oxide release. *Proceedings of the National Academy of Sciences of the United States of America*. 2009;106(8):2829-34.
78. Oberleithner H, Riethmüller C, Schillers H, MacGregor GA, de Wardener HE, Hausberg M. Plasma sodium stiffens vascular endothelium and reduces nitric oxide release. *Proceedings of the National Academy of Sciences of the United States of America*. 2007;104(41):16281-6.
79. Szczygiel AM, Brzezinka G, Targosz-Korecka M, Chlopicki S, Szymonski M. Elasticity changes anti-correlate with NO production for human endothelial cells stimulated with TNF- $\alpha$ . *Pflugers Arch*. 2012;463(3):487-96.
80. Fels J, Kusche-Vihrog K. Endothelial Nanomechanics in the Context of Endothelial (Dys)function and Inflammation. *Antioxid Redox Signal*. 2019;30(7):945-59.
81. Kondrikov D, Fonseca FV, Elms S, Fulton D, Black SM, Block ER, et al. Beta-actin association with endothelial nitric-oxide synthase modulates nitric oxide and superoxide generation from the enzyme. *J Biol Chem*. 2010;285(7):4319-27.
82. Fels J, Jeggle P, Kusche-Vihrog K, Oberleithner H. Cortical actin nanodynamics determines nitric oxide release in vascular endothelium. *PloS one*. 2012;7(7):e41520.
83. Galán C, Dionisio N, Smani T, Salido GM, Rosado JA. The cytoskeleton plays a modulatory role in the association between STIM1 and the Ca<sup>2+</sup> channel subunits Orail and TRPC1. *Biochem Pharmacol*. 2011;82(4):400-10.
84. Knudsen HL, Frangos JA. Role of cytoskeleton in shear stress-induced endothelial nitric oxide production. *The American journal of physiology*. 1997;273(1 Pt 2):H347-55.
85. Kuchan MJ, Frangos JA. Role of calcium and calmodulin in flow-induced nitric oxide production in endothelial cells. *The American journal of physiology*. 1994;266(3 Pt 1):C628-36.
86. Chen X, Feng L, Jin H. Constant or fluctuating hyperglycemias increases cytomembrane stiffness of human umbilical vein endothelial cells in culture: roles of cytoskeletal rearrangement and nitric oxide synthesis. *BMC Cell Biol*. 2013;14:22.
87. Arita R, Hata Y, Nakao S, Kita T, Miura M, Kawahara S, et al. Rho kinase inhibition by fasudil ameliorates diabetes-induced microvascular damage. *Diabetes*. 2009;58(1):215-26.
88. Kolavennu V, Zeng L, Peng H, Wang Y, Danesh FR. Targeting of RhoA/ROCK signaling ameliorates progression of diabetic nephropathy independent of glucose control. *Diabetes*. 2008;57(3):714-23.
89. Tang J, Kusaka I, Massey AR, Rollins S, Zhang JH. Increased RhoA translocation in aorta of diabetic rats. *Acta Pharmacol Sin*. 2006;27(5):543-8.

90. Sehgel NL, Vatner SF, Meininger GA. "Smooth Muscle Cell Stiffness Syndrome"-Revisiting the Structural Basis of Arterial Stiffness. *Front Physiol.* 2015;6:335.
91. Sehgel NL, Sun Z, Hong Z, Hunter WC, Hill MA, Vatner DE, et al. Augmented vascular smooth muscle cell stiffness and adhesion when hypertension is superimposed on aging. *Hypertension (Dallas, Tex : 1979).* 2015;65(2):370-7.
92. Sehgel NL, Zhu Y, Sun Z, Trzeciakowski JP, Hong Z, Hunter WC, et al. Increased vascular smooth muscle cell stiffness: a novel mechanism for aortic stiffness in hypertension. *American journal of physiology Heart and circulatory physiology.* 2013;305(9):H1281-7.
93. Qiu H, Zhu Y, Sun Z, Trzeciakowski JP, Gansner M, DePre C, et al. Short communication: vascular smooth muscle cell stiffness as a mechanism for increased aortic stiffness with aging. *Circulation research.* 2010;107(5):615-9.
94. Zhu Y, Qiu H, Trzeciakowski JP, Sun Z, Li Z, Hong Z, et al. Temporal analysis of vascular smooth muscle cell elasticity and adhesion reveals oscillation waveforms that differ with aging. *Aging Cell.* 2012;11(5):741-50.
95. DeMarco VG, Habibi J, Jia G, Aroor AR, Ramirez-Perez FI, Martinez-Lemus LA, et al. Low-Dose Mineralocorticoid Receptor Blockade Prevents Western Diet-Induced Arterial Stiffening in Female Mice. *Hypertension (Dallas, Tex : 1979).* 2015;66(1):99-107.
96. Ramirez-Perez FI, Cabral-Amador FJ, Whaley-Connell AT, Aroor AR, Morales-Quinones M, Woodford ML, et al. Cystamine reduces vascular stiffness in Western diet-fed female mice. *American journal of physiology Heart and circulatory physiology.* 2022;322(2):H167-h80.
97. Kizub IV, Pavlova OO, Johnson CD, Soloviev AI, Zholos AV. Rho kinase and protein kinase C involvement in vascular smooth muscle myofilament calcium sensitization in arteries from diabetic rats. *British journal of pharmacology.* 2010;159(8):1724-31.
98. Hirshman CA, Emala CW. Actin reorganization in airway smooth muscle cells involves Gq and Gi-2 activation of Rho. *The American journal of physiology.* 1999;277(3):L653-61.
99. Bézie Y, Lamazière JM, Laurent S, Challande P, Cunha RS, Bonnet J, et al. Fibronectin expression and aortic wall elastic modulus in spontaneously hypertensive rats. *Arteriosclerosis, thrombosis, and vascular biology.* 1998;18(7):1027-34.
100. Lim RR, Grant DG, Olver TD, Padilla J, Czajkowski AM, Schnurbusch TR, et al. Young Ossabaw Pigs Fed a Western Diet Exhibit Early Signs of Diabetic Retinopathy. *Invest Ophthalmol Vis Sci.* 2018;59(6):2325-38.
101. Martinez-Lemus LA, Aroor AR, Ramirez-Perez FI, Jia G, Habibi J, DeMarco VG, et al. Amiloride Improves Endothelial Function and Reduces Vascular Stiffness in Female Mice Fed a Western Diet. *Front Physiol.* 2017;8:456.
102. Jia G, Habibi J, Bostick BP, Ma L, DeMarco VG, Aroor AR, et al. Uric acid promotes left ventricular diastolic dysfunction in mice fed a Western diet. *Hypertension (Dallas, Tex : 1979).* 2015;65(3):531-9.

103. Tian L, Wang Z, Liu Y, Eickhoff JC, Eliceiri KW, Chesler NC. Validation of an arterial constitutive model accounting for collagen content and crosslinking. *Acta Biomater.* 2016;31:276-87.
104. Aronson D. Cross-linking of glycated collagen in the pathogenesis of arterial and myocardial stiffening of aging and diabetes. *Journal of hypertension.* 2003;21(1):3-12.
105. Stirban A, Gawlowski T, Roden M. Vascular effects of advanced glycation endproducts: Clinical effects and molecular mechanisms. *Molecular metabolism.* 2014;3(2):94-108.
106. Eckert RL, Kaartinen MT, Nurminskaya M, Belkin AM, Colak G, Johnson GV, et al. Transglutaminase regulation of cell function. *Physiological reviews.* 2014;94(2):383-417.
107. Nurminskaya MV, Belkin AM. Cellular functions of tissue transglutaminase. *Int Rev Cell Mol Biol.* 2012;294:1-97.
108. Jandu SK, Webb AK, Pak A, Sevinc B, Nyhan D, Belkin AM, et al. Nitric oxide regulates tissue transglutaminase localization and function in the vasculature. *Amino Acids.* 2013;44(1):261-9.
109. Penumatsa KC, Falcão-Pires I, Leite S, Leite-Moreira A, Bhedi CD, Nasirova S, et al. Increased Transglutaminase 2 Expression and Activity in Rodent Models of Obesity/Metabolic Syndrome and Aging. *Front Physiol.* 2020;11:560019.
110. Steppan J, Bergman Y, Viegas K, Armstrong D, Tan S, Wang H, et al. Tissue Transglutaminase Modulates Vascular Stiffness and Function Through Crosslinking-Dependent and Crosslinking-Independent Functions. *J Am Heart Assoc.* 2017;6(2).
111. Uemura S, Matsushita H, Li W, Glassford AJ, Asagami T, Lee KH, et al. Diabetes mellitus enhances vascular matrix metalloproteinase activity: role of oxidative stress. *Circulation research.* 2001;88(12):1291-8.
112. Han SY, Jee YH, Han KH, Kang YS, Kim HK, Han JY, et al. An imbalance between matrix metalloproteinase-2 and tissue inhibitor of matrix metalloproteinase-2 contributes to the development of early diabetic nephropathy. *Nephrol Dial Transplant.* 2006;21(9):2406-16.
113. Cabral-Pacheco GA, Garza-Veloz I, Castruita-De la Rosa C, Ramirez-Acuña JM, Perez-Romero BA, Guerrero-Rodriguez JF, et al. The Roles of Matrix Metalloproteinases and Their Inhibitors in Human Diseases. *Int J Mol Sci.* 2020;21(24).
114. Kologrivova IV, Suslova TE, Koshel'skaya OA, Vinnitskaya IV, Trubacheva OA. System of matrix metalloproteinases and cytokine secretion in type 2 diabetes mellitus and impaired carbohydrate tolerance associated with arterial hypertension. *Bull Exp Biol Med.* 2014;156(5):635-8.
115. Hong Z, Reeves KJ, Sun Z, Li Z, Brown NJ, Meininger GA. Vascular smooth muscle cell stiffness and adhesion to collagen I modified by vasoactive agonists. *PLoS one.* 2015;10(3):e0119533.
116. Hong Z, Sun Z, Li M, Li Z, Bunyak F, Ersoy I, et al. Vasoactive agonists exert dynamic and coordinated effects on vascular smooth muscle cell elasticity, cytoskeletal remodelling and adhesion. *The Journal of physiology.* 2014;592(6):1249-66.
117. Hong Z, Sun Z, Li Z, Mesquitta WT, Trzeciakowski JP, Meininger GA. Coordination of fibronectin adhesion with contraction and relaxation in microvascular smooth muscle. *Cardiovasc Res.* 2012;96(1):73-80.



118. Sun Z, Martinez-Lemus LA, Hill MA, Meininger GA. Extracellular matrix-specific focal adhesions in vascular smooth muscle produce mechanically active adhesion sites. *Am J Physiol Cell Physiol*. 2008;295(1):C268-78.
119. Bouissou C, Lacolley P, Dabire H, Safar ME, Gabella G, Duchatelle V, et al. Increased stiffness and cell-matrix interactions of abdominal aorta in two experimental nonhypertensive models: long-term chemically sympathectomized and sinoaortic denervated rats. *Journal of hypertension*. 2014;32(3):652-8.
120. Intengan HD, Thibault G, Li JS, Schiffrin EL. Resistance artery mechanics, structure, and extracellular components in spontaneously hypertensive rats : effects of angiotensin receptor antagonism and converting enzyme inhibition. *Circulation*. 1999;100(22):2267-75.
121. Takasaki I, Chobanian AV, Sarzani R, Brecher P. Effect of hypertension on fibronectin expression in the rat aorta. *J Biol Chem*. 1990;265(35):21935-9.
122. Belmadani S, Zerfaoui M, Boulares HA, Palen DI, Matrougui K. Microvessel vascular smooth muscle cells contribute to collagen type I deposition through ERK1/2 MAP kinase,  $\alpha$ v $\beta$ 3-integrin, and TGF- $\beta$ 1 in response to ANG II and high glucose. *American journal of physiology Heart and circulatory physiology*. 2008;295(1):H69-76.
123. Cagliero E, Roth T, Roy S, Lorenzi M. Characteristics and mechanisms of high-glucose-induced overexpression of basement membrane components in cultured human endothelial cells. *Diabetes*. 1991;40(1):102-10.
124. Green J, Yurdagul A, Jr., McInnis MC, Albert P, Orr AW. Flow patterns regulate hyperglycemia-induced subendothelial matrix remodeling during early atherogenesis. *Atherosclerosis*. 2014;232(2):277-84.
125. Kanters SD, Banga JD, Algra A, Frijns RC, Beutler JJ, Fijnheer R. Plasma levels of cellular fibronectin in diabetes. *Diabetes care*. 2001;24(2):323-7.
126. Kakou A, Bézie Y, Mercier N, Louis H, Labat C, Challande P, et al. Selective reduction of central pulse pressure under angiotensin blockage in SHR: role of the fibronectin- $\alpha$ 5 $\beta$ 1 integrin complex. *American journal of hypertension*. 2009;22(7):711-7.
127. Koffi I, Lacolley P, Kirchengaast M, Pomiès JP, Laurent S, Benetos A. Prevention of arterial structural alterations with verapamil and trandolapril and consequences for mechanical properties in spontaneously hypertensive rats. *European journal of pharmacology*. 1998;361(1):51-60.
128. Banerjee S, Ghoshal S, Girardet C, DeMars KM, Yang C, Niehoff ML, et al. Adropin correlates with aging-related neuropathology in humans and improves cognitive function in aging mice. *NPJ Aging Mech Dis*. 2021;7(1):23.
129. Zhang S, Chen Q, Lin X, Chen M, Liu Q. A Review of Adropin as the Medium of Dialogue between Energy Regulation and Immune Regulation. *Oxidative Medicine and Cellular Longevity*. 2020;2020:3947806.
130. Bozic J, Kumric M, Ticinovic Kurir T, Males I, Borovac JA, Martinovic D, et al. Role of Adropin in Cardiometabolic Disorders: From Pathophysiological Mechanisms to Therapeutic Target. *Biomedicines*. 2021;9(10).
131. Stein LM, Yosten GLC, Samson WK. Adropin acts in brain to inhibit water drinking: potential interaction with the orphan G protein-coupled receptor, GPR19.

- American journal of physiology Regulatory, integrative and comparative physiology. 2016;310(6):R476-R80.
132. Rao A, Herr DR. G protein-coupled receptor GPR19 regulates E-cadherin expression and invasion of breast cancer cells. *Biochim Biophys Acta Mol Cell Res.* 2017;1864(7):1318-27.
133. Foster SR, Hauser AS, Vedel L, Strachan RT, Huang XP, Gavin AC, et al. Discovery of Human Signaling Systems: Pairing Peptides to G Protein-Coupled Receptors. *Cell.* 2019;179(4):895-908.e21.
134. Wong CM, Wang Y, Lee JT, Huang Z, Wu D, Xu A, et al. Adropin is a brain membrane-bound protein regulating physical activity via the NB-3/Notch signaling pathway in mice. *J Biol Chem.* 2014;289(37):25976-86.
135. Yu L, Lu Z, Burchell S, Nowrangi D, Manaenko A, Li X, et al. Adropin preserves the blood-brain barrier through a Notch1/Hes1 pathway after intracerebral hemorrhage in mice. *J Neurochem.* 2017;143(6):750-60.
136. Stokar J, Gurt I, Cohen-Kfir E, Yakubovsky O, Hallak N, Benyamini H, et al. Hepatic adropin is regulated by estrogen and contributes to adverse metabolic phenotypes in ovariectomized mice. *Molecular metabolism.* 2022;60:101482.
137. Meda C, Dolce A, Vegeto E, Maggi A, Della Torre S. ER $\alpha$ -Dependent Regulation of Adropin Predicts Sex Differences in Liver Homeostasis during High-Fat Diet. *Nutrients.* 2022;14(16):3262.
138. Stevens JR, Kearney ML, St-Onge MP, Stanhope KL, Havel PJ, Kanaley JA, et al. Inverse association between carbohydrate consumption and plasma adropin concentrations in humans. *Obesity (Silver Spring, Md).* 2016;24(8):1731-40.
139. Chang J-B, Chu N-F, Lin F-H, Hsu J-T, Chen P-Y. Relationship between plasma adropin levels and body composition and lipid characteristics amongst young adolescents in Taiwan. *Obes Res Clin Pract.* 2018;12(Suppl 2):101-7.
140. Davoodi M, Hesamabadi BK, Ariabood E, Izadi MR, Ghardashi-Afousi A, Bigi MAB, et al. Improved blood pressure and flow-mediated dilatation via increased plasma adropin and nitrate/nitrite induced by high-intensity interval training in patients with type 2 diabetes. *Experimental physiology.* 2022;107(8):813-24.
141. Smith JA, Soares RN, McMillan NJ, Jurrissen TJ, Martinez-Lemus LA, Padilla J, et al. Young women are protected against vascular insulin resistance induced by adoption of an obesogenic lifestyle. *Endocrinology.* 2022.
142. Choi HN, Yim JE. Plasma Adropin as a Potential Marker Predicting Obesity and Obesity-associated Cancer in Korean Patients With Type 2 Diabetes Mellitus. *J Cancer Prev.* 2018;23(4):191-6.
143. Butler AA, St-Onge MP, Siebert EA, Medici V, Stanhope KL, Havel PJ. Differential Responses of Plasma Adropin Concentrations To Dietary Glucose or Fructose Consumption In Humans. *Scientific Reports.* 2015;5:14691.
144. Chen X, Xue H, Fang W, Chen K, Chen S, Yang W, et al. Adropin protects against liver injury in nonalcoholic steatohepatitis via the Nrf2 mediated antioxidant capacity. *Redox Biol.* 2019;21:101068-.
145. Yang W, Liu L, Wei Y, Fang C, Liu S, Zhou F, et al. Exercise suppresses NLRP3 inflammasome activation in mice with diet-induced NASH: a plausible role of adropin. *Lab Invest.* 2021;101(3):369-80.

146. Li N, Xie G, Zhou B, Qu A, Meng H, Liu J, et al. Serum Adropin as a Potential Biomarker for Predicting the Development of Type 2 Diabetes Mellitus in Individuals With Metabolic Dysfunction-Associated Fatty Liver Disease. *Front Physiol.* 2021;12:696163.
147. Sayın O, Tokgöz Y, Arslan N. Investigation of adropin and leptin levels in pediatric obesity-related nonalcoholic fatty liver disease. *J Pediatr Endocrinol Metab.* 2014;27(5-6):479-84.
148. Yosae S, Khodadost M, Esteghamati A, Speakman JR, Shidfar F, Nazari MN, et al. Metabolic Syndrome Patients Have Lower Levels of Adropin When Compared With Healthy Overweight/Obese and Lean Subjects. *Am J Mens Health.* 2017;11(2):426-34.
149. Chen X, Sun X, Shen T, Chen Q, Chen S, Pang J, et al. Lower adropin expression is associated with oxidative stress and severity of nonalcoholic fatty liver disease. *Free Radic Biol Med.* 2020;160:191-8.
150. Kutlu O, Altun Ö, Dikker O, Aktaş Ş, Özsoy N, Arman Y, et al. Serum Adropin Levels Are Reduced in Adult Patients with Nonalcoholic Fatty Liver Disease. *Med Princ Pract.* 2019;28(5):463-9.
151. Aydın P, Uzunçakmak SK, Tör İ H, Bilen A, Özden A. Comparison of Serum Adropin Levels in Patients with Diabetes Mellitus, COVID-19, and COVID-19 with Diabetes Mellitus. *Eurasian J Med.* 2022;54(2):197-201.
152. Chen S, Zeng K, Liu Q-C, Guo Z, Zhang S, Chen X-R, et al. Adropin deficiency worsens HFD-induced metabolic defects. *Cell Death Dis.* 2017;8(8):e3008-e.
153. Es-Haghi A, Al-Abyadh T, Mehrad-Majd H. The Clinical Value of Serum Adropin Level in Early Detection of Diabetic Nephropathy. *Kidney Blood Press Res.* 2021;46(6):734-40.
154. Hu W, Chen L. Association of Serum Adropin Concentrations with Diabetic Nephropathy. *Mediators of inflammation.* 2016;2016:6038261-.
155. Li B, Tian X, Guo S, Zhang M, Li J, Zhai N, et al. Pentraxin-3 and adropin as inflammatory markers of early renal damage in type 2 diabetes patients. *Int Urol Nephrol.* 2020;52(11):2145-52.
156. Li S, Sun J, Hu W, Liu Y, Lin D, Duan H, et al. The association of serum and vitreous adropin concentrations with diabetic retinopathy. *Ann Clin Biochem.* 2019;56(2):253-8.
157. Polkowska A, Pasierowska IE, Paśławska M, Pawluczuk E, Bossowski A. Assessment of Serum Concentrations of Adropin, Afamin, and Neudesin in Children with Type 1 Diabetes. *Biomed Res Int.* 2019;2019:6128410.
158. Zang H, Jiang F, Cheng X, Xu H, Hu X. Serum adropin levels are decreased in Chinese type 2 diabetic patients and negatively correlated with body mass index. *Endocr J.* 2018;65(7):685-91.
159. Beigi A, Shirzad N, Nikpour F, Nasli Esfahani E, Emamgholipour S, Bandarian F. Association between serum adropin levels and gestational diabetes mellitus; a case-control study. *Gynecol Endocrinol.* 2015;31(12):939-41.
160. Dincer E, Topçuoğlu S, Arman D, Kaya A, Yavuz T, Karatekin G. Inflammation Markers in Infants of Mothers with Gestational Diabetes. *Fetal Pediatr Pathol.* 2022;41(4):616-26.

161. Hosseini A, Shanaki M, Emamgholipour S, Nakhjavani M, Razi F, Golmohammadi T. Elevated serum levels of adropin in patients with type 2 diabetes mellitus and its association with insulin resistance. *J Biol Today's World*. 2016;5:44-9.
162. Palizban AA, Yazdani AH, Jahanbani-Ardakani H. Role of rs7903146 polymorphism and adropin serum level in patients with diabetes mellitus; a case-control study from Isfahan, Iran. *Arch Physiol Biochem*. 2022;128(2):378-81.
163. Dąbrowski FA, Jarmużek P, Gondek A, Cudnoch-Jędrzejewska A, Bomba-Opoń D, Wielgoś M. First and third trimester serum concentrations of adropin and copeptin in gestational diabetes mellitus and normal pregnancy. *Ginekol Pol*. 2016;87(9):629-34.
164. Kuhla A, Hahn S, Butschkau A, Lange S, Wree A, Vollmar B. Lifelong caloric restriction reprograms hepatic fat metabolism in mice. *J Gerontol A Biol Sci Med Sci*. 2014;69(8):915-22.
165. Ulupinar S, Ozbay S, Gencoglu C, Altinkaynak K, Sebin E, Oymak B. Exercise in the cold causes greater irisin release but may not be enough for adropin. *Chin J Physiol*. 2021;64(3):129-34.
166. Mikus CR, Fairfax ST, Libla JL, Boyle LJ, Vianna LC, Oberlin DJ, et al. Seven days of aerobic exercise training improves conduit artery blood flow following glucose ingestion in patients with type 2 diabetes. *Journal of applied physiology (Bethesda, Md : 1985)*. 2011;111(3):657-64.
167. Sanchis-Gomar F, Alis R, Rampinini E, Bosio A, Ferioli D, La Torre A, et al. Adropin and apelin fluctuations throughout a season in professional soccer players: Are they related with performance? *Peptides*. 2015;70:32-6.
168. Afşin A, Bozyılan E, Asoğlu R, Yavuz F, Dündar A. Effects of eight weeks exercise training on serum levels of adropin in male volleyball players. *Hormone molecular biology and clinical investigation*. 2021.
169. Moustafa A, Arisha AH. Swim therapy-induced tissue specific metabolic responses in male rats. *Life sciences*. 2020;262:118516.
170. Fujie S, Hasegawa N, Horii N, Uchida M, Sanada K, Hamaoka T, et al. Aerobic Exercise Restores Aging-Associated Reductions in Arterial Adropin Levels and Improves Adropin-Induced Nitric Oxide-Dependent Vasorelaxation. *J Am Heart Assoc*. 2021;10(10):e020641.
171. Chen TC, Huang TH, Tseng WC, Tseng KW, Hsieh CC, Chen MY, et al. Changes in plasma C1q, apelin and adropin concentrations in older adults after descending and ascending stair walking intervention. *Scientific Reports*. 2021;11(1):17644.
172. Hody S, Croisier JL, Bury T, Rogister B, Leprince P. Eccentric Muscle Contractions: Risks and Benefits. *Front Physiol*. 2019;10:536.
173. Altamimi TR, Gao S, Karwi QG, Fukushima A, Rawat S, Wagg CS, et al. Adropin regulates cardiac energy metabolism and improves cardiac function and efficiency. *Metabolism*. 2019;98:37-48.
174. Thapa D, Xie B, Zhang M, Stoner MW, Manning JR, Huckestein BR, et al. Adropin treatment restores cardiac glucose oxidation in pre-diabetic obese mice. *Journal of molecular and cellular cardiology*. 2019;129:174-8.

175. Han W, Zhang C, Wang H, Yang M, Guo Y, Li G, et al. Alterations of irisin, adropin, preptin and BDNF concentrations in coronary heart disease patients comorbid with depression. *Ann Transl Med.* 2019;7(14):298.
176. Wu L, Fang J, Yuan X, Xiong C, Chen L. Adropin reduces hypoxia/reoxygenation-induced myocardial injury via the reperfusion injury salvage kinase pathway. *Exp Ther Med.* 2019;18(5):3307-14.
177. Celik A, Balin M, Kobat MA, Erdem K, Baydas A, Bulut M, et al. Deficiency of a new protein associated with cardiac syndrome X; called adropin. *Cardiovasc Ther.* 2013;31(3):174-8.
178. Lin D, Yong J, Ni S, Ou W, Tan X. Negative association between serum adropin and hypertensive disorders complicating pregnancy. *Hypertens Pregnancy.* 2019;38(4):237-44.
179. Çelik HT, Akkaya N, Erdamar H, Gok S, Kazanci F, Demircelik B, et al. The Effects of Valsartan and Amlodipine on the Levels of Irisin, Adropin, and Perilipin. *Clin Lab.* 2015;61(12):1889-95.
180. Durham AL, Speer MY, Scatena M, Giachelli CM, Shanahan CM. Role of smooth muscle cells in vascular calcification: implications in atherosclerosis and arterial stiffness. *Cardiovasc Res.* 2018;114(4):590-600.
181. Dodd WS, Patel D, Lucke-Wold B, Hosaka K, Chalouhi N, Hoh BL. Adropin decreases endothelial monolayer permeability after cell-free hemoglobin exposure and reduces MCP-1-induced macrophage transmigration. *Biochemical and biophysical research communications.* 2021;582:105-10.
182. Yang C, DeMars KM, Hawkins KE, Candelario-Jalil E. Adropin reduces paracellular permeability of rat brain endothelial cells exposed to ischemia-like conditions. *Peptides.* 2016;81:29-37.
183. Wang L, Jin F, Wang P, Hou S, Jin T, Chang X, et al. Adropin Inhibits Vascular Smooth Muscle Cell Osteogenic Differentiation to Alleviate Vascular Calcification via the JAK2/STAT3 Signaling Pathway. *Biomed Res Int.* 2022;2022:9122264.
184. Thapa D, Xie B, Mushala BAS, Zhang M, Manning JR, Bugga P, et al. Diet-induced obese mice are resistant to improvements in cardiac function resulting from short-term adropin treatment. *Curr Res Physiol.* 2022;5:55-62.
185. Yang C, Lavayen BP, Liu L, Sanz BD, DeMars KM, Laroche J, et al. Neurovascular protection by adropin in experimental ischemic stroke through an endothelial nitric oxide synthase-dependent mechanism. *Redox Biol.* 2021;48:102197.
186. Cecelja M, Chowienczyk P. Role of arterial stiffness in cardiovascular disease. *JRSM Cardiovasc Dis.* 2012;1(4).
187. Mattace-Raso FU, van der Cammen TJ, Hofman A, van Popele NM, Bos ML, Schalekamp MA, et al. Arterial stiffness and risk of coronary heart disease and stroke: the Rotterdam Study. *Circulation.* 2006;113(5):657-63.
188. Ertem AG, Ünal S, Efe TH, Açar B, Yayla Ç, Kuyumcu MS, et al. Association between serum adropin level and burden of coronary artery disease in patients with non-ST elevation myocardial infarction. *Anatol J Cardiol.* 2017;17(2):119-24.
189. Grzegorzewska AE, Niepolski L, Mostowska A, Warchoń W, Jagodziński PP. Involvement of adropin and adropin-associated genes in metabolic abnormalities of hemodialysis patients. *Life sciences.* 2016;160:41-6.

190. Wang B, Xue Y, Shang F, Ni S, Liu X, Fan B, et al. Association of serum adropin with the presence of atrial fibrillation and atrial remodeling. *J Clin Lab Anal.* 2019;33(2):e22672-e.
191. Maciorkowska M, Musiałowska D, Małyszko J. Adropin and irisin in arterial hypertension, diabetes mellitus and chronic kidney disease. *Adv Clin Exp Med.* 2019;28(11):1571-5.
192. Moore MP, Cunningham RP, Meers GM, Johnson SA, Wheeler AA, Ganga RR, et al. Compromised hepatic mitochondrial fatty acid oxidation and reduced markers of mitochondrial turnover in human NAFLD. *Hepatology.* 2022.
193. Pettit-Mee RJ, Power G, Cabral-Amador FJ, Ramirez-Perez FI, Soares RN, Sharma N, et al. Endothelial HSP72 is not reduced in type 2 diabetes nor is it a key determinant of endothelial insulin sensitivity. *American journal of physiology Regulatory, integrative and comparative physiology.* 2022;323(1):R43-r58.
194. Hwang MH, Yoo JK, Kim HK, Hwang CL, Mackay K, Hemstreet O, et al. Validity and reliability of aortic pulse wave velocity and augmentation index determined by the new cuff-based SphygmoCor Xcel. *J Hum Hypertens.* 2014;28(8):475-81.
195. Soares RN, Ramirez-Perez FI, Cabral-Amador FJ, Morales-Quinones M, Foote CA, Ghiarone T, et al. SGLT2 inhibition attenuates arterial dysfunction and decreases vascular F-actin content and expression of proteins associated with oxidative stress in aged mice. *Geroscience.* 2022.
196. Hales CM, Carroll MD, Fryar CD, Ogden CL. Prevalence of obesity and severe obesity among adults: United States, 2017–2018. 2020.
197. Manrique-Acevedo C, Padilla J, Naz H, Woodford ML, Ghiarone T, Aroor AR, et al. Mineralocorticoid Receptor in Myeloid Cells Mediates Angiotensin II-Induced Vascular Dysfunction in Female Mice. *Front Physiol.* 2021;12:588358.
198. Vesey CJ, Stringer M, Cole PV. Decay of nitroprusside. I: In vitro. *Br J Anaesth.* 1990;64(6):696-703.
199. Bailey JD, Shaw A, McNeill E, Nicol T, Diotallevi M, Chuaiphichai S, et al. Isolation and culture of murine bone marrow-derived macrophages for nitric oxide and redox biology. *Nitric Oxide.* 2020;100-101:17-29.
200. Cox RD, Frank CW. Determination of nitrate and nitrite in blood and urine by chemiluminescence. *J Anal Toxicol.* 1982;6(3):148-52.
201. Pelletier MM, Kleinbongard P, Ringwood L, Hito R, Hunter CJ, Schechter AN, et al. The measurement of blood and plasma nitrite by chemiluminescence: pitfalls and solutions. *Free Radic Biol Med.* 2006;41(4):541-8.
202. McEniery CM, Qasem A, Schmitt M, Avolio AP, Cockcroft JR, Wilkinson IB. Endothelin-1 regulates arterial pulse wave velocity in vivo. *Journal of the American College of Cardiology.* 2003;42(11):1975-81.
203. Hill MA, Yang Y, Zhang L, Sun Z, Jia G, Parrish AR, et al. Insulin resistance, cardiovascular stiffening and cardiovascular disease. *Metabolism.* 2021;119:154766.
204. Maruhashi T, Noma K, Iwamoto Y, Iwamoto A, Oda N, Kajikawa M, et al. Critical role of exogenous nitric oxide in ROCK activity in vascular smooth muscle cells. *PloS one.* 2014;9(10):e109017.
205. Griffin CT, Curtis CD, Davis RB, Muthukumar V, Magnuson T. The chromatin-remodeling enzyme BRG1 modulates vascular Wnt signaling at two levels. *Proceedings*

- of the National Academy of Sciences of the United States of America. 2011;108(6):2282-7.
206. Lan J, Li H, Luo X, Hu J, Wang G. BRG1 promotes VEGF-A expression and angiogenesis in human colorectal cancer cells. *Exp Cell Res*. 2017;360(2):236-42.
207. Staiculescu MC, Galiñanes EL, Zhao G, Ulloa U, Jin M, Beig MI, et al. Prolonged vasoconstriction of resistance arteries involves vascular smooth muscle actin polymerization leading to inward remodelling. *Cardiovasc Res*. 2013;98(3):428-36.
208. Touyz RM, Alves-Lopes R, Rios FJ, Camargo LL, Anagnostopoulou A, Arner A, et al. Vascular smooth muscle contraction in hypertension. *Cardiovasc Res*. 2018;114(4):529-39.
209. Zhou N, Lee JJ, Stoll S, Ma B, Costa KD, Qiu H. Rho Kinase Regulates Aortic Vascular Smooth Muscle Cell Stiffness Via Actin/SRF/Myocardin in Hypertension. *Cell Physiol Biochem*. 2017;44(2):701-15.
210. Ben-Shlomo Y, Spears M, Boustred C, May M, Anderson SG, Benjamin EJ, et al. Aortic pulse wave velocity improves cardiovascular event prediction: an individual participant meta-analysis of prospective observational data from 17,635 subjects. *Journal of the American College of Cardiology*. 2014;63(7):636-46.
211. Vlachopoulos C, Aznaouridis K, Stefanadis C. Prediction of cardiovascular events and all-cause mortality with arterial stiffness: a systematic review and meta-analysis. *Journal of the American College of Cardiology*. 2010;55(13):1318-27.
212. Vlachopoulos C, Terentes-Printzios D, Laurent S, Nilsson PM, Protogerou AD, Aznaouridis K, et al. Association of Estimated Pulse Wave Velocity With Survival: A Secondary Analysis of SPRINT. *JAMA Netw Open*. 2019;2(10):e1912831.
213. Nichols WW, Singh BM. Augmentation index as a measure of peripheral vascular disease state. *Current opinion in cardiology*. 2002;17(5):543-51.
214. Rizzoni D, Porteri E, Boari GE, De Ciuceis C, Sleiman I, Muiesan ML, et al. Prognostic significance of small-artery structure in hypertension. *Circulation*. 2003;108(18):2230-5.
215. Mitchell GF, Vita JA, Larson MG, Parise H, Keyes MJ, Warner E, et al. Cross-sectional relations of peripheral microvascular function, cardiovascular disease risk factors, and aortic stiffness: the Framingham Heart Study. *Circulation*. 2005;112(24):3722-8.
216. Cooper LL, Palmisano JN, Benjamin EJ, Larson MG, Vasan RS, Mitchell GF, et al. Microvascular Function Contributes to the Relation Between Aortic Stiffness and Cardiovascular Events: The Framingham Heart Study. *Circ Cardiovasc Imaging*. 2016;9(12).
217. Frisbee JC. Remodeling of the skeletal muscle microcirculation increases resistance to perfusion in obese Zucker rats. *American journal of physiology Heart and circulatory physiology*. 2003;285(1):H104-11.
218. Stapleton PA, Goodwill AG, James ME, D'Audiffret AC, Frisbee JC. Differential impact of familial hypercholesterolemia and combined hyperlipidemia on vascular wall and network remodeling in mice. *Microcirculation*. 2010;17(1):47-58.
219. Alicandri CL, Fariello R, Agabiti-Rosei E, Romanelli G, Muiesan G. Influence of the sympathetic nervous system on aortic compliance. *Clinical science (London, England : 1979)*. 1980;59 Suppl 6:279s-82s.

220. Nardone M, Floras JS, Millar PJ. Sympathetic neural modulation of arterial stiffness in humans. *American journal of physiology Heart and circulatory physiology*. 2020;319(6):H1338-h46.
221. Foote CA, Castorena-Gonzalez JA, Staiculescu MC, Clifford PS, Hill MA, Meininger GA, et al. Brief serotonin exposure initiates arteriolar inward remodeling processes in vivo that involve transglutaminase activation and actin cytoskeleton reorganization. *American journal of physiology Heart and circulatory physiology*. 2016;310(2):H188-98.
222. Klein A, Joseph PD, Christensen VG, Jensen LJ, Jacobsen JCB. Lack of tone in mouse small mesenteric arteries leads to outward remodeling, which can be prevented by prolonged agonist-induced vasoconstriction. *American journal of physiology Heart and circulatory physiology*. 2018;315(3):H644-h57.
223. Kim HR, Gallant C, Leavis PC, Gunst SJ, Morgan KG. Cytoskeletal remodeling in differentiated vascular smooth muscle is actin isoform dependent and stimulus dependent. *Am J Physiol Cell Physiol*. 2008;295(3):C768-78.
224. Wainright KS, Fleming NJ, Rowles JL, Welly RJ, Zidon TM, Park YM, et al. Retention of sedentary obese visceral white adipose tissue phenotype with intermittent physical activity despite reduced adiposity. *American journal of physiology Regulatory, integrative and comparative physiology*. 2015;309(5):R594-602.
225. Bubb MR, Spector I, Beyer BB, Fosen KM. Effects of jasplakinolide on the kinetics of actin polymerization. An explanation for certain in vivo observations. *J Biol Chem*. 2000;275(7):5163-70.
226. Laurent S, Briet M, Boutouyrie P. Large and small artery cross-talk and recent morbidity-mortality trials in hypertension. *Hypertension (Dallas, Tex : 1979)*. 2009;54(2):388-92.
227. Plows JF, Yu X, Broadhurst R, Vickers MH, Tong C, Zhang H, et al. Absence of a gestational diabetes phenotype in the LepRdb/+ mouse is independent of control strain, diet, misty allele, or parity. *Scientific Reports*. 2017;7:45130.
228. Yu M, Wang D, Zhong D, Xie W, Luo J. Adropin Carried by Reactive Oxygen Species-Responsive Nanocapsules Ameliorates Renal Lipid Toxicity in Diabetic Mice. *ACS Appl Mater Interfaces*. 2022;14(33):37330-44.
229. Hughes TM, Craft S, Lopez OL. Review of 'the potential role of arterial stiffness in the pathogenesis of Alzheimer's disease'. *Neurodegener Dis Manag*. 2015;5(2):121-35.



## APPENDIX A: Curriculum Vitae

### **Education**

**Ph.D. in Nutrition and Exercise Physiology - University of Missouri**                      **2015-**  
**current**

- Dissertation: *Role of adropin in arterial stiffening associated with obesity and type 2 diabetes*

Supervisor: Jaume Padilla, Ph.D.

I interrogated the contributions of circulating adropin, a secreted peptide that is largely expressed in the liver and is associated with energy regulation, on arterial stiffening associated with obesity and type 2 diabetes. Adropin concentrations are inversely associated with obesity, insulin resistance, and arterial stiffness. I determined the lack of adropin is sufficient to induce arterial stiffening, while adropin treatment decreased diabetic-associated arterial stiffness through an eNOS-dependent pathway.

**MSc in Exercise Science - Appalachian State University**

**2013-2015**

- Thesis: *Effects of watermelon supplementation on insulin resistance and intake in overweight, postmenopausal women*

Supervisor: Jennifer J. Zwetsloot, Ph.D, | Co-supervisor: Kevin A. Zwetsloot, Ph.D. and R. Andrew Shanely, Ph.D.

We investigated whether watermelon supplementation via frozen puree would be sufficient to induce alteration in insulin resistance and food intake in overweight, postmenopausal women.

## **BSc in Exercise Science - Appalachian State University**

**2008-2013**

- Minor in Biology and Psychology

## **Research Experience**

08/2015 – present      Ph.D. Cardiometabolic Physiology Lab. University of Missouri.

Learned

and gained experience in 1) Western blot analyses; 2) Tissue dissection and isolation of aortic, femoral, and mesenteric arteries; 3) Wire and pressure myography of isolated arteries; 4) Confocal and multiphoton microscopy; 5) Enzyme-linked immunoassy; 6) Introductory cell culture techniques; 7) Implementation of exercise protocols in mouse and swine models.

08/2013-05/2015      MSc. Exercise Physiology Lab. Appalachian State University.

Learned and gained experience in 1) Implementation of gavage and running

exercise protocol in mice; 2) Collection and preparation of blood samples; 3)  
Enzyme-linked immunoassay multiplex assays.

## **Academic Positions**

2020	<b>University of Missouri</b> , Nutrition and Exercise Physiology Teaching Assistant (Gable) NEP 2222: Landscape of obesity
2016 – 2020	<b>University of Missouri</b> , Nutrition and Exercise Physiology Teaching Assistant (Kanaley) NEP 3850: Exercise Physiology Laboratory
2019	<b>University of Missouri</b> , Nutrition and Exercise Physiology Teaching Assistant (Fritsche) NEP 2340: Human Nutrition I
2018	<b>University of Missouri</b> , Nutrition and Exercise Physiology Instructor led for an independent study course (Mann) NEP 4200: Sport Performance and conditioning
2015	<b>University of Missouri</b> , Nutrition and Exercise Physiology

Teaching Assistant (Ball)

NEP 1340: Introduction to exercise and fitness

2013 - 2015

**Appalachian State University** – Department of Exercise

Science

Human performance laboratory manager

2014

**Appalachian State University**

Teaching Assistant (Merritt)

ES 2010: Anatomy and physiology laboratory

2014

**Appalachian State University**

Teaching Assistant (Merritt)

ES 2010: Exercise physiology laboratory

## **Peer Reviewed Research Publications**

1. **Jurrissen TJ**, Ramirez-Perez FI, Cabral-Amador FJ, Soares RN, Pettit-Mee RJ, Betancourt-Cortes EE, McMillan NJ, Sharma N, Rocha HNM, Fujie S, Morales-Quinones M, Lazo-Fernandez Y, Butler AA, Banerjee S, Sacks HS, Ibdah JA, Parks EJ, Rector RS, Manrique-Acevedo C, Martinez-Lemus LA, Padilla J. (2022). Role of adropin in arterial stiffening associated with obesity and type 2 diabetes. *American Journal of Physiology-Heart and Circulation Physiology*. PMID: 36083795
  - **Selected for American Physiological Society press release program.**
2. Smith JA, Soares RN, McMillan NJ, **Jurrissen TJ**, Martinez-Lemus LA, Padilla J, Manrique-Acevedo C. (2022). Young women are protected against vascular insulin

- resistance induced by adoption of an obesogenic lifestyle. *Endocrinology*. PMID: 35974454
3. Ramirez-Perez FI, Cabral-Amador FJ, Whaley-Connell AT, Aroor AR, Morales-Quinones M, Woodford ML, Ferrerira-Santos L, **Jurrissen TJ**, Manrique-Acevedo CM, Jia G, DeMarco VG, Padilla J, Martinez-Lemus LA, Lastra G. (2022). Cystamine reduces vascular stiffness in Western diet-fed female mice. *American Journal of Physiology-Heart and Circulation Physiology*. PMID: 34890280
  4. Dirkes RK, Winn NC, **Jurrissen TJ**, Lubahn DB, Vieira-Potter VJ, Padilla J, Hinton PS. (2021). Voluntary wheel running partially compensates for the effects of global estrogen receptor- $\alpha$  knockout on cortical bone in young male mice. *International Journal of Molecular Sciences*. PMID: 33572215
  5. Shanely RA, Zwetsloot JJ, **Jurrissen TJ**, Hannan LC, Zwetsloot KA, Needle AR, Bishop AE, Wu G, Perkins-Veazie P. (2020). Daily watermelon consumption decreases plasma sVCAM-1 levels in overweight and obese postmenopausal women. *Nutrition Research*. PMID: 32142970
  6. **Jurrissen TJ**, Grunewald ZI, Woodford ML, Winn NC, Ball JR, Smith TN, Wheeler AA, Rawlings AL, Staveley-O'Carroll KF, Ji Y, Fay WP, Paradis P, Schiffrin, EL, Vieira-Potter VJ, Fadel PJ, Martinez-Lemus LA, Padilla J. (2019). Overproduction of endothelin-1 impairs glucose tolerance but does not promote visceral adipose tissue inflammation or limit metabolic adaptations to exercise. *American Journal of Physiology-Endocrinology and Metabolism*. PMID: 31310581
    - o **APSselect article**
  7. McDonald MW, Olver TD, Dotzert MS, **Jurrissen TJ**, Nobel EG, Padilla J, Melling CJ. (2019) Aerobic exercise training improves insulin-induced vasorelaxation in a vessel-specific manner in rats with insulin-treated experimental diabetes. *Diabetes and Vascular Disease Research*. PMID: 30537862
  8. Grunewald ZI, **Jurrissen TJ**, Woodford ML, Ramirez-Perez FI, Park LK, Pettit-Mee P, Gharone T, Brown SM, Morales-Quinones M, Ball JR, Staveley-O'Carroll KF, Aroor AR, Fadel PJ, Paradis P, Schiffrin EL, Bender SB, Martinez-Lemus LA, Padilla. (2019). Chronic elevation of endothelin-1 alone may not be sufficient to impair endothelium-dependent relaxation. *Hypertension*. PMID: 31630572
  9. Olver TD, Edwards JC, **Jurrissen TJ**, Veteto AB, Jones JL, Gao C, Rau C, Warren CM, Klutho PJ, Alex L, Ferreira-Nichols SC, Ivey JR, Thorne PK, McDonald KS, Krenz M, Baines CP, Solaro RJ, Wang Y, Ford DA, Domeier TL, Padilla J, Rector RS, Emter CA. (2019) Western diet-fed, aortic-banded Ossabaw Swine: a preclinical model of cardio-metabolic heart failure. *Journal of the American College of Cardiology: Basic to translational Science*. PMID: 31312763
  10. Winn NC, **Jurrissen TJ**, Grunewald ZI, Cunningham RP, Woodford ML, Kanaley JA, Lubahn DB, Manrique-Acevedo C, Vieira-Potter VJ, Padilla J. (2019). Estrogen receptor-alpha signaling maintains immunometabolic function in males and is obligatory for exercise-induced amelioration of nonalcoholic fatty liver. *American Journal of Physiology-Endocrinology and Metabolism*. PMID: 30512987
  11. Olver TD, Grunewald ZI, **Jurrissen TJ**, Macpherson REK, LeBlanc PJ, Schnurbush TR, Czajkowski AM, Laughlin MH, Rector RS, Bender SB, Walters EM, Emter CA, Padilla J. (2018) Microvascular insulin resistance 1 in skeletal muscle and brain

occurs early in the development of juvenile obesity in pigs. *American Journal of Physiology Regulatory, Integrative and Comparative Physiology*. PMID: 29141949

○ **APSselect article**

12. **Jurrissen TJ**, Olver TD, Lin GS, Winn NC, Gastecki ML, Welly RJ, Grunewald ZI, Emter CA, Vieira-Potter VJ, Padilla J. (2018). Endothelial dysfunction occur independently of adipose tissue inflammation and insulin resistance in ovariectomized Yucatan swine. *Adipocyte*. PMID: 29283284
13. **Jurrissen TJ**, Sheldon RD, Gastecki ML, Woodford ML, Zidon TM, Rector RS, Vieira-Potter VJ, Padilla J. (2016). Ablation of eNOS does not promote adipose tissue inflammation. *American Journal of Physiology Regulatory, Integrative and Comparative Physiology*. PMID: 26864812

## **Invited Oral Scientific Presentations**

1. **Jurrissen TJ**, Ramirez-Perez FI, Cabral-Amador FJ, Soares RN, Pettit-Mee RJ, Betancourt-Cortes EE, McMillan NJ, Sharma N, Rocha HNM, Fujie S, Morales-Quinones M, Lazo-Fernandez Y, Butler AA, Banerjee S, Sacks HS, Ibdah JA, Parks EJ, Rector RS, Manrique-Acevedo C, Martinez-Lemus LA, Padilla J. Role of adropin in arterial stiffening associated with obesity and type 2 diabetes. (2022). *Missouri American Physiological Society*. Columbia, MO.
2. **Jurrissen TJ**, Ramirez-Perez FI, Cabral-Amador FJ, McMillan NJ, Fujie S, Butler AA, Banerjee S, Sacks HS, Manrique-Acevedo C, Martinez-Lemus LA, Padilla J. Role of adropin in reducing arterial stiffness in type 2 diabetes. (2022). *Experimental Biology*. Philadelphia, PA.
3. **Jurrissen TJ**, Fujie S, Ramirez-Perez FI, Butler AA, Banerjee S, Sacks HS, Manrique-Acevedo C, Martinez-Lemus LA, Padilla J. Loss of adropin causes arterial stiffening in mouse femoral and mesenteric arteries. (2021). *Experimental Biology*. (Virtual)
4. **Jurrissen TJ**, Castorena-Gonzalez JA, Ramirez-Perez FI, Hill MA, Meininger GA, Padilla J, Martinez-Lemus LA. Age-related changes in skeletal muscle and small mesenteric arterial function in spontaneously hypertensive rats. (2019). *Experimental Biology*. Orlando, FL.
5. **Jurrissen TJ**, Grunewald ZI, Ball JR, Ramirez-Perez FI, Woodford ML, Aroor AR, Ayedun LA, Winn NC, Paradis P, Schiffrin EL, Martinez-Lemus LA, Padilla J. Regular exercise reduces adipose tissue inflammation and improves glycemic control in Western diet-fed mice despite hyperendothelinemia. (2018). *Experimental Biology*. San Diego, CA.
6. **Jurrissen TJ**, Olver TD, Lin GS, Winn NC, Gastecki ML, Well RJ, Grunewald ZI, Emter CA, Vieira-Potter VJ, Padilla J. Endothelial dysfunction occurs independently of adipose tissue inflammation and insulin resistance in ovariectomized Yucatan swine. (2017). *Experimental Biology*. Chicago, IL.

7. **Jurrissen TJ**, Sheldon RD, Gastecki ML, Woodford ML, Zidon TM, Rector RS, Vieira-Potter VJ, Padilla J. Ablation of eNOS does not promote adipose tissue inflammation. (2016). *Experimental Biology*. San Diego, CA.
8. **Jurrissen TJ**, Carson LT, Bishop AE, Woerner SM, Zwetsloot, Neiman DC, Perkins-Veazie P, Collier SC, Shanely RA, Zwetsloot JJ. Effects of watermelon supplementation on insulin resistance and intake signaling in free-living, overweight, postmenopausal women. (2015) *American College of Sports Medicine Conference*, San Diego, CA.

### **Guest Lectures**

- 2020      Lecture Title: Hunger and satiety hormones  
Department of Nutrition and Exercise Physiology  
University of Missouri  
Course: Landscape of Obesity
- 2020      Lecture Title: Physical inactivity and sleep  
Department of Nutrition and Exercise Physiology  
University of Missouri  
Course: Landscape of Obesity

### **Funding Grants/Awards**

- 2021      Dale E. Brigham Nutrition and Exercise Physiology Teaching Assistant Award
- 2021      Human Environmental Sciences Distinguished Graduate Student Teacher Award
- 2021      Donald K. Anderson Graduate Teaching Assistant Award
- 2021      Zweifach Student Travel Award from the Microcirculatory Society
- 2020      James L. McGregor Scholarship in Health and Exercise Science
- 2015      Nutrition and Exercise Physiology Corporate Advisory Board Research Grant
- 2015      Nutrition and Exercise Physiology Corporate Advisory Board Travel Grant
- 2015      Appalachian State University Office of Student Research Grant

### **Service/Community Outreach**

- Nutrition and Exercise Physiology/Exercise is Medicine (2017-2019)
- Nutrition and Exercise Physiology outreach to local high schools (2018-2020)

- Nutrition and Exercise Physiology Graduate Professional Council representative (2016-2018)
- Steering Member of Nutrition and Exercise Physiology Graduate Student Association (2016-2019)

### **Professional Membership**

- Microcirculation Society (2019-present)
- American Physiology Society (2017-present)
- American College of Sports Medicine Student Member (2012-2016)
- American Nutrition Society (2016-2019)



## APPENDIX B: Abstracts of Published Manuscripts

### **Role of Adropin in Arterial Stiffening Associated with Obesity and Type 2 Diabetes.**

Citation:

**Jurrissen TJ**, Ramirez-Perez FI, Cabral-Amador FJ, Soares RN, Pettit-Mee RJ, Betancourt-Cortes EE, McMillan NJ, Sharma N, Rocha HNM, Fujie S, Morales-Quinones M, Lazo-Fernandez Y, Butler AA, Banerjee S, Sacks HS, Ibdah JA, Parks EJ, Rector RS, Manrique-Acevedo C, Martinez-Lemus LA, Padilla J. *Am J Physiol Heart Circ Physiol*. 2022 Sep 9. doi: 10.1152/ajpheart.00385.2022. Online ahead of print. PMID: 36083795

Abstract:

Adropin is a peptide largely secreted by the liver and known to regulate energy homeostasis; however, it also exerts cardiovascular effects. Herein, we tested the hypothesis that low circulating levels of adropin in obesity and type 2 diabetes (T2D) contribute to arterial stiffening. In support of this hypothesis, we report that obesity and T2D is associated with reduced levels of adropin (in liver and plasma) and increased arterial stiffness in mice and humans. Establishing causation, we show that mesenteric arteries from adropin knockout mice are also stiffer, relative to arteries from wild-type counterparts, thus recapitulating the stiffening phenotype observed in T2D db/db mice. Given the above, we performed a set of follow-up experiments, in which we found that: 1) exposure of endothelial cells or isolated mesenteric arteries from db/db mice to adropin reduces filamentous actin (F-actin) stress fibers and stiffness; 2) adropin-induced reduction of F-actin and stiffness in endothelial cells and db/db mesenteric arteries is abrogated by inhibition of nitric oxide (NO) synthase; and 3) stimulation of smooth muscle cells or db/db mesenteric arteries with a NO mimetic reduces stiffness. Last, we demonstrated that in vivo treatment of db/db mice with adropin for four weeks reduces stiffness in mesenteric arteries. Collectively, these findings indicate that adropin can regulate arterial stiffness, likely via endothelial-derived NO, and thus support the notion that "hyoadropinemia" should be considered as a putative target for the prevention and treatment of arterial stiffening in obesity and T2D.

### **Young Women are Protected Against Vascular Insulin Resistance Induced by Adoption of an Obesogenic Lifestyle**

Citation:

Smith JA, Soares RN, McMillan NJ, **Jurrissen TJ**, Martinez-Lemus LA, Padilla J, Manrique-Acevedo C. Young women are protected against vascular insulin resistance induced by adoption of an obesogenic lifestyle. *Endocrinology*. 2022. bqac137, <https://doi.org/10.1210/endocr/bqac137>. PMID: 35974454.

Abstract:

Vascular insulin resistance is a feature of obesity and type 2 diabetes that contributes to the genesis of vascular disease and glycemic dysregulation. Data from preclinical models indicate that vascular insulin resistance is an early event in the disease course preceding the development of insulin resistance in metabolically-active tissues. Whether this is translatable to humans requires further investigation. To this end, we examined if vascular insulin resistance develops when young healthy individuals (n = 18 men, n = 18 women) transition to an obesogenic lifestyle that would ultimately cause whole-body insulin resistance. Specifically, we hypothesized that short-term (10 days) exposure to reduced ambulatory activity (from >10,000 to <5,000 steps/day) and increased consumption of sugar-sweetened beverages (six cans/day) would be sufficient to prompt vascular insulin resistance. Furthermore, given that incidence of insulin resistance and cardiovascular disease is lower in premenopausal women compared to men, we postulated that young females would be protected against vascular insulin resistance. Consistent with this hypothesis, we report that after reduced ambulation and increased ingestion of carbonated beverages high in sugar, young healthy men, but not women, exhibited a blunted leg blood flow response to insulin, as well as suppressed skeletal muscle microvascular perfusion. These findings were associated with a decrease in plasma adiponin and nitrite concentrations. This is the first evidence in humans that vascular insulin resistance can be provoked by short-term adverse lifestyle changes. It is also the first documentation of a sexual dimorphism in the development of vascular insulin resistance in association with changes in adiponin levels.

## Cystamine Reduces Vascular Stiffness in Western Diet-Fed Female Mice.

Citation:

Ramirez-Perez FI, Cabral-Amador FJ, Whaley-Connell AT, Aroor AR, Morales-Quinones M, Woodford ML, Ghiarone T, Ferreira-Santos L, **Jurrissen TJ**, Manrique-Acevedo CM, Jia G, DeMarco VG, Padilla J, Martinez-Lemus LA, Lastra G. *Am J Physiol Heart Circ Physiol*. 2022 Feb 1;322(2):H167-H180. doi: 10.1152/ajpheart.00431.2021. Epub 2021 Dec 10.

Abstract:

Consumption of diets high in fat, sugar, and salt (Western diet, WD) is associated with accelerated arterial stiffening, a major independent risk factor for cardiovascular disease (CVD). Women with obesity are more prone to develop arterial stiffening leading to more frequent and severe CVD compared with men. As tissue transglutaminase (TG2) has been implicated in vascular stiffening, our goal herein was to determine the efficacy of cystamine, a nonspecific TG2 inhibitor, at reducing vascular stiffness in female mice chronically fed a WD. Three experimental groups of female mice were created. One was fed regular chow diet (CD) for 43 wk starting at 4 wk of age. The second was fed a WD for the same 43 wk, whereas a third cohort was fed WD, but also received cystamine (216 mg/kg/day) in the drinking water during the last 8 wk on the diet (WD + C). All vascular stiffness parameters assessed, including aortic pulse wave velocity and the incremental modulus of elasticity of isolated femoral and mesenteric arteries, were significantly increased in WD- versus CD-fed mice, and reduced in WD + C versus WD-fed mice. These changes coincided with respectively augmented and diminished vascular wall collagen and F-actin content, with no associated effect in blood pressure. In cultured human vascular smooth muscle cells, cystamine reduced TG2 activity, F-actin:G-actin ratio, collagen compaction capacity, and cellular stiffness. We conclude that cystamine treatment represents an effective approach to reduce vascular stiffness in female mice in the setting of WD consumption, likely because of its TG2 inhibitory capacity.

## **Voluntary Wheel Running Partially Compensates for the Effects of Global Estrogen Receptor- $\alpha$ Knockout on Critical Bone in Young Male Mice.**

Citation:

Dirkes RK, Winn NC, **Jurrissen TJ**, Lubahn DB, Vieira-Potter VJ, Padilla J, Hinton PS. Int J Mol Sci. 2021 Feb 9;22(4):1734. doi: 10.3390/ijms22041734. PMID: 33572215. PMCID: [PMC7915374](https://pubmed.ncbi.nlm.nih.gov/33572215/)

Abstract:

Estrogen receptor- $\alpha$  knockout (ERKO) in female, but not male, mice results in an impaired osteogenic response to exercise, but the mechanisms behind this ability in males are unknown. We explored the main and interactive effects of ERKO and exercise on cortical geometry, trabecular microarchitecture, biomechanical strength, and sclerostin expression in male mice. At 12 weeks of age, male C57BL/6J ERKO and WT animals were randomized into two groups: exercise treatment (EX) and sedentary (34) controls, until 22 weeks of age. Cortical geometry and trabecular microarchitecture were measured via  $\mu$ CT; biomechanical strength was assessed via three-point bending; sclerostin expression was measured via immunohistochemistry. Two-way ANOVA was used to assess sclerostin expression and trabecular microarchitecture; two-way ANCOVA with body weight was used to assess cortical geometry and biomechanical strength. ERKO positively impacted trabecular microarchitecture, and exercise had little effect on these outcomes. ERKO significantly impaired cortical geometry, but exercise was able to partially reverse these negative alterations. EX increased cortical thickness regardless of genotype. There were no effects of genotype or exercise on sclerostin expression. In conclusion, male ERKO mice retain the ability to build bone in response to exercise, but altering sclerostin expression is not one of the mechanisms involved.

## Daily watermelon Consumption Decreases Plasma sVCAM-1 Levels in Overweight and Obese Postmenopausal Women.

Citation:

Shanely RA, Zwetsloot JJ, **Jurrissen TJ**, Hannan LC, Zwetsloot KA, Needle AR, Bishop AE, Wu G, Perkins-Veazie P. *Nutr Res.* 2020 Apr;76:9-19. doi: 10.1016/j.nutres.2020.02.005. Epub 2020 Feb 8. PMID: 32142970.

Abstract:

Postmenopausal status is associated with an increase in total and abdominal body fat as well as increased incidence of insulin resistance and cardiovascular disease. The purpose of this study was to determine if watermelon supplementation affects select systemic markers of atherosclerosis and measures of insulin resistance in overweight and obese postmenopausal women. We hypothesized that overweight and obese postmenopausal women consuming 100% watermelon puree daily for 6 weeks would have improved levels of select systemic markers connected with cardiovascular disease without changing markers of insulin resistance. To test this hypothesis, overweight and obese postmenopausal women were recruited to participate in this study. Participants were randomly assigned to either the control group (no intervention) or the watermelon puree group (WM) for 6 weeks. Plasma concentration of markers connected with atherosclerosis and glycemic control were measured pre- and poststudy. A significant 6% decrease in soluble vascular cell adhesion molecule-1 occurred pre- to poststudy in WM,  $P = .003$ . The pattern of change in fasting blood glucose ( $P = .633$ ), insulin ( $P = .158$ ), and homeostatic model assessment-estimated insulin resistance ( $P = .174$ ) did not differ between groups. Pre- to poststudy increases were measured in the fasting plasma concentration of l-arginine (8%,  $P = .005$ ), cis-lycopene (32%,  $P = .003$ ), and trans-lycopene (42%,  $P = .003$ ) in WM. We conclude that 6 weeks of watermelon supplementation improved soluble vascular cell adhesion molecule-1 levels, a marker connected to atherogenesis, independent of changes in body composition or glycemic control.

## **Chronic Elevation of Endothelin-1 Alone May Not Be Sufficient to Impair Endothelium-Dependent Relaxation.**

Citation:

Grunewald ZI, **Jurrissen TJ**, Woodford ML, Ramirez-Perez FI, Park LK, Pettit-Mee R, Ghiarone T, Brown SM, Morales-Quinones M, Ball JR, Staveley-O'Carroll KF, Aroor AR, Fadel PJ, Paradis P, Schiffrin EL, Bender SB, Martinez-Lemus LA, Padilla J. *Hypertension*. 2019 Dec;74(6):1409-1419. doi: 10.1161/HYPERTENSIONAHA.119.13676. Epub 2019 Oct 21. PMID: 31630572.

Abstract:

Endothelin-1 (ET-1) is a powerful vasoconstrictor peptide considered to be causally implicated in hypertension and the development of cardiovascular disease. Increased ET-1 is commonly associated with reduced NO bioavailability and impaired vascular function; however, whether chronic elevation of ET-1 directly impairs endothelium-dependent relaxation (EDR) remains elusive. Herein, we report that (1) prolonged ET-1 exposure (ie, 48 hours) of naive mouse aortas or cultured endothelial cells did not impair EDR or reduce eNOS (endothelial NO synthase) activity, respectively ( $P>0.05$ ); (2) mice with endothelial cell-specific ET-1 overexpression did not exhibit impaired EDR or reduced eNOS activity ( $P>0.05$ ); (3) chronic (8 weeks) pharmacological blockade of ET-1 receptors in obese/hyperlipidemic mice did not improve aortic EDR or increase eNOS activity ( $P>0.05$ ); and (4) vascular and plasma ET-1 did not inversely correlate with EDR in resistance arteries isolated from human subjects with a wide range of ET-1 levels ( $r=0.0037$  and  $r=-0.1258$ , respectively). Furthermore, we report that prolonged ET-1 exposure downregulated vascular UCP-1 (uncoupling protein-1;  $P<0.05$ ), which may contribute to the preservation of EDR in conditions characterized by hyperendothelinemia. Collectively, our findings demonstrate that chronic elevation of ET-1 alone may not be sufficient to impair EDR.

**Western Diet-Fed, Aortic-Banded Ossabaw Swine: a Preclinical Model of Cardiometabolic Heart Failure.**

Citation:

Olver TD, Edwards JC, **Jurrissen TJ**, Veteto AB, Jones JL, Gao C, Rau C, Warren CM, Klutho PJ, Alex L, Ferreira-Nichols SC, Ivey JR, Thorne PK, McDonald KS, Krenz M, Baines CP, Solaro RJ, Wang Y, Ford DA, Domeier TL, Padilla J, Rector RS, Emter CA. JACC Basic Transl Sci. 2019 Jun 24;4(3):404-421. doi: 10.1016/j.jacbts.2019.02.004. eCollection 2019 Jun. PMID: 31312763

Abstract:

The development of new treatments for heart failure lack animal models that encompass the increasingly heterogeneous disease profile of this patient population. This report provides evidence supporting the hypothesis that Western Diet-fed, aortic-banded Ossabaw swine display an integrated physiological, morphological, and genetic phenotype evocative of cardio-metabolic heart failure. This new preclinical animal model displays a distinctive constellation of findings that are conceivably useful to extending the understanding of how pre-existing cardio-metabolic syndrome can contribute to developing HF.

**Overproduction of Endothelin-1 Impairs Glucose Tolerance But Does Not Promote Visceral Adipose Tissue Inflammation or Limit Metabolic Adaptations to Exercise.**

Citation:

**Jurrissen TJ**, Grunewald ZI, Woodford ML, Winn NC, Ball JR, Smith TN, Wheeler AA, Rawlings AL, Staveley-O'Carroll KF, Ji Y, Fay WP, Paradis P, Schiffrin EL, Vieira-Potter VJ, Fadel PJ, Martinez-Lemus LA, Padilla J. *Am J Physiol Endocrinol Metab.* 2019 Sep 1;317(3):E548-E558. doi: 10.1152/ajpendo.00178.2019. Epub 2019 Jul 16. PMID: 31310581

Abstract:

Endothelin-1 (ET-1) is a potent vasoconstrictor and proinflammatory peptide that is upregulated in obesity. Herein, we tested the hypothesis that ET-1 signaling promotes visceral adipose tissue (AT) inflammation and disrupts glucose homeostasis. We also tested if reduced ET-1 is a required mechanism by which exercise ameliorates AT inflammation and improves glycemic control in obesity. We found that 1) diet-induced obesity, AT inflammation, and glycemic dysregulation were not accompanied by significantly increased levels of ET-1 in AT or circulation in wild-type mice and that endothelial overexpression of ET-1 and consequently increased ET-1 levels did not cause AT inflammation yet impaired glucose tolerance; 2) reduced AT inflammation and improved glucose tolerance with voluntary wheel running was not associated with decreased levels of ET-1 in AT or circulation in obese mice nor did endothelial overexpression of ET-1 impede such exercise-induced metabolic adaptations; 3) chronic pharmacological blockade of ET-1 receptors did not suppress AT inflammation in obese mice but improved glucose tolerance; and 4) in a cohort of human subjects with a wide range of body mass indexes, ET-1 levels in AT, or circulation were not correlated with markers of inflammation in AT. In aggregate, we conclude that ET-1 signaling is not implicated in the development of visceral AT inflammation but promotes glucose intolerance, thus representing an important therapeutic target for glycemic dysregulation in conditions characterized by hyperendothelinemia. Furthermore, we show that the salutary effects of exercise on AT and systemic metabolic function are not contingent on the suppression of ET-1 signaling.

**Aerobic Exercise Training Improves Insulin-induced Vasorelaxation in a Vessel-specific Manner in Rats with Insulin-treated Experimental Diabetes.**

Citation:



McDonald MW, Olver TD, Dotzert MS, **Jurrissen TJ**, Noble EG, Padilla J, Melling CJ. *Diab Vasc Dis Res*. 2019 Jan;16(1):77-86. doi: 10.1177/1479164118815279. Epub 2018 Dec 11. PMID: 30537862

**Abstract:**

Vascular insulin resistance often precedes endothelial dysfunction in type 1 diabetes mellitus. Strategies to limit vascular dysfunction include intensive insulin therapy (4-9 mM) and aerobic training. To avoid the risk of hypoglycaemia, individuals often prescribed conventional insulin therapy (9-15 mM) and participate in resistance training. In a model of type 1 diabetes mellitus, this study examined insulin-induced vasomotor function in the aorta and femoral artery to determine (1) whether resistance training with conventional insulin therapy provides the same benefits as aerobic training with conventional insulin therapy, (2) whether aerobic training or resistance training, when paired with conventional insulin therapy, results in superior vasomotor function compared to intensive insulin therapy alone and (3) whether vessel-specific adaptations exist. Groups consisted of conventional insulin therapy, intensive insulin therapy, aerobic training with conventional insulin therapy and resistance training with conventional insulin therapy. Following multiple low doses of streptozotocin, male Sprague-Dawley rats were supplemented with insulin to maintain blood glucose concentrations (9-15 mM: conventional insulin therapy, aerobic training and resistance training; 4-9 mM: intensive insulin therapy) for 12 weeks. Aerobic training performed treadmill exercise and resistance training consisted of weighted climbing. Coinciding with increased Akt signalling, aerobic training resulted in enhanced insulin-induced vasorelaxation in the femoral artery. Intensive insulin therapy displayed increased mitogen-activated protein kinase signalling and no improvement in insulin-stimulated vasorelaxation compared to all other groups. These data suggest that aerobic training may be more beneficial for limiting the pathogenesis of vascular disease in type 1 diabetes mellitus than merely intensive insulin therapy.

**Estrogen Receptor- $\alpha$  Signaling Maintains Immunometabolic Function in Males and is Obligatory for Exercise-induced Amelioration of Nonalcoholic Fatty Liver.**

Citation:

Winn NC, **Jurrissen TJ**, Grunewald ZI, Cunningham RP, Woodford ML, Kanaley JA, Lubahn DB, Manrique-Acevedo C, Rector RS, Vieira-Potter VJ, Padilla J. *Am J Physiol Endocrinol Metab.* 2019 Feb 1;316(2):E156-E167. doi: 10.1152/ajpendo.00259.2018. Epub 2018 Dec 4. PMID: 30512987

Abstract:

The role of estrogen receptor- $\alpha$  (ER $\alpha$ ) signaling in immunometabolic function is established in females. However, its necessity in males, while appreciated, requires further study. Accordingly, we first determined whether lower metabolic function in male mice compared with females is related to reduced ER $\alpha$  expression. ER $\alpha$  protein expression in metabolically active tissues was lower in males than in females, and this lower expression was associated with worse glucose tolerance. Second, we determined whether ER $\alpha$  is required for optimal immunometabolic function in male mice consuming a chow diet. Despite lower expression of ER $\alpha$  in males, its genetic ablation (KO) caused an insulin-resistant phenotype characterized by enhanced adiposity, glucose intolerance, hepatic steatosis, and metaflammation in adipose tissue and liver. Last, we determined whether ER $\alpha$  is essential for exercise-induced metabolic adaptations. Twelve-week-old wild-type (WT) and ER $\alpha$  KO mice either remained sedentary (34) or were given access to running wheels (WR) for 10 wk while fed an obesogenic diet. Body weight and fat mass were lower in WR mice regardless of genotype. Daily exercise obliterated immune cell infiltration and inflammatory gene transcripts in adipose tissue in both genotypes. In the liver, however, wheel running suppressed hepatic steatosis and inflammatory gene transcripts in WT but not in KO mice. In conclusion, the present findings indicate that ER $\alpha$  is required for optimal immunometabolic function in male mice despite their reduced ER $\alpha$  protein expression in metabolically active tissues. Furthermore, for the first time, we show that ER $\alpha$  signaling appears to be obligatory for exercise-induced prevention of hepatic steatosis.

**Endothelial Dysfunction Occurs Independently of Adipose Tissue Inflammation and Insulin Resistance in Ovariectomized Yucatan Miniature-swine.**

Citation:

**Jurrissen TJ**, Olver TD, Winn NC, Grunewald ZI, Lin GS, Hiemstra JA, Edwards JC, Gastecki ML, Welly RJ, Emter CA, Vieira-Potter VJ, Padilla J. Adipocyte. 2018 Jan 2;7(1):35-44. doi: 10.1080/21623945.2017.1405191. Epub 2017 Dec 28. PMID: 29283284

Abstract:

In rodents, experimentally-induced ovarian hormone deficiency increases adiposity and adipose tissue (AT) inflammation, which is thought to contribute to insulin resistance and increased cardiovascular disease risk. However, whether this occurs in a translationally-relevant large animal model remains unknown. Herein, we tested the hypothesis that ovariectomy would promote visceral and perivascular AT (PVAT) inflammation, as well as subsequent insulin resistance and peripheral vascular dysfunction in female swine. At sexual maturity (7 months of age), female Yucatan mini-swine either remained intact (control, n = 9) or were ovariectomized (OVX, n = 7). All pigs were fed standard chow (15-20 g/kg), and were euthanized 6 months post-surgery. Uterine mass and plasma estradiol levels were decreased by ~10-fold and 2-fold, respectively, in OVX compared to control pigs. Body mass, glucose homeostasis, and markers of insulin resistance were not different between control and OVX pigs; however, OVX animals exhibited greater plasma triglycerides and triglyceride:HDL ratio. Ovariectomy enhanced visceral adipocyte expansion, although this was not accompanied by brachial artery PVAT adipocyte expansion, AT inflammation in either depot, or increased systemic inflammation assessed by plasma C-reactive protein concentrations. Despite the lack of AT inflammation and insulin resistance, OVX pigs exhibited depressed brachial artery endothelial-dependent vasorelaxation, which was rescued with blockade of endothelin receptor A. Together, these findings indicate that in female Yucatan mini-swine, increased AT inflammation and insulin resistance are not required for loss of ovarian hormones to induce endothelial dysfunction.

### **Microvascular Insulin Resistance in Skeletal Muscle and Brain Occurs Early in the Development of Juvenile Obesity in Pigs.**

Citation:

Olver TD, Grunewald ZI, **Jurrissen TJ**, MacPherson REK, LeBlanc PJ, Schnurbusch TR, Czajkowski AM, Laughlin MH, Rector RS, Bender SB, Walters EM, Emter CA, Padilla J. Am J Physiol Regul Integr Comp Physiol. 2018 Feb

1;314(2):R252-R264. doi: 10.1152/ajpregu.00213.2017. Epub 2017 Dec 4. PMID: 29141949

Abstract:

Impaired microvascular insulin signaling may develop before overt indices of microvascular endothelial dysfunction and represent an early pathological feature of adolescent obesity. Using a translational porcine model of juvenile obesity, we tested the hypotheses that in the early stages of obesity development, impaired insulin signaling manifests in skeletal muscle (triceps), brain (prefrontal cortex), and corresponding vasculatures, and that depressed insulin-induced vasodilation is reversible with acute inhibition of protein kinase C $\beta$  (PKC $\beta$ ). Juvenile Ossabaw miniature swine (3.5 mo of age) were divided into two groups: lean control (n = 6) and obese (n = 6). Obesity was induced by feeding the animals a high-fat/high-fructose corn syrup/high-cholesterol diet for 10 wk. Juvenile obesity was characterized by excess body mass, hyperglycemia, physical inactivity (accelerometer), and marked lipid accumulation in the skeletal muscle, with no evidence of overt atherosclerotic lesions in athero-prone regions, such as the abdominal aorta. Endothelium-dependent (bradykinin) and -independent (sodium nitroprusside) vasomotor responses in the brachial and carotid arteries (wire myography), as well as in the skeletal muscle resistance and 2A pial arterioles (pressure myography) were unaltered, but insulin-induced microvascular vasodilation was impaired in the obese group. Blunted insulin-stimulated vasodilation, which was reversed with acute PKC $\beta$  inhibition (LY333-531), occurred alongside decreased tissue perfusion, as well as reduced insulin-stimulated Akt signaling in the prefrontal cortex, but not the triceps. In the early stages of juvenile obesity development, the microvasculature and prefrontal cortex exhibit impaired insulin signaling. Such adaptations may underscore vascular and neurological derangements associated with juvenile obesity.

### **Ablation of eNOS Does Not Promote Adipose Tissue Inflammation.**

Citation:

**Jurrissen TJ**, Sheldon RD, Gastecki ML, Woodford ML, Zidon TM, Rector RS, Vieira-Potter VJ, Padilla J. *Am J Physiol Regul Integr Comp Physiol*. 2016 Apr 15;310(8):R744-51. doi: 10.1152/ajpregu.00473.2015. Epub 2016 Feb 10. PMID: 26864812

Abstract:

Adipose tissue (AT) inflammation is a hallmark characteristic of obesity and an important determinant of insulin resistance and cardiovascular disease; therefore, a better understanding of factors regulating AT inflammation is critical. It is well established that reduced vascular endothelial nitric oxide (NO) bioavailability promotes arterial inflammation; however, the role of NO in modulating inflammation in AT remains disputed. In the present study, 10-wk-old C57BL6 wild-type and endothelial nitric oxide synthase (eNOS) knockout male mice were randomized to either a control diet (10% kcal from fat) or a Western diet (44.9% kcal from fat, 17% sucrose, and 1% cholesterol) for 18 wk (n= 7 or 8/group). In wild-type mice, Western diet-induced obesity led to increased visceral white AT expression of inflammatory genes (e.g., MCP1, TNF- $\alpha$ , and CCL5 mRNAs) and markers of macrophage infiltration (e.g., CD68, ITGAM, EMR1, CD11C mRNAs, and Mac-2 protein), as well as reduced markers of mitochondrial content (e.g., OXPHOS complex I and IV protein). Unexpectedly, these effects of Western diet on visceral white AT were not accompanied by decreases in eNOS phosphorylation at Ser-1177 or increases in eNOS phosphorylation at Thr-495. Also counter to expectations, eNOS knockout mice, independent of the diet, were leaner and did not exhibit greater white or brown AT inflammation compared with wild-type mice. Collectively, these findings do not support the hypothesis that reduced NO production from eNOS contributes to obesity-related AT inflammation.

## VITA

Thomas Jacob Jurrissen, III was born to Thomas and Brigitte Jurrissen in Summit, New Jersey. Following completion of high school at Reidsville High School in 2008, Thomas attended Appalachian State University in Boone, North Carolina where he received a Bachelor of Science degree and Master of Science degree in Exercise Science in 2013 and 2015, respectively. During his Master's in Exercise Science, Thomas became interested in research related the influence of exercise on chronic diseases, specifically metabolic and cardiovascular disease. This led him to pursue a PhD in Exercise Physiology at the University of Missouri, under the mentorship of Dr. Jaume Padilla. Thomas obtained his doctorate degree in 2022 and is planning to pursue a post-doctoral fellowship.